UiO : Department of Geosciences
University of Oslo

High and Low Flow Trends in Norway - Co-occurrence and Causing Factors

Sunniva Nordeide

Master's Thesis, Spring 2022

Abstract

Climate change has impacted the global water cycle and has changed how streamflow behaves in Norway. Knowledge about high and low flows are important to be prepared for future changes, such as changes in water availability for humans, electricity production, agriculture and more. This thesis investigates historical changes (01.01.1991-31.12.2019) in seasonal high and low flow in Norway and their co-occurrence, and uses machine learning to identify which catchment characteristics, climate indices or other trends in seasonal high and low flow are important predictors to explain these trends. Discharge data from the Norwegian Water Resources and Energy Directorate (NVE) is used to calculate trends in high and low flow. Low flow was divided into two periods: summer low flow (June-September) and winter low flow (October-May), and high flow was divided into two periods: spring high flow (March-August) and autumn high flow (September-February). The trends were calculated over smoothing intervals of minimum/maximum discharge over 7 and 30 days. Precipitation, temperature, evaporation and snow data from seNorge is used to create climate indices while catchment characteristics are from NVE. The machine learning methods decision tree and random forest were applied to find the most important predictors for each seasonal trend. The trend results showed a clear divide in trend direction between southern and northern Norway across all seasonal trends. Southern Norway displayed only significantly increasing trends for summer low flow and autumn high flow, where as some decreasing trends showed up in the western part of southern Norway for winter low flow and spring high flow. Northern Norway displayed mostly significantly decreasing trends across all seasons, except for Troms and Finnmark which had increasing trends in winter low flow. The increasing trends in southern Norway may be because southern Norway experienced increased precipitation across all seasons during the research period, while the decreasing trends in northern Norway may be due to increasing winter temperatures and less snow melting in spring and summer. Increasing winter temperature may lead to more frequent melting during the winter period in Troms and Finnmark, explaining the increasing trends in winter low flow. The machine learning highlighted latitude and longitude as important predictors, within top tree for at least one machine learning model for all trends except $AM(7)_{low,winter}$. Precipitation, temperature and streamflow often showed up as important as well. Other seasonal trends were not often used as predictors, probably because a catchment displaying a significant trend for one season did not always show trends in the other seasons. This thesis provides insight into trends in high and low flow their co-occurrence during the current climate period, and main predictors explaining the observed changes.

Acknowledgements

I am grateful to everyone helping me working with this thesis during the past year. Thank you to my great supervisors, Sigrid Jørgensen Bakke, Lena M. Tallaksen and Kolbjørn Engeland. This thesis would not have been possible without your help and expertise, and especially not without your support, optimism, and enthusiasm for the thesis. Thank you to the Norwegian Water Resources and Energy Directorate, for letting me use your data and sharing your expertise freely. Special thanks to Jess Andersen at NVE for helping me download the data used for the climate indices.

I would also like to give a special thank you to my friends and family, for all the support, kind words and revision help on the thesis. To my study room buddies, thank you for all the coffee breaks and quizzes.

Contents

List of Figures

List of Tables

1 Introduction

1.1 Motivation

The Intergovernmental Panel on Climate Change (IPCC) states in its most recent report that global warming has intensified the global water cycle, and further warming will further intensify the water cycle (IPCC, 2021). The mean global temperature has increased by 1.1°C since the start of the industrial revolution, and this increase is unequivocally partially caused by human impacts. Human impacts are also very likely to have caused observed changes in extreme weather, and the severity of wet and dry events has intensified. Climate is changing, and we now live in a world with less permafrost, snow cover, ocean ice sheets and lake and sea ice than a hundred years ago. At the same time, we need to expect extreme heat spells, forest fires, droughts, heavy precipitation and river floods, more frequent and severe than previously (IPCC, 2021).

The changing climate affects the water cycle and thereby influence the seasonality and dynamics of streamflow. Changes in the water cycle can lead to more extreme events like floods and droughts, while also increasing the probability of multiple extreme events happening after each other (Catto & Dowdy, 2021; IPCC, 2021). For water resources management it is of utter importance to identify expected changes since we today make decisions about investments in utilities and infrastructure for domestic water supply and electricity production that should be reliable also in the expected future climate. Knowledge about extreme flood sizes is important for land use planning, urban development, design of dam spillways and infrastructure (Wilson et al., 2011). In addition, we might need to "retrofit" existing infrastructure to expected changes.

Changes in the global water cycle will affect discharge in Norwegian catchments (Hanssen-Bauer et al., 2017). This will in turn affect water resources management, local ecosystems and water supply for drinking and electricity production. To understand what changes may happen in the future, it is important to be aware of the changes that has already happened in our catchments. Norway has already experienced increasing mean precipitation, temperature and streamflow during the past century (Hanssen-Bauer et al., 2017). By discovering trend patterns across the country, the patterns of change in mean and extreme streamflow may help uncover how climate change has affected

the water cycle in Norway, and how it will further affect the water cycle in the future.

1.2 Background

The hydrological cycle, or the water cycle, describes the process of how water interacts between the ocean, the atmosphere and land, and is driven by solar energy and gravity (Yang et al., 2021). Incoming solar radiation warm up the Earth's surface and evaporate water either from ocean surfaces, other open water sources like lakes or rivers or directly from the ground. Water may be evaporated directly from plants due to a process called transpiration. The evaporated water is transported up into the atmosphere, where it is cooled down and condensates to clouds. These clouds lose water when it falls as precipitation, either over land or over the ocean. The precipitation that falls over land either fall into in lakes and rivers, percolates through the ground and is stored as soil or groundwater, or it ends up being evaporated again, directly from the soil or from plants or water bodies. If the precipitation falls as snow it can be stored as snow or ice for a while, or in a glacier. Eventually, the water will return to the ocean and the cycle starts anew (Dingman, 2015).

In this study we focus on water changes and trends within a catchment. A catchment is defined as: "the area that topographically appears to contribute all the water that passes through a specified cross section of a stream" (Dingman, 2015). When looking at how water moves within a catchment, it is important to know the key characteristics of the catchment. Such characteristics can be the catchment area, average height above sea level, the amount of forest or agricultural areas within the catchment or length of the main river in the catchment. An important characteristic is the location of the catchment, since that decides the climatic influences on streamflow. Streamflow in a river depends on precipitation amount, temperature, evaporation, storage capacity in the catchment, vegetation, groundwater input, and snow melt, among others. Norway is a diverse country, leading to large differences between these variables.

To further understand the streamflow generation one must be aware of the different flow regimes in Norway. A flow regime is defined as the river's seasonality in its flow and is governed by climate and physiography (Gottschalk et al., 1979). Critical components to flow regime is magnitude, frequency, duration, timing, and rate of change of hydrological conditions (Poff et al., 1997). When Gottschalk et al. (1979) defined the runoff regimes in the Nordic region, six possible combinations of regime types were defined, as can be seen in Figure 1.1. The regime type were decided based on the time of year when low flow and high flow in the Nordic countries occurred, both natural parts of the flow regime and important factors of this thesis. The most common regime type in Norway was the combination winter low flow and spring high flow, appearing in in mid and inland southern Norway and inland northern Norway.

Trøndelag and southern parts of south Norway experience mixed high flow processes with winter low flow, while all coastal parts of the country have regimes based on autumn high flow and summer low flow (Gottschalk et al., 1979).

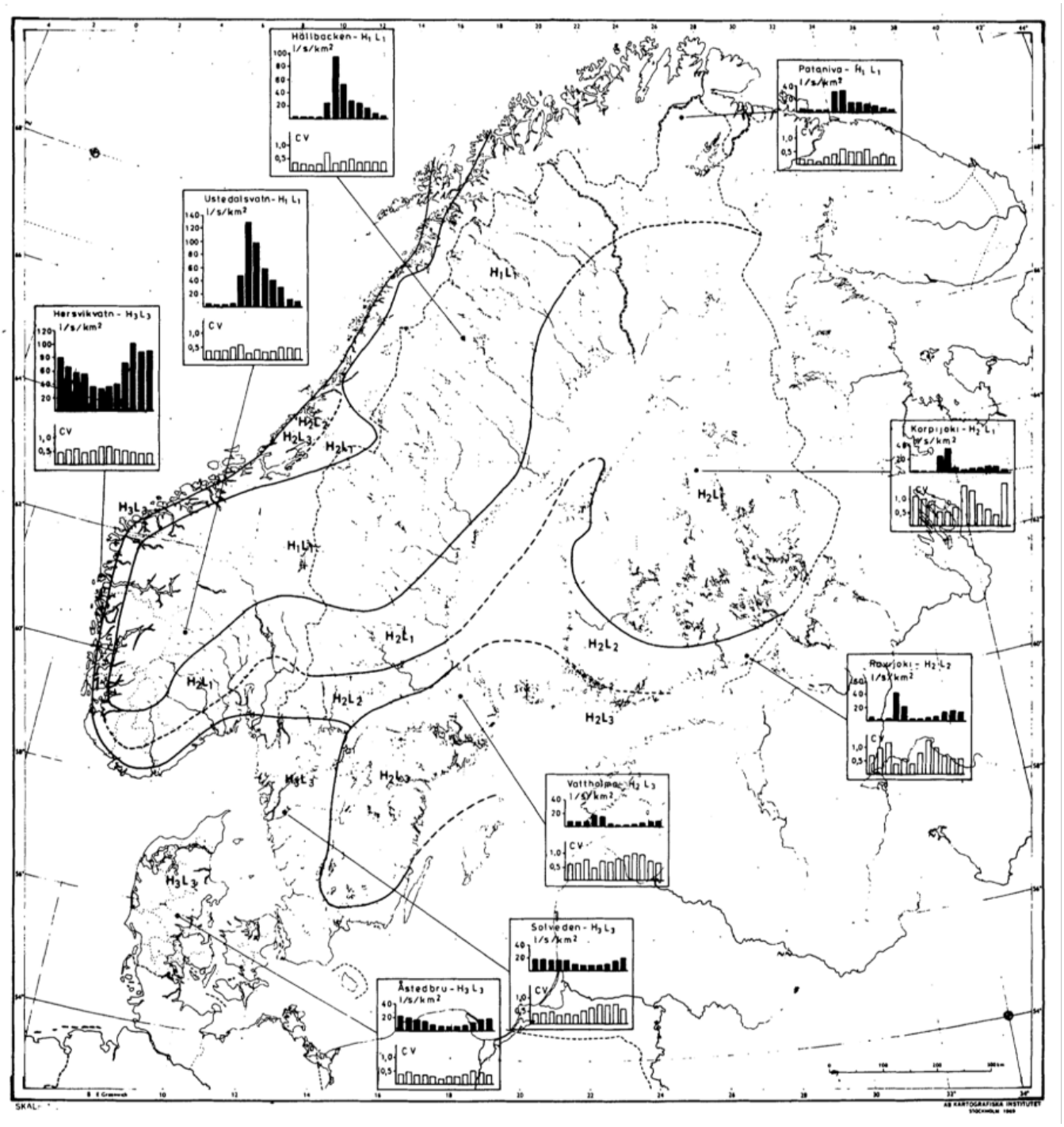

Figure 1.1: Runoff regions in the Nordic countries. High (low) flow regime is decided by if the two months of the year experiencing the highest (lowest) flow is in the same season. H_1: Both months are in the spring, the snow melt season (typically May-July). H_2: The two months are in different seasons. H_3: Both months are in autumn/early winter (typically November-December). L_1: Both months are in the winter season, when low flow is caused by snow accumulation (typically February-March). L_2: The two months are in different seasons. L_3: Both months are in the summer season, when low flow is caused by high evaporation and low precipitation (typically June-August). Figure taken from Gottschalk et al. (1979).

Low flow and drought

Low flow is a natural part of the flow regime in a river, and is a seasonal phenomenon (Smakhtin, 2001). In Norway, different processes lead to low flow in summer and winter. Winter low flow is usually caused by snow being stored as snow and ice, meaning that precipitation accumulates in the catchment and less water escapes the catchment as runoff in rivers. Summer low flow is caused by less precipitation and higher evaporation (Engeland & Hisdal, 2009). There is not one fixed way to calculate low flow. It is therefore important to define what method is used, as there are many different ways of analyzing a time series of daily flow to characterize the low flow regime of a river. These include: as a yearly minimum; as a percentile (for example, the flow exceeded 95% of the time in a river); as how long the flow in a river is below a given threshold; or as minimum mean flow during a given period within a year (WMO, 2009). Gottschalk et al. (1979) defined two separate periods of low flow: snow and ice accumulation dominated low flow during the winter months, and high evaporation and/or low precipitation dominated low flow during the autumn and winter months.

Extended periods of low flow can be a driver for hydrological droughts. A drought can be defined as "a sustained and regional extensive occurrence of below average natural water availability" (Tallaksen & Van Lanen, 2004), and is a deviation from the normal streamflow, precipitation, soil water and groundwater situation (Hanssen-Bauer et al., 2017). It appears gradually and can affect a large spatial scale. Due to the gradual evolution of a drought, it can occur as three different types, each reflecting the stage of propagation through the hydrological cycle. These are meteorological drought, reflecting lack of precipitation; soil moisture drought, reflecting both lack in precipitation and lack of water through evapotranspiration; and hydrological (streamflow and groundwater) drought (Tallaksen & Van Lanen, 2004). Droughts lead to water deficit, and impacts not only agriculture, energy production and public water supply, but aquaculture, ecosystems, humans, public safety and may lead to forest fires (Blauhut et al., 2021; Hanssen-Bauer et al., 2017).

High flow and flood

High flow is the natural counterpart to low flow, periods with higher streamflow in the river than the mean. It is also a seasonal phenomenon, but with different underlying drivers. Gottschalk et al. (1979) defined two separate periods of high flow: snow melt dominated high flow during the spring and early summer months, and rainfall dominated high flow during the autumn and early winter months. High flow can be calculated using some of the same methods as low flow, including: as a yearly maximum; as a percentile (the flow exceeded only 5% of the time); or as a minimum mean flow during a given period within a year (Hannaford & Marsh, 2008).

High flows is a natural part of a flow regime, but when the water rises too high to be considered "normal", it is called a flood. A flood occurs when the water level in rivers or lakes rises above a certain level, such as the river-bank, and causes damages to the surroundings (Roald, 2020). Floods are the result of seasonal interplay between precipitation, soil moisture and snow process (Blöschl et al., 2017). Different regions of Norway experience different main dominating flood-generating processes (FGPs). In Norway, the two dominating FGPs are snow melt floods and rainfall floods (Roald, 2020). However, different types of floods could be generated from these FGPs. Five flood process types have been proposed: Long-rain floods, generated by rainfall over several days, possibly weeks; Short-rain floods, generated by short but high-intensity rainfall which saturates part of the area; Flash-floods, again short and high-intensity rainfall, but on a very local scale; Rain-on-Snow floods, where rainfall over a snow cover may enhance snow melt leading to large amount of runoff at once; and finally Snow melt floods, when a period of warmer weather lead to accumulated snow over the winter melting (Merz & Blöschl, 2003). The largest floods in Norway have occurred in years where the snow melt started late, followed by a sudden increase in temperature combine with rainfall (Hanssen-Bauer et al., 2017)). A flood is typically a smaller-scaled spatial and temporal event than a drought(Tallaksen & Van Lanen, 2004).

The interplay between high and low flows

Through the seasonality of the hydrological cycle, high flows and low flows are inherently linked. Lower low flows in the winter caused by most precipitation being stored as snow and ice yield large high flows in the spring from the resulting melting. When melting in a catchment occurs in spring affect summer low flow, due to the soil water and groundwater storage capacity in the catchment. Accordingly, a warmer winter with less precipitation falling as snow, and higher winter low flow, affects spring high flow by decreasing the amount of snow melt, which in turn may affect summer low flow due to low soil water and groundwater capacity in the catchment during the summer. Due to climate change, temperatures in Norway are expected to increase, as well as precipitation amount. An increase in these two climate variables will lead to increases in both high flow and low flow, during all seasons.

1.3 Approaches for detecting Climate Change impacts on high and low flow

Ever since we learned climate change may have been caused by human impacts, we have tried different methods and approaches to projecting the future climate, as well as analyzing how humans already have impacted it. This has been done by using methods varying from simple linear methods to find trends in measured data, to large, computation-heavy global circulation models to project the future climate system.

There are many different approaches to calculating trends in discharge. One way is to look at changes over time using linear regression, drawing a regression line and using its slope as an indicator of the magnitude and direction of the changes. Finding changes in streamflow using linear regression methods is a well-used method in hydrology (Hannaford & Marsh, 2006; Stahl et al., 2010; Wilson et al., 2010).

Trends in streamflow

A study of streamflow trends in the Nordic countries found increasing streamflow trends in south-western Norway during the period 1961-2000 (Wilson et al., 2010). The same study also looked at trends in seasonal streamflow, and found that streamflow were increasing in southern Norway for the winter, spring and summer season. Decreasing trends were found in autumn season for the whole country, while northern Norway showed decreasing trends during winter season. A recent study from Norway looked at trends in daily streamflow between Western and Eastern Norway during 1983-2012, and found earlier spring flow timing in both regions, increased summer streamflow and slightly increased winter streamflow in the east (Skålevåg & Vormoor, 2021). This same pattern has been found in multiple studies, where less snow in winter and higher spring temperatures cause earlier snow melt. A study from the Czech Republic found that less snow accumulated in the mountains in the winter, leading to earlier snowmelt, less groundwater recharge and therefore a decrease in summer low flow (Jenicek & Ledvinka, 2020). Similar trends are seen for Norway. Rizzi et al. (2017) found that in the period 1961-2010, the snow cover extent in large parts of Norway decreased, with the largest decrease at the end of the snow season. In the same period, mean air temperature increased in all seasons, with the highest increase in winter and spring. However, trends towards higher SWE was found in the mountain regions of Norway (Rizzi et al., 2017).

Trends in high flow and floods

The report Climate in Norway 2100 (Hanssen-Bauer et al., 2017) produced trend maps for floods and droughts predicted from 2030-2100. 200-year floods are projected to increase for most catchments, especially in the regions Vestlandet and Nordland. The decreasing trends belong to catchments in the far north, the southeast and some weak decreases in the mountains in the mid-south. The increases in flood magnitudes affect the catchments with rainfall-dominated FGPs, since more rain is incoming from the coast, while the decreases affect the catchments with snow melt-dominated FGPs, caused by warmer temperatures. With a warmer future climate scenario, the bigger the flood magnitude increase.

Flood-frequency studies from Norway have shown that flood magnitudes in all catchments with rainfall-dominated regimes are expected to increase (Lawrence, 2020). The Climate in Norway 2100 report (Hanssen-Bauer et al., 2017) concluded that snow melt floods will become more rare and smaller in magnitude, while rainfall-dominated floods will be larger and occur more often. This is also reported in a European study (Blöschl et al., 2017), which conclude that spring floods (driven by snow melt) occur earlier, while winter floods (rainfall driven) arrive later in the year.

Trends in low flow and droughts

A study from 2010 (Stahl et al., 2010) that presented summer low flow trends for the period 1962-2004 over Europe, found opposite trends in AM7 summer flow and monthly streamflow. Most Norwegian catchments in the study had low flow during the months February-march, signifying winter low flow. Summer low flow showed decreasing trends for catchments in southern and coastal parts of Norway, while mountain regions inland had increasing trends.

The Norwegian Centre for Climate Services (NCCS) does not present any trends for hydrological droughts or low flow as they do for floods. However, they do present a map of predicted soil water deficit during the summer months. There is a decrease of at least 5mm in soil water deficit for most of Norway, with the largest changes in northern and western Norway, with decreases in soil water by more than 15mm (Hanssen-Bauer et al., 2017). These changes are explained by increased evaporation in southern Norway, while in northern Norway it is mostly due to earlier snow melt.

Co-occurrence of high and low flow in Norway

Few studies have previously tried to look at trends in both high and low flow in Norway. Wilson et al. (2010) looked at trends in flood timing and drought deficit volume in Norway. The Climate in Norway 2100 report (Hanssen-Bauer et al., 2017) presented the past and future changes in flood magnitude and soil moisture deficit.

Using machine learning to predict high and low flow

To the authors knowledge, no studies have tried to predict trends in high and low flow using machine learning, to find the most important predictors among climate indices and catchment descriptors to explain the trends. A study from late 2021 (Laimighofer et al., 2022) used different machine learning methods to predict low flow, to find which performed the best. An American study used random forest machine learning algorithm to find the most important predictors for three different drought regimes (Konapala & Mishra, 2020). An Austrian study used multiple regression to find which climate and catchment characteristics could explain hydrological drought severity, and found that both climate indices and catchment characteristics are important predictors (Van Loon & Laaha, 2015).

1.4 Aim of this study

This study aims to provide new insights in trends in high and low flows in Norway for the period 01.01.1991-31.12.2019. These trends calculated in this study will add to the knowledge of how streamflow in Norwegian unregulated catchments have changed, as well as the co-occurrence of the trends regarding their location and the direction of the trend.

Further, in using machine learning to first, make a model predicting trends in high and low flow, then assess which predictors play the most important role when predicting these trends, will provide a new understanding of streamflow in Norwegian catchments. The predictors used will be climate indices and their trends, and catchment characteristics. Seasonal trends will have other seasonal trend results used as predictors as well, to further the study of co-occurrence between high flow and low flow by examining if other trends are picked by the machine learning algorithm as important predictor.

The research questions for this study are:

(i) How has low and high flow for Norwegian unregulated catchments changed during the period 01.01.1991 - 31.12.2019?

(ii) If there are changes, do they display co-occurrence in their location and directions?

(iii) Can we, using machine learning, find which of the climate indices and catchment characteristics available are the most important predictor for the trends?

The thesis will be structured like this. Firstly, Chapter 2 describes the study area in this thesis and data is used. Then, Chapter 3, Methods, explains all methods used to produce the results, which are presented in the Chapter 4, Results. Chapter 5 includes the discussion. Conclusions are drawn in Chapter 6, followed by references and appendices.

2 Study Area and Data

This chapter gives an introduction to the study area of the study. First, a description of Norway and its climatic and hydrological situation is introduced. Then the data used in this study are presented.

Norway is a country located in northwestern Europe and borders to Sweden, Finland and Russia. It has a long coastline stretching from the south to the north of the country across more than ten latitude degrees and 25 longitude degrees. It is a diverse country with height differences from ocean level to 2469 m.a.s.l, mean annual temperature ranging from -4 to +8 °C, and mean annual precipitation reaching 3500-4000 mm in the western parts of the country (Hanssen-Bauer et al., 2017; Ketzler et al., 2021). The coldest temperature recorded in Norway was -51.4 °C at Finnmarksvidda, while the highest temperature was recorded in south-eastern Norway, at +35.6 °C (Ketzler et al., 2021).

The large differences in Norway's latitude, longitude, temperature, precipitation, height as well as other climatological and physiographical characteristics greatly impact its hydrological components. Figure 2.1 shows Norway divided by its runoff regions. Norway has six runoff regions, each with their separate flow regimes. It is by these regions I will refer to the different parts of the country during this thesis. In the following sections, the climate of Norway, its hydrological regions and its physiographical characteristics will be presented.

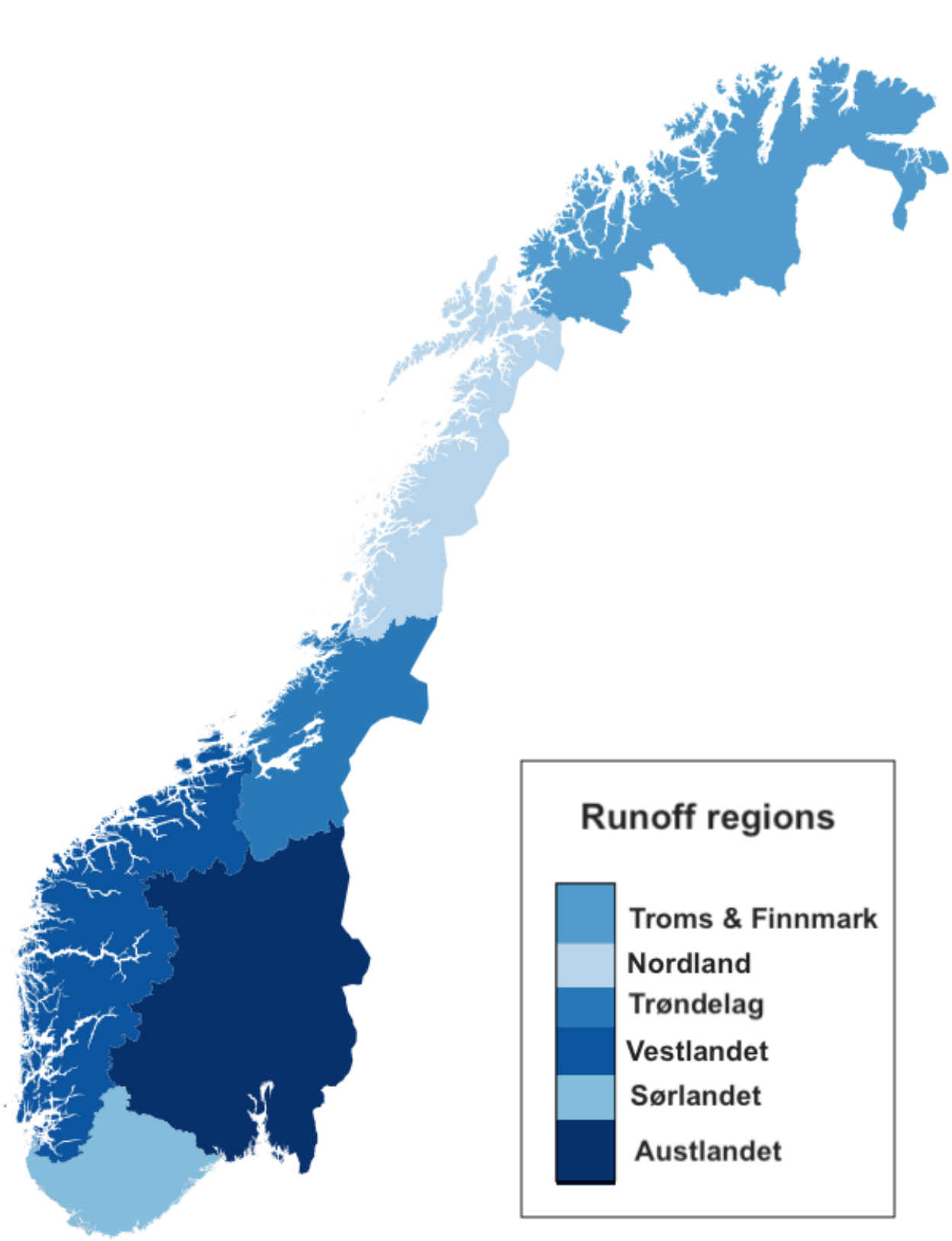

Figure 2.1: Runoff regions of Norway defined by NVE. Shapefiles downloaded from https://nedlasting.nve.no/gis/

2.1 Norwegian hydroclimatology

2.1.1 Mean temperature and precipitation

Mean annual air temperature [°C] and mean annual precipitation [mm] over Norway for the current climate normal period 1991-2020 can be seen in Figure 2.2. The mean temperature (Figure 2.2a) is lowest in the mountainous areas in the middle of southern Norway and inland Troms and Finnmark, with temperature below 0°C. The warmest mean temperatures during this period (at between 6-10 °C) can be seen along the coast of southern Norway, especially Sørlandet and Austlandet. There is a north-south gradient in temperature, with generally lower temperatures in the northern part of the country. This is due to the large difference in latitude, resulting in different amounts of solar radiation. Temperatures in the north are generally higher along the coast due to the Gulf Stream, an ocean current bringing warm, tropical water from the Mexican Gulf. This explain the west-east gradient in mean temperatures (Ketzler et al., 2021).

Mean annual precipitation (Figure 2.2b) is highest at the western coast in southern Norway, especially in Vestlandet and Sørlandet, with some high precipitation areas in Trøndelag and Nordland. Purple values are mean yearly precipitation above 2000 mm. The areas of Norway experiencing the least mean precipitation are inland Troms and Finnmark, and Austlandet, with mean values below 750mm per year. Precipitation is high along the coast of Norway due to its nearness to the Atlantic ocean and the rain currents the ocean brings in. This is why there is a clear rainfall gradient from west to east. Bergen, a city at the cost of Vestlandet, had a mean annual precipitation of 2300 mm in the past normal period 1961-1990, while Dovrefjell, a mountain area in Austlandet had less than 500 mm during the same period (Ketzler et al., 2021).

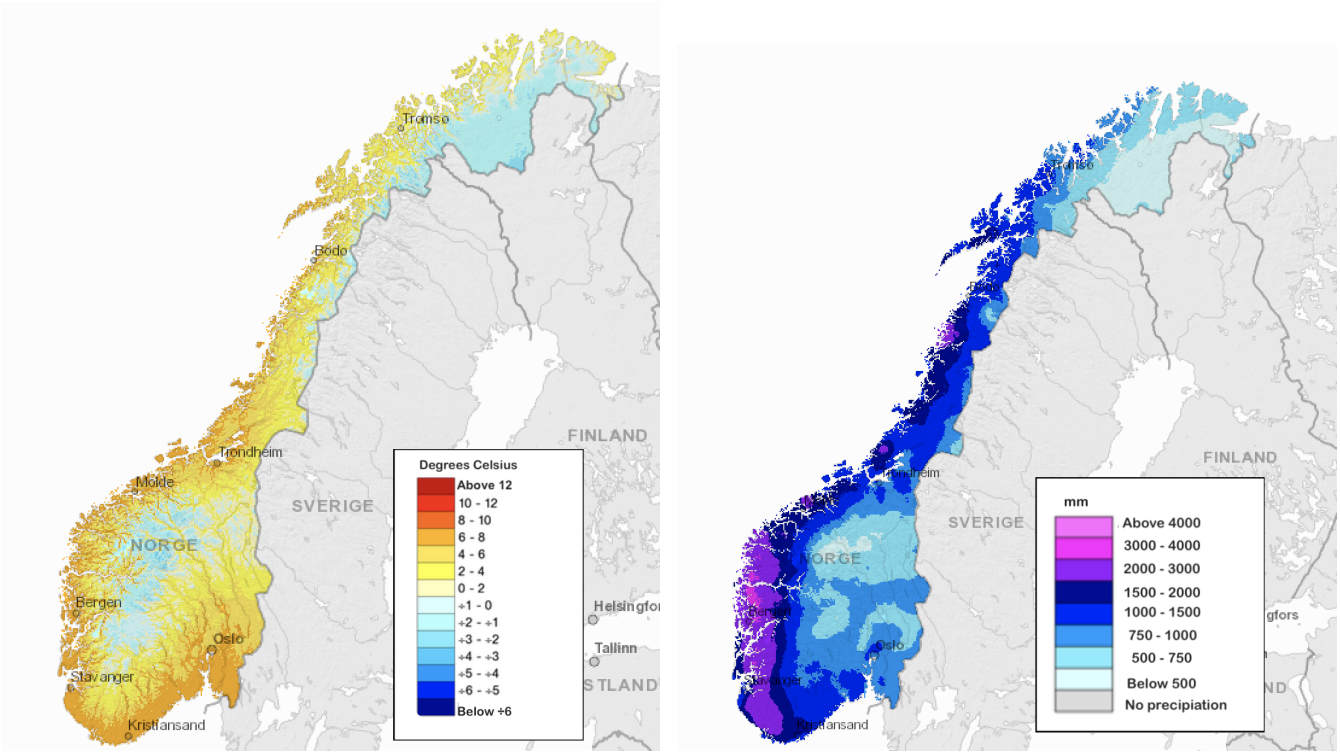

(a) (b)

Figure 2.2: Mean annual temperature (a) and precipitation (b) over Norway for the period 1991-2020 collected from seNorge.no. Retrieved 05.05.2022 from https://www.senorge.no/map

2.1.2 Hydrology of Norway

Due to the large differences in mean temperature and precipitation in the country, Norway have different streamflow patterns depending on the location in the country, hence the runoff regions in Figure 2.1. The regions are divided by main runoff generating processes and mean daily runoff (Hanssen-Bauer et al., 2017). Figure 2.3 shows the mean annual runoff map for the past normal period 1961-1990. It largely follows the precipitation map in Figure 2.2b, with Vestlandet and Nordland having the highest runoff values, above 1500 mm per year. The areas of Norway who showed the least annual precipitation and temperature are also the regions with the lowest annual runoff, below 600 mm per year. Figure 2.4 show mean runoff divided by the four seasons. Vestlandet and coastal Nordland has a high level of runoff throughout the year. The country experience most runoff in the spring, followed by autumn. The winter is the season with the least runoff for most of the country.

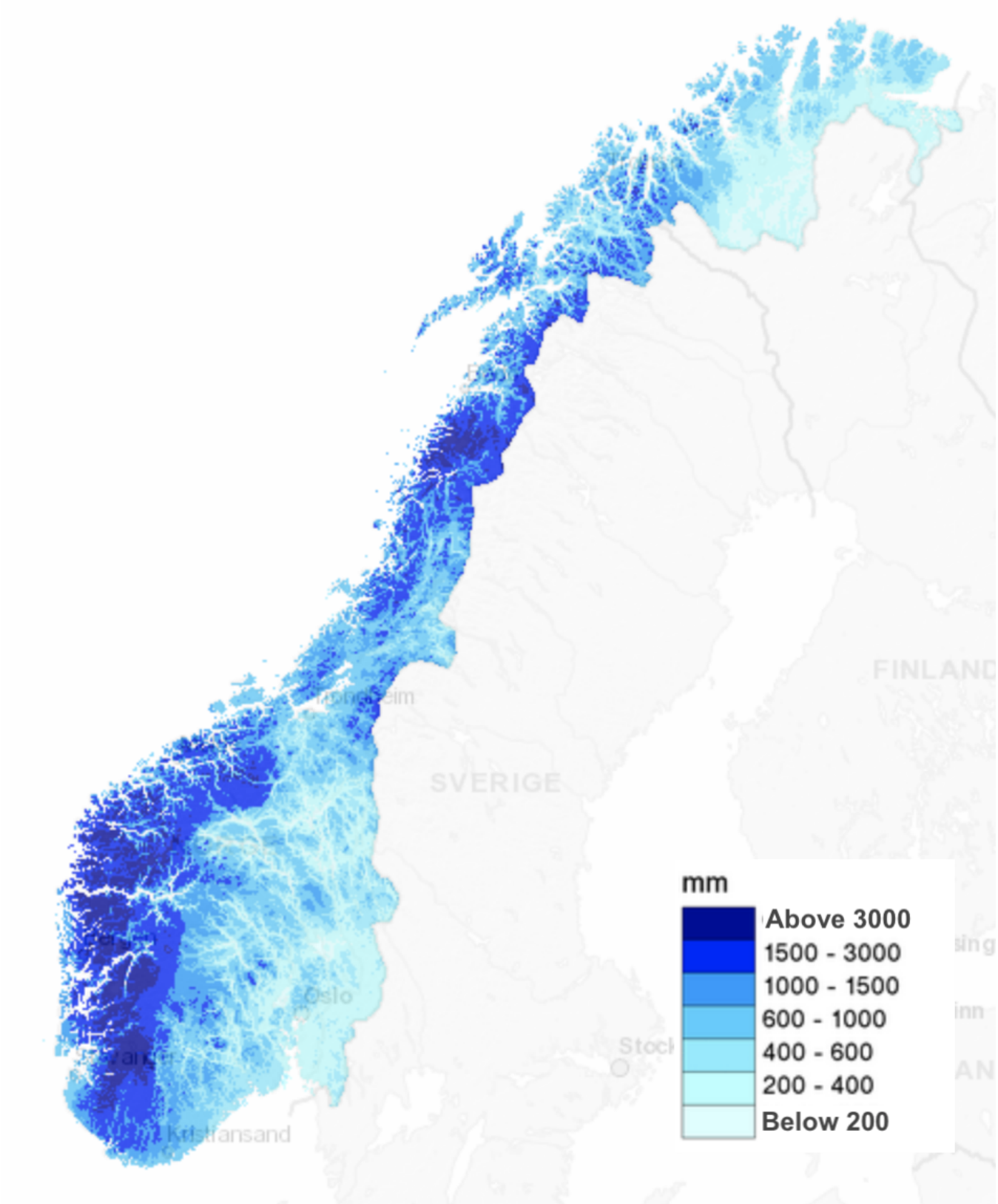

Figure 2.3: Mean annual runoff over Norway during the period 1961-1990. Figure from retro.seNorge.no. Downloaded 05.05.2022 from http://retro.senorge.no/?p=klima

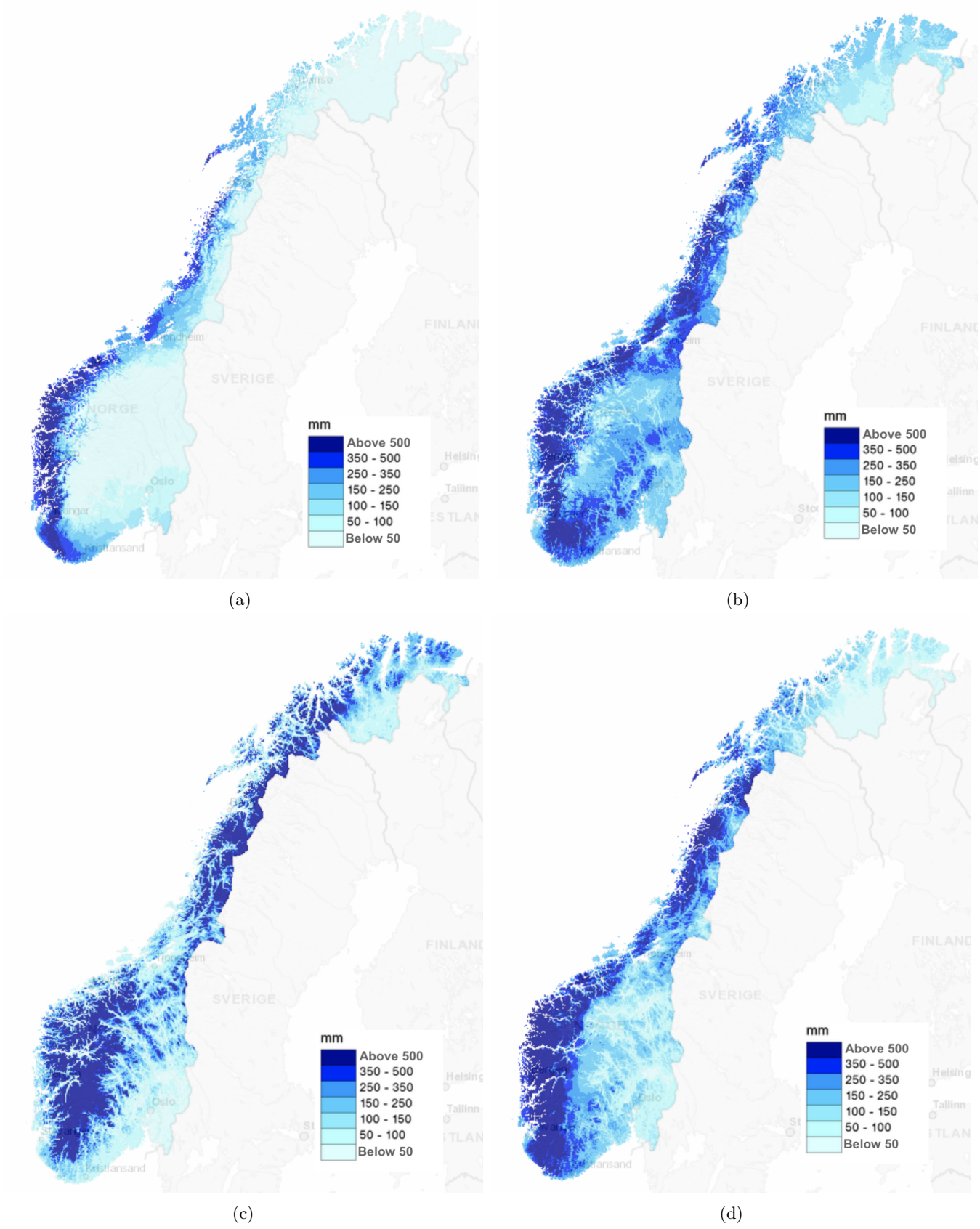

(a) (b)

(c) (d)

Figure 2.4: Mean winter (December-February) runoff (a), spring (March-May) runoff (b), summer (June-August) runoff (c) and autumn (September-November) runoff over Norway for the period 1961-1990. Figures from retro.seNorge.no. Retrieved 05.05.2022 from http://retro.senorge.no/?p=klima

2.2 Data

This section describes the data used for the analysis in this thesis and where the data is from. In this thesis, climatic data including precipitation, temperature, evaporation as well as different snow data have been used. The precipitation and temperature are provided from the Nordic Gridded Climate Dataset (NGCD). This is a dataset made based on gridded precipitation and temperature data from the seNorge dataset, but while the seNorge dataset varies in number of stations and station density during its time period, the NGCD consist of a fixed number of stations (CCCS, 2018). The other climatic characteristics are collected from the seNorge snow model or the Gridded Water Balance model (GWB). The GWB is a model calculating the water balance over square grid cell landscape elements, and is based on the Hydrologiska Byråns Vattenbalansavdelning model (the HBV model) (**Roald2006**; Beldring et al., 2003; Bergström, 1995).

2.2.1 Climate data

Evaporation

Evaporation is calculated based on the GWB model (Beldring et al., 2003). This model is a grid-based version of the hydrological model HBV (Bergström, 1995). It performs water balance calculations on a grid of 1x1 km characterized by altitude and land use. It runs on daily time steps with daily mean air temperature [°C] and daily precipitation total [mm] as input variables. The evaporation data collected for this study were forced with seNorge1 data. It considers seasonally varying effects from vegetation on potential evapotranspiration (**Roald2002**)). The data were provided to the author by NVE.

Snow

All climate characteristics concerning snow were provided from the seNorge snow model v1.1.1, forced with seNorge2018 data. This snow model is a revised model, following the first version of the seNorge snow model, v1.1, which was launched in 2004 by NVE with the help of the Norwegian Meteorological Institute (MET) and the Norwegian Mapping Authority (T. M. Saloranta, 2012). The input forcing is daily mean air temperature [°C] and daily sum of precipitation [mm], and the main modules consist of the Snow Water Equivalent (SWE) model for snow pack water balance and the snow compaction and density routine. The SWE model is based on the HBV models' snow routine. The SWE model calculates if precipitation falls as liquid or solid (D.1 and D.2), the daily melt rate or refreezing (D.3-D.5), ice content and potential and actual liquid water content in the snow (D.6-D.8), SWE (D.9) and the runoff out of the snow pack (D.10). The snow compaction and density routine are used to convert the SWE to snow depth (SD) using three steps, net decrease in SWE due to melting, compaction of the snow pack due to weight of new snow and finally the combination of these with a gradual compaction due to snow being a viscous medium. The steps are

further explained in Appendix D, equations D.11-D.15.

The snow model v1.1.1 consists of several revisions (improvements) to the original v1.1 model, including a revised melt rate and calculation for SWE and snow density. Melt rate was revised for the snow model v1.1.1 with the help of approximately 3350 observations from 31 snow-pillow stations across Norway, providing melt rates from daily snow water equivalent time series (T. Saloranta, 2014). This was also used to develop a temperature-independent melt term, which only depend on solar radiation (A.16). Also in the seNorge snow model v1.1.1, a sub grid variability within the 1x1 km grid cells was added, to better describe the spatial variability in snow distribution. Based on 580 observations from approximately 200 snow stations of SWE and snow density, the calculations for these were adjusted, and main adjustments were related to reducing precipitation falling as snow with higher elevation and revising the snow compaction and density routine.

From the snow model three characteristics are used in this thesis: total snow depth (SD) [mm], snow melt (M) [mm], and snow water equivalent (SWE) [mm]. All three characteristics are given as a grid covering the whole of Norway with spatial resolution of 1x1 km. The data were provided to the author by NVE.

Precipitation and temperature

The seNorge2018 dataset is a collection of observational gridded daily values for precipitation and minimum, mean and maximum temperature, covering the whole of mainland Norway, as well as a strip of land expanding into Russia, Sweden, and Finland to reduce boundary effects (Lussana et al., 2019). It originally contained data from 1957 to 2017 and is updated continuously. It is a high-resolution dataset with a 1x1 km grid, where the precipitation and air temperature data are 24h averages between 06:00 UTC of the current day and the previous day. The core statistical interpolation method is optimal interpolation and the gridded analysis produce areal averages where for each grid point a weighted average of nearest observations are calculated. The larger the extensions of the spatial support for these averages, the lower the effective resolution of the analysis fields and the larger the uncertainty in areal estimates.

The input data is in situ observations from MET's measuring stations covering Norway, and some from the bordering countries from the European Climate Assessment and Dataset. The precipitation data has been adjusted for wind-induced under-catch. The seNorge observational data is based on measuring stations for precipitation and temperature but are not always based on a fixed set of stations. In fact, this number changes notably during the period 1957 to 2017, with the number of temperature stations being twice as high in 2017 as in 1957 (Lussana et al., 2019). Northern and southern Norway also has a difference in station density, with a higher density in southern Norway, making the data perform better than in the north. In the article documenting seNorge2018, Lussana et al.

(2019) warn users of the dataset to be aware since "variations in the observational network over time will affect temporal trends derived from this dataset". To combat this, a dataset known as the Nordic Gridded Climate Dataset (NGCD), was made. This dataset is based on seNorge2018 and consists of high-resolution observational gridded daily precipitation and temperature data from a fixed set of observations to ensure time consistency. The dataset covers all of Norway, Finland and Sweden (Fennoscandia) for the period 1957-present, with a spatial resolution of 1x1 km. The NGCD comes in two versions – type 1 and type 2 – based on different spatial interpolation methods used to produce the datasets. In this study the NGCD Type 2 dataset is used since it is based on the same statistical interpolation method used to create the seNorge2 datasets (CCCS, 2018; Lussana et al., 2018).

The NGCD is updated every half year. In this study data from v20.05 (version uploaded May 2020) are used for the first half of our study period 1981-2000, and the latest version, v21.09, is used for the data 2001-2020. This is for practical reasons, since the v20.05 contain a compressed file including all data from 1981-2000, while the rest of the years from 2001 till today must be downloaded one by one. The NGCD data was downloaded from the MET Norway Thredds service
(https://thredds.met.no/thredds/catalog/ngcd/catalog.html) (CCCS, 2018).

2.2.2 Discharge data

Data used for the high and low flow analysis were daily discharge $[m^3 s^{-1}]$ data from the Norwegian Water Resources and Energy Directorate (NVE), the national institution for hydrology. The discharge data was downloaded from NVE's Hydrological database Hydra II, using their API named HydAPI to collect the data. Selection of which gauging station data should be used in this thesis was based on a reference dataset. NVE published the first hydrological reference dataset for climate change studies (HRD) in 2013 (Fleig et al., 2013). Since then, the dataset was updated in 2017 (unpublished), and in late 2021 the dataset was again updated using a new methodology for identifying which stations are fit for the different types of data analysis (Dahl & Pedersen, 2021).

The HRD is a collection of measuring stations across Norway with long time series and good data quality for catchments which are little to not affected by human activity. The current version consists of 157 active and unregulated streamflow stations in Norway. The streamflow data in the HRD are collected from NVE's Hydra II database. To be chosen as a reference station, the measuring station and its catchment must follow these criteria: the catchment must have less than 10% urban area, the catchment must be unregulated, the time series must include at least 20 years of good quality data, the station must be an active data collecting one, and the data must be accurate with adequate metadata (Dahl & Pedersen, 2021).

For this analysis I wanted to select measuring stations that fulfill the following criteria: daily discharge data; suitable for studying high and low flows both summer and winter; no land use change in the catchment; the start of daily data record in the HRD were in the latest in 1990. Since the purpose of this thesis is to study changes in flow affected by climate change, a period of at least 30 years is needed, since this is the recommended data length for climate studies (Fleig et al., 2013). By following these criteria using the old HRD, I got a dataset containing 123 catchments with data over the period 01.01.1991-31.12.2019.

In this analysis I first wanted to use the updated HRD from 2021. However, this dataset included fewer catchments recommended for both high flow and low flow studies, and especially fewer stations recommended for low flow studies. As a result a compromise was made. I decided to use mainly stations recommended from the original HRD from 2013, but cross-referenced with the new dataset from 2021. If a station recommended in the old HRD was no longer included in the new HRD, it fell out of my dataset. If a new catchment previously not included in the HRD from 2013, but now included in HRD 2021 and suitable for my study, it was included into my dataset. This resulted in a dataset with daily discharge data from 123 gauging stations. All catchment locations can be seen in Figure 2.5 and their respective area and gauging station coordinates are listed in Appendix A.1.

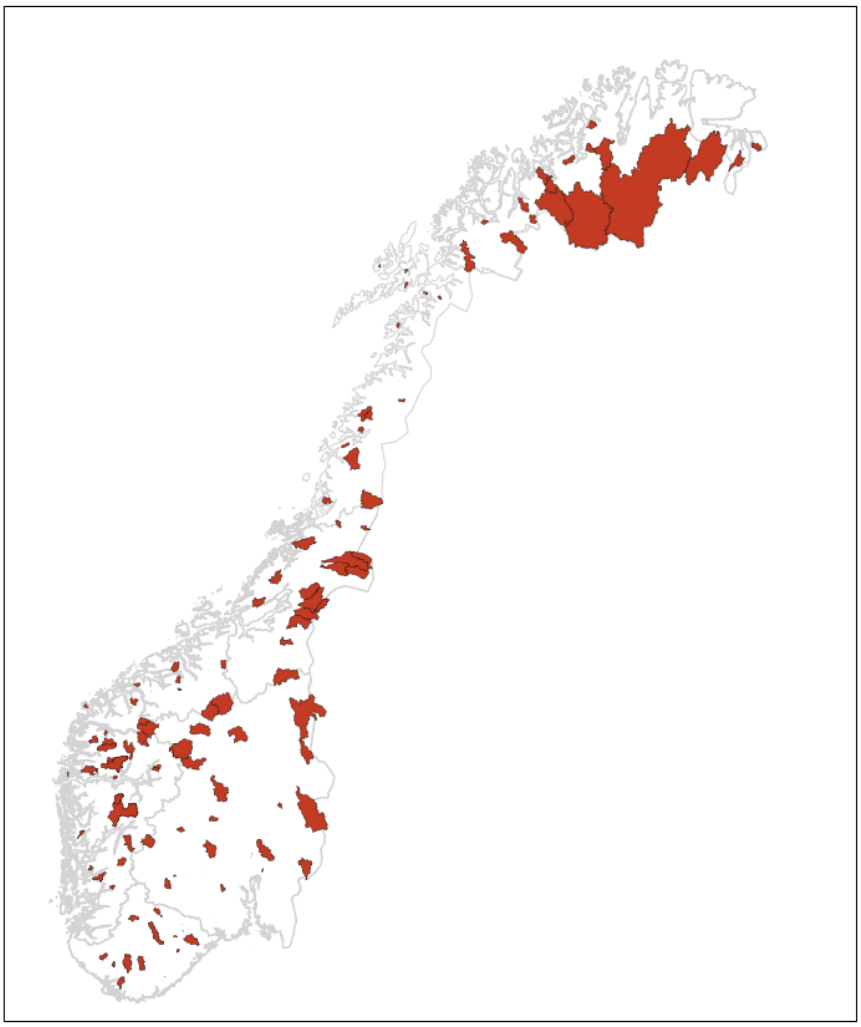

Figure 2.5: The catchments used in this thesis. Catchment shapefiles were downloaded from NVE's shapefile downloading webpage https://nedlasting.nve.no/gis/.

2.2.3 Catchment characteristics

Along with the discharge dataset, catchment characteristics belonging to each of the catchments in Figure 2.5 were collected from NVE's HydAPI. A list of all characteristics can be seen in Table 3.1. Notable characteristics, which can also be seen in Figure 2.6, are minimum and maximum height above sea level [m.a.s.l.], percentage of glacier within the catchment and the catchment length [km]. The rest of the catchment characteristics are presented in Appendix C (Figure C.1 and C.2).

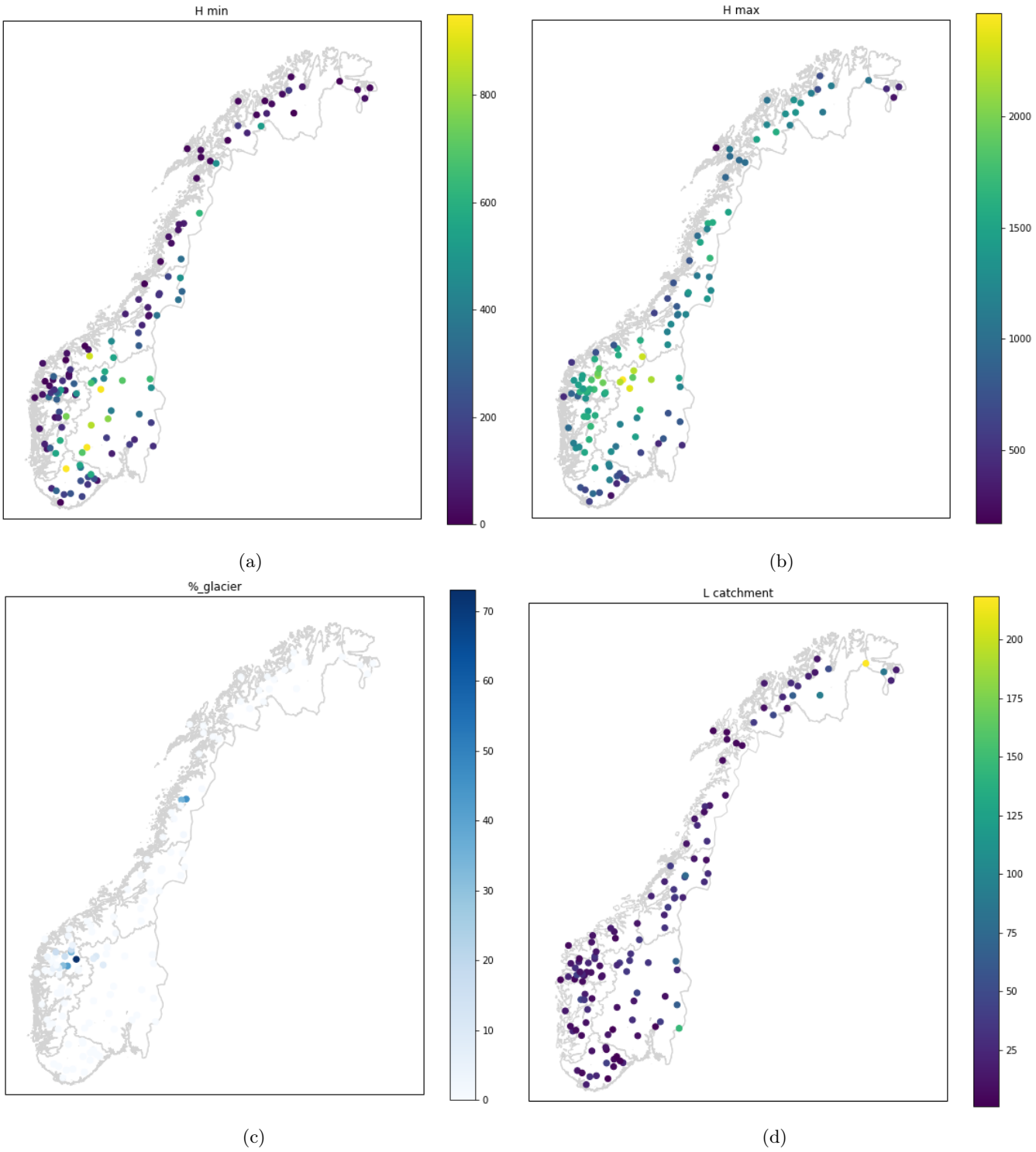

Figure 2.6: Four characteristics for each catchment. (a) minimum catchment height [m.a.s.l], (b) maximum catchment height [m.a.s.l.], (c) percentage glacier within the catchment [%] and (d) catchment length [km].

3 Methods

All calculations and figures are made using Python and Jupyter Notebook. The Python version used is mainly 3.9.4, downloaded from Anaconda Inc. The trend analysis was done using the Mann-Kendall method using the Python package pymannkendall (Hussain, 2019). To visualize the results in maps, map data from naturalearthdata.com (Natural Earth) and NVE's HydAPI was applied, as well as the python packages geopandas and cartopy. Machine learning methods were done using python packages from SciKit Learn (Pedregosa et al., 2011). The code is available on GitHub, following the link in Appendix E.

This section will be structured as seen in Figure 3.1. Catchment characteristics have already been introduced in Section 2.2.3, while climate indices and moving averages of discharge will be presented in Section 3.1 and 3.2, respectively. Trend calculation is presented in Section 3.3. The rest of the schematic follow the machine learning process and is explained at the start of Section 3.4.

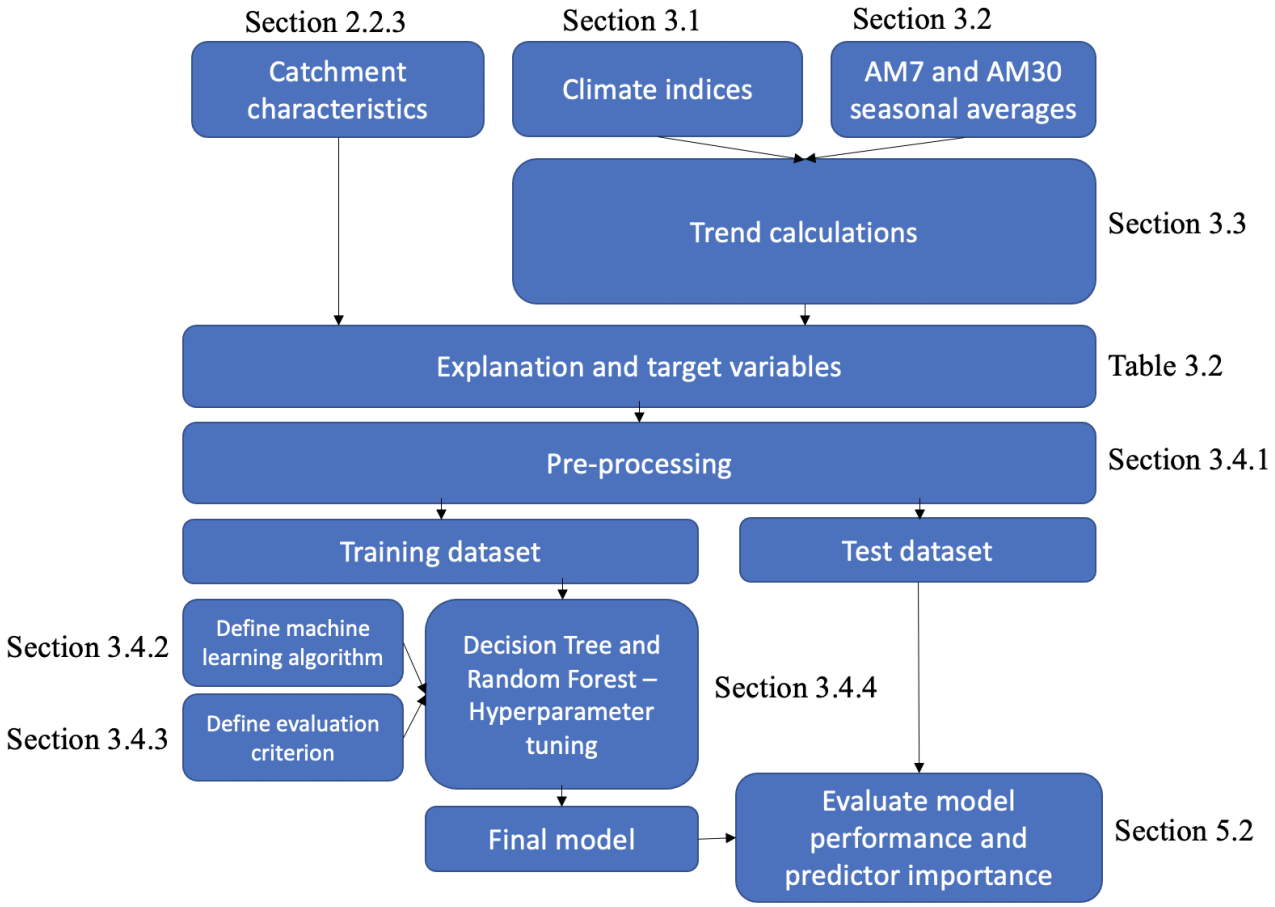

Figure 3.1: Schematic description of the Method structure.

3.1 Climate indices and catchment descriptors

The term climate indices refer to all data describing long term statistical properties of meteorological and hydrological variables. The indices used in this thesis can be seen in Table 3.1 together with their respective trends and catchment characteristics. The climate indices comprise mean annual precipitation [mm/yr], mean annual air temperature [°C/yr], annual maximum snow depth [mm/yr], mean daily snow melt [mm], mean daily snow water equivalent [mm], precipitation as rain [mm] and evaporation [mm]. Additionally, mean annual specific discharge and its 95% and 5% exceedance frequencies are included.

Mean annual precipitation, temperature, evaporation and the snow indices were calculated based on daily values. Maximum (minimum) annual precipitation and temperature was calculated by picking the highest (lowest) value out of each year within each catchment. The snow indices were calculated over the hydrological year starting in the year before, e.g. maximum snow depth for 1991 were calculated based on the snow depths of the hydrological year starting 01.10.1990-31.09.1991.

All these data sets were originally large gridded (1x1km) files covering the whole of Norway. For each of these climate

Table 3.1: Table containing the catchment characteristics and climate indices used in this study.

Catchment descriptors and climate indices					
Catchment descriptors		Climate indices		Trends in climate indices	
Area	[km^2]	$\bar{T}$	[°C/year]	$\bar{T}$ trend	[-]
Longitude	[-]	$\bar{T}_{min}$	[°C/year]		
Latitude	[-]	$\bar{T}_{max}$	[°C/year]		
% agriculture	[-]	P	[mm/year]	P trend	[-]
% bog	[-]	P_{min}	[mm/year]		
% lake	[-]	P_{max}	[mm/year]		
% effective lake	[-]	Mean SWE	[mm]	Mean SWE trend	[-]
% forest	[-]	Mean SM	[mm]	Mean SM trend	[-]
% mountain	[-]	Mean SDmax	[mm/yr]	Mean SDmax trend	[-]
% glacier	[-]	Mean E	[mm]	Mean E trend	[-]
% urban	[-]	$\bar{Q_s}$	[m/s]	$\bar{Q_s}$ trend	
H_{min}	[m.a.s.l.]	$\bar{Q}_{s,95}$	[m/s]	$\bar{Q}_{s,95}$ trend	
H_{max}	[m.a.s.l.]	$\bar{Q}_{s,5}$	[m/s]	$\bar{Q}_{s,5}$ trend	
$L_{catchment}$	[km]				

indices, the grid cells within each catchment were masked out and averaged using shapefiles of the catchment borders obtained from NVE's HydAPI and the python package regionmask (https://regionmask.readthedocs.io/en/stable/). This resulted in each catchment having their own set of daily time series, one for each hydrological variable.

Mean annual specific discharge is calculated by first finding the annual mean of the daily discharge values, before dividing these values on the catchments' area. The exceedance frequencies are found by calculating a flow duration curve for each catchment, and deriving the 5% and 95% percentiles of the curves, respectively.

3.2 High and low flow definition

In this analysis we want to find where the lowest (highest) flow during chosen periods of the year occurs and find the trend over these values to see of the magnitude of low (high) flow in Norway has changed. An often-applied method for this type of analysis is the annual minima (maxima) series method – the AMS – as it is used to determine the minima (maxima) flow over a given X-day period per year (Hannaford & Marsh, 2006; Stahl et al., 2010; Wilson et al., 2010). This method is used to remove short-term fluctuations from the data set, as well as uncertainty in the measurements, to better study the general behavior (WMO, 2009). Two smoothing intervals were used, the 7-day minima (maxima) annual series and the 30-day minima (maxima) annual series.

Before starting the analysis in trends of low and high flow for the different catchments, the discharge measurements for the catchments were divided into different periods based on when in the year the lowest (highest) flow occurs. A divide between summer low flow and winter low flow is made based on the generating process behind the flow pattern. Winter low flow is caused by precipitation falling as snow and being stored in the catchment

as snow and ice, or frost in the ground keeping precipitation from reaching rivers, while summer low flow occurs based on the combination of less precipitation and higher evapotranspiration, or low storage of water in the soil and low groundwater levels. Previous studies have shown that the period with snow on the ground in Norway is mainly between October and May (Rizzi et al., 2017). Based on this, we split into two low flow periods as follows: winter low flow in the snow season between October-May, while summer low flow is in the (mostly) snowless season between June-September. This resulted in four periods of minimum flow: $AM(7)_{low,summer}$, $AM(30)_{low,summer}$, $AM(7)_{low,winter}$ and $AM(30)_{low,winter}$

The high flow is divided between the flood generating processes: snowmelt or rainfall. In Norway the snowmelt season differs heavily based on the location in the country and the catchment characteristics. The snowmelt season had to be long enough to cover all snowmelt generated events, but not too long as to catch some of the rainfall generated events in late summer/early autumn. As well, the rainfall season had to include the rainfall generated events in early autumn and mid-winter. The chosen periods are therefore between March-July for the spring high flow, while summer/autumn high flow are between August-February. This resulted in four periods of minimum flow: $AM(7)_{high,spring}$, $AM(30)_{high,spring}$, $AM(7)_{high,autumn}$ and $AM(30)_{high,autumn}$

3.3 Trend calculations

To calculate the trends for high and low flow, as well as the climate indices and mean streamflow, the Mann-Kendall trend test was applied. The trends' slope is estimated by the Theil-Sen slope estimation method. The trend and slope estimation methods were chosen since they are widely used in literature to find trends in hydrological data (Hannaford & Marsh, 2006; Stahl et al., 2010; Wilson et al., 2010).

The Mann-Kendall test is based on correlation between the rank and order of points in a time series (Kendall, 1975; Mann, 1945). The test looks for a trend by the relationship between the Mann-Kendall score S and its standard variance σ_s. One first find the score S by summing all consecutive values in the data series, and if this value is positive or negative.

$$S = \sum_{i=1}^{n-1} \sum_{j=i-1}^{n} Sgn(X_j - X_i) \tag{3.1}$$

Where $X_j - X_i$ are two sequential data points, and n is the length of the data series.

$$S = \sum_{k=1}^{\frac{n(n-1)}{2}} \begin{cases} -1 & \text{if } \theta < 0 \\ 0 & \text{if } \theta = 0 \\ 1 & \theta > 0 \end{cases} \tag{3.2}$$

Where $\theta = X_j - X_i$. The variance σ_s of S is found by:

$$\sigma_s = \frac{n(n-1)(2n+5)}{18} \tag{3.3}$$

It then checks if the standardized test statistic Z_s is not equal to zero and if the absolute value of Z_s is larger than the significance level. If both are true, there exists a trend in the direction given by the sign of Z_s.

$$Z_s = \begin{cases} \frac{S-1}{\sqrt{\sigma_s}} & \text{if } S > 0 \\ 0 & \text{if } S = 0 \\ \frac{S+1}{\sqrt{\sigma_s}} & \text{if } S < 0 \end{cases} \tag{3.4}$$

Theil-Sen slope estimator is used to find the median of all slopes m_k of consecutive pairs of values (Stahl et al., 2010):

$$m_k = \frac{(X_j - X_i)}{(t_j - t_i)} \tag{3.5}$$

In this trend analysis, the 5% significance level was first used, and if this significance level yielded few or no significant trends, a 30% significance level was applied additionally. A 5% (30%) significance level means there is below 5% (30%) probability of wrongly rejecting the 'no trend'-hypothesis which is the null hypothesis of the test. The Mann-Kendall test variation used in this thesis is a two-tailed test, meaning the critical area of the distribution is two-sided, and tests whether the sample is greater than or less than a certain range of values. The result of this test is either the null hypothesis 'no trend', an increasing trend or a decreasing trend.

Since there is a slight probability of wrongly assigning trends where there should be none, trends in clusters will have more weight than single trends in an area. When the chosen significance level is high (5%), the trends are more reliable. Positive trends show an increase in the value of interest, while negative trends show decreases. All trends are calculated over the period 01.01.1991 – 31.12.2019.

3.4 Trend Attribution using Machine learning

The following section will be divided as seen in the second part of Figure 3.1. Firstly the predictors used in the machine learning will be pre-processed and split into a train set and a test set. Then the machine learning algorithm and evaluation criterion will be chosen, before we have a final algorithm to use on our data.

Table 3.2 show all trends calculated over the two smoothing averages, 7-day and 30-day AMS. The seasonal AM

Table 3.2: All values present in the table used in machine learning. Yearly trend results are only used as explanation variables. Seasonal trend results are used as target variables as well as explanation variables.

Trends	
AM7yearly 5%	AM30yearly 5%
AM7summer 5%	AM30summer 5%
AM7winter 5%	AM30winter 5%
AM7spring 30%	AM30spring 30%
AM7autumn 30%	AM30autumn 30%

trends will be the ones predicted by the machine learning methods (target variables), and the yearly trends will only be used as predictors (explanation variables).

3.4.1 Selecting predictors and preprocessing

When all the trend calculations were complete, the results were collected in a table together with the catchment characteristics of each catchment. This resulted in a table with 123 rows (number of catchments) and 33 columns (number of parameters - predictors and target variables). However, some catchments failed to produce masked climate indices through the process described in Section 3.1, resulting in a need to shorten the dataset to 105 catchments. The catchment characteristics and climate indices were used as explanation variables, or predictors. Trend results could be used as both target variables and predictors based on what aspect was aimed to be the predicted. The AM7 trends were not used as predictors for the AM30 trends of the same index/variable, as these are too similar and would stump the machine learning, since the algorithm would use the other as main predictor and get a good accuracy score without testing other predictors.

To see if any of the predictors were unfit to be used as predictors for any of the trends, the correlation between each variable in Table 3.1 and Table 3.2 is calculated. Correlation is calculated based on the Pearson method, which measure the linear association between the predictors. Correlation is given on a scale of -1 to 1, where -1 is complete negative correlation, 0 is no correlation and 1 is complete positive correlation, or all data points lying exactly on a line.

In machine learning we want to avoid overfitting our data. Overfitting is when the model is too well-fitted to the training dataset, to the extent that it negatively affects the performance of the model on new data. To prevent

this our dataset is split into a training dataset and a test dataset. The split was done in a 67%/33% split. This mean 67% of the catchments were put as training catchments, and 33% of catchments are test catchments. This was done by using the train_test_split function from the sklearn python module (Pedregosa et al., 2011).

When the trend direction results are used as target variables, this machine learning problem is a classification problem. The result of the trend is one of three possibilities: an increasing trend, a decreasing trend, or no trend. We want to have approximately equal proportion of each result class ("no trend", "increasing", "decreasing") in my training and test datasets, to ensure the model will be equally good at predicting the different classes. The "stratify"-argument in the train_test_split makes sure this is fulfilled. One class – the "no trend" - will always be larger than the other two since most of the catchments selected got this result.

It is possible to split the dataset in three parts to combat the possibility of overfitting, with the third part as a validation dataset. However, our dataset is already short for a machine learning dataset, and even fewer values in the training dataset will lead to poor fittings to any model.

3.4.2 Machine learning algorithm

I applied the decision tree classifier method (DT), which is a non-parametric supervised learning method. The goal of a DT is to create a model that predicts the value of a target variable by learning simple decision rules inferred from the parameters. It uses a set of if-then-else decisions to learn from the training data, as illustrated in Figure 3.2. This splits the dataset by the different parameters and their values, and the deeper the tree is, the more accurate to the dataset it typically is. This is where the danger of overfitting lies, as the deeper the tree, the better the fit, but it is more prone to overfitting. To combat this, we can prune the tree – cutting some of the decisions it makes before the result – or set a maximum depth to the tree.

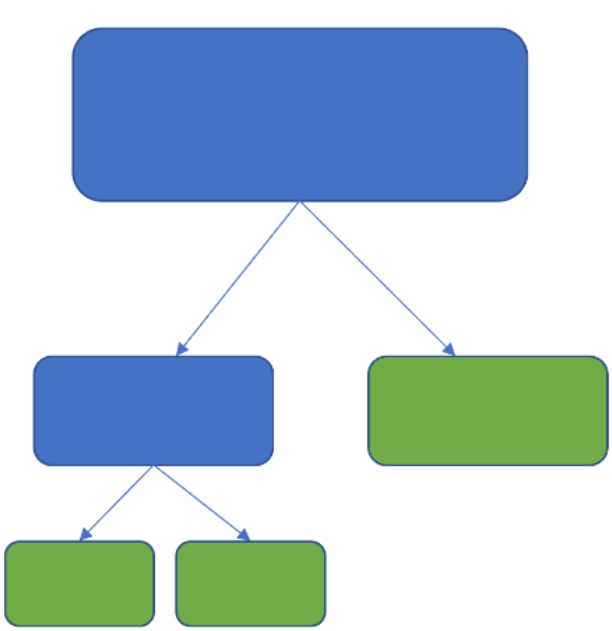

Figure 3.2: Schematic description of a Decision Tree. The top box is called the root node, and is the first split in the tree. If the statement in this box is false, it moves right, to the right branch of the tree. If the statement in the root node is true, it moves to the left branch of the tree. Green boxes in this figure is the leaf nodes, where the final decision of the branch is made.

Additionally, the random forest method (RF) was applied as a second non-parametric supervised learning method. The RF method was first developed by Breiman (2001) and consists of several decision trees all predicting as a DT would, then selecting the best performing features from all trees in the "forest", making a final tree with the best prediction. The standard RF algorithm was used to predict the trend directions. This model come with number of estimators (number of DTs in the RF) of 100, a max depth of none and several other defaults.

3.4.3 Evaluation criterion

There are multiple ways to evaluate how effective a machine learning model is at estimating the model result. The method used in this thesis is the classification accuracy. The classification accuracy ranges from a score of 0 to 1, and gives the proportion of correctly predicted data points (i.e. the number of correctly predicted data points divided by the total number of predicted data points). Here, a higher return value is better than a lower return value, and a score of 1 is a perfectly predicted result.

3.4.4 Hyperparameter tuning

The default version of both models may perform well, but there is always something to tweak to make the models perform better at predicting. The accuracy of the models can be increased by tuning their hyperparameters. This is

done by using the randomized search cross validation, RSCV. Several hyperparameters were chosen for tuning with RSCV. Among these were number of estimators, max features, max depth, min split samples, min samples leaf and if the data should be bootstrapped or not.

3.4.5 Feature importance

To figure out which predictors show the most importance when predicting trends for each of the seasonal periods, feature importance for each predictor was calculated. This was done by using Scikit Learn's package feature_imporances_ (Pedregosa et al., 2011). Feature importance of a predictor is calculated by the mean and standard deviation of the impurity decrease the predictor brings to the split of the tree. The deviation is computed based on the gini impurity of the predictor.

4 Results

4.1 Trends

4.1.1 Yearly mean annual and seasonal streamflow trends

Trends in yearly mean streamflow $\bar{Q}$ are shown in Figure 4.1. Trends towards increasing streamflow is colored dark blue at 5% significance level (strong positive trend) and light blue at 30% significance level (weak positive trend). Trends towards decreasing streamflow is colored red at 5% significance level (strong negative trend) and orange at 30% significance level (weak negative trend). Most stations show no significant trend (green), but among the stations with 5% significant trends there is a clear divide between southern and northern Norway. All 5% significant positive trends can be found in southern Norway, where as 5% significantly negative trends are in northern Norway. There is a cluster of decreasing trends at the coast of Troms and Finnmark and two on the coast of Nordland. Of the significantly increasing trends, three are in Vestlandet, and all are stations with more than 30% glacier in its catchment (Figure 2.6c). The remaining increasing trend stations in southern Norway are in Sørlandet and Austlandet. For the 30% significance level, a similar trend pattern appears as for the 5% significance level, with weaker increasing trends clustered in the south and weaker decreasing trends in mid-Norway and the north. This further show the divide in streamflow trends between northern and southern Norway. The cluster of positive trends in Vestlandet has increased in number of stations, while several trends have shown up in Sørlandet and Austlandet. Some negative trends have been added to the cluster in Troms and Finnmark, while multiple additional negative trends are now present in Trøndelag and Nordland. Three negative trends are found near the coast of Vestlandet.

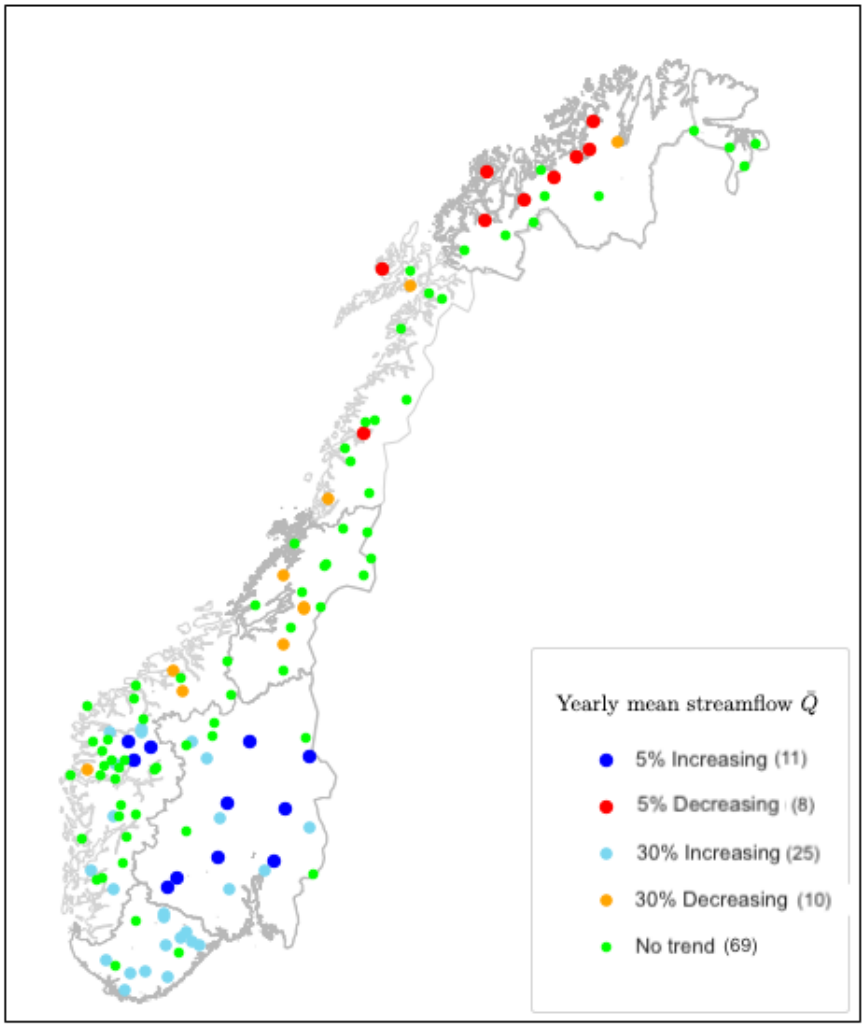

Figure 4.1: Yearly mean specific discharge trends for both the 5% and 30% significance levels, calculated over the period 01.01.1991-31.12.2019. Number in brackets indicate the number of stations with 5% increasing, 5% decreasing, 30% increasing, 30% decreasing, or no trend, respectively.

The trends showing up for $AM(7)_{year}$ and $AM(30)_{year}$ are almost identical (Figure 4.2), with the only difference in trends being one less catchment in Troms and Finnmark showing decreasing trends between the 7-day moving average (8) and 30-day moving average (7) period. Both show 10 increasing trends, all in southern Norway. The decreasing trends are found in Nordland and Troms and Finnmark, and match the pattern of 5% significant trends for mean annual streamflow $\bar{Q}$ in Figure 4.1.

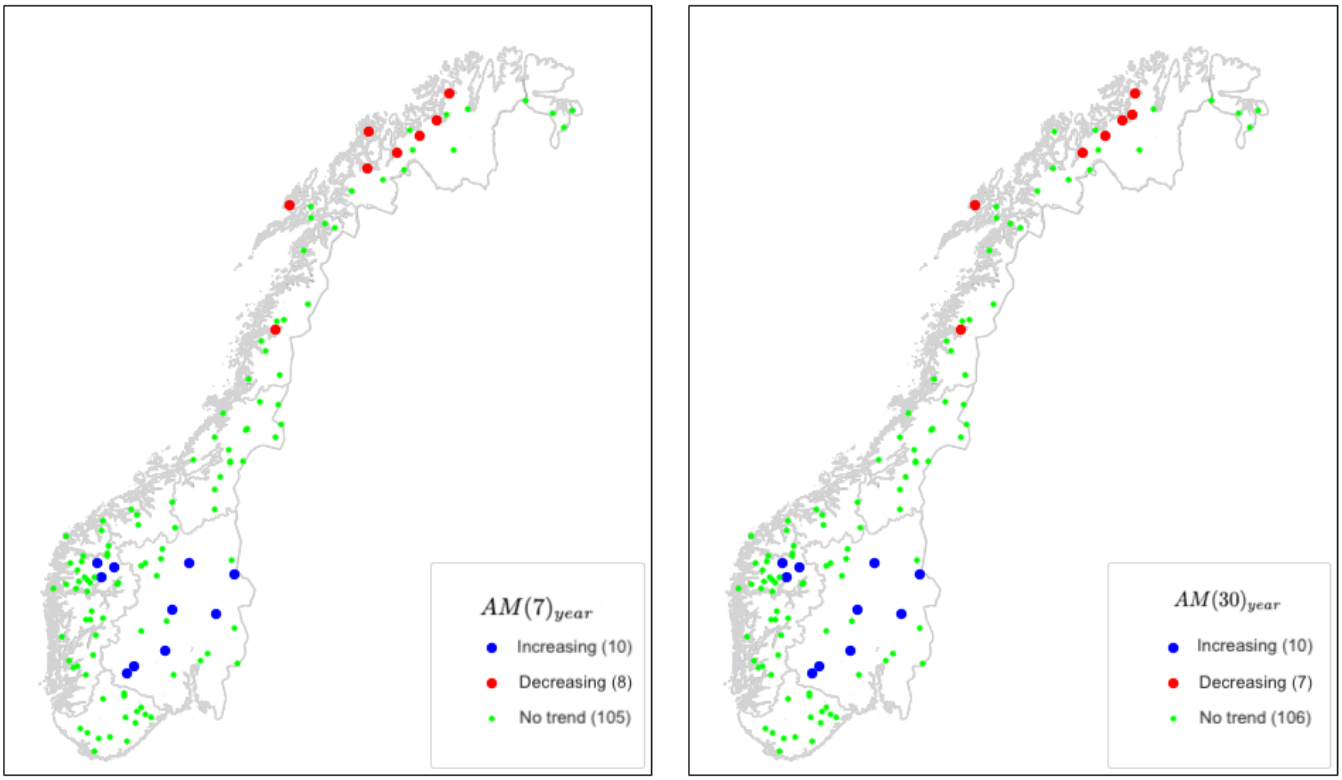

(a) (b)

Figure 4.2: Mean discharge trends for the 5% significance level calculated over the period 01.01.1991-31.12.2019 on a 7-day moving average (left) and on a 30-day moving average (right). Number in brackets indicate the number of stations with increasing, decreasing or no trend, respectively.

4.1.2 Seasonal trends in low flow

Figure 4.3a shows the trend results for the AM7 summer low flow ($AM(7)_{low,summer}$). As for mean flow there is a divide between southern and northern Norway, but there is a higher number of positive trends (18) and a lower number of negative trends (5). The negative trends are located in Trøndelag, north Nordland and Troms and Finnmark, where as the positive trends are scattered over southern Norway, most in Sørlandet and Austlandet.

Figure 4.3b shows the trend results for $AM(30)_{low,summer}$ (AM30 summer low flow). The same divide between north and south as the $AM(7)_{low,summer}$ can be seen. However, compared to $AM(7)_{low,summer}$, there are more negative trends (7) and less positive trends (16). Trends showing increasing streamflow have moved from being clustered in the middle of southern Norway to forming a larger cluster in Sørlandet, while two positive trends in Vestlandet have disappeared. Among the negative trends, one additional trend has appeared in Trøndelag and one in Nordland.

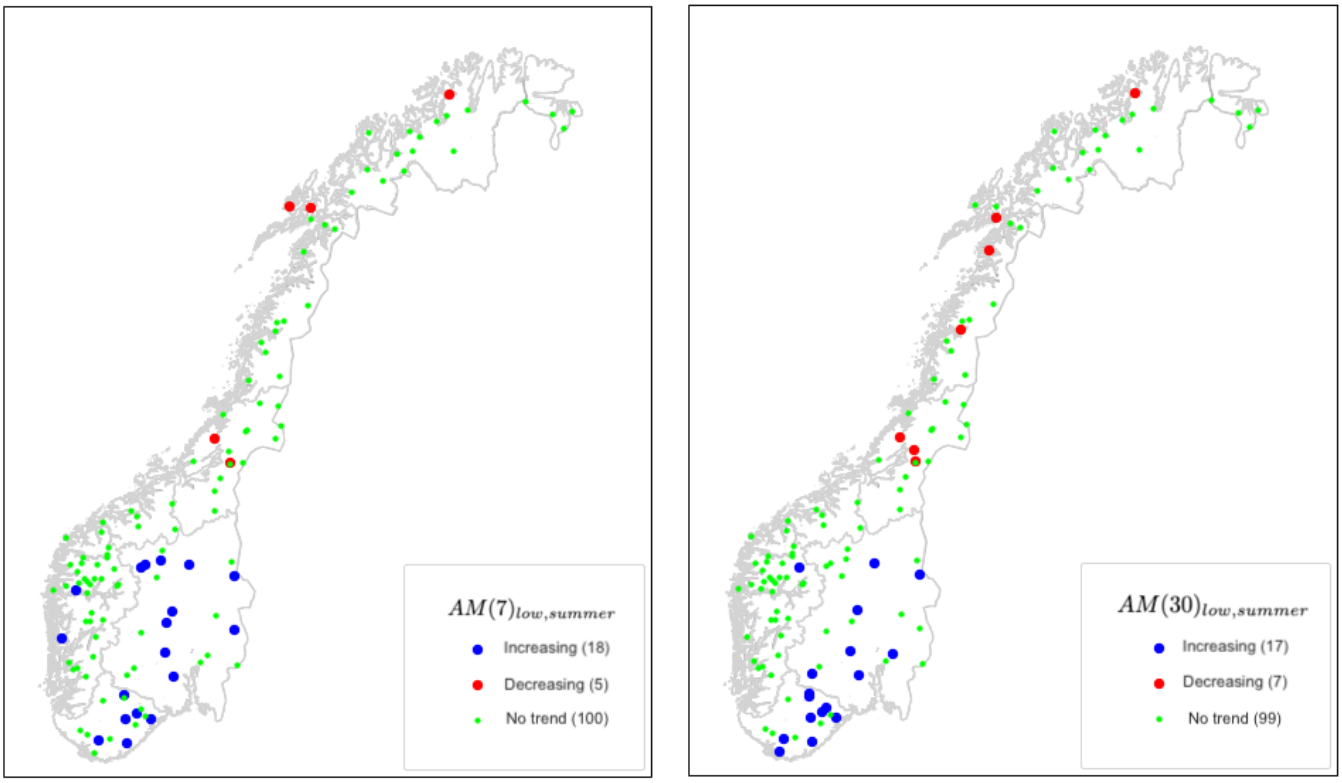

(a) (b)

Figure 4.3: Summer low flow trends calculated for the months June-September, over the period 01.01.1991-31.12.2019 with 5% significance level. Trends are calculated over a 7-day minimum moving average (left), or a 30-day minimum moving average (right).

Trends in AM7 winter low flow ($AM(7)_{low,winter}$) can be seen in Figure 4.4a. There are more trends showing increasing winter low flow (16) than decreasing (8). The negative trends are well distributed, one in Troms and Finnmark, two in north Nordland, two in mid-Nordland, one in Trøndelag and two in Vestlandet. One of the negative trends in Vestlandet is located at the station with ca. 70% glacier (76.5.0 in Table A.1 in Appendix A), while one in mid-Nordland belongs to a station with ca. 30% glacier (156.10.0 in Table A.1 in Appendix A). There is a cluster of positive trends in inland Troms and Finnmark and another cluster, although more spatially distributed, in south-eastern Norway.

The $AM(30)_{low,winter}$ (AM30 winter low flow) trends are similar, shown in Figure 4.4b, with two less significant positive trends and three less negative, equal to 14 positive trends and 5 negative trends. There are three less negative trends in northern Norway than for $AM(7)_{low,winter}$, while one negative trend has appeared closer to the negative glacier trend in western Norway. As for the positive trends, the one in western Norway is gone, as well as one in south Norway.

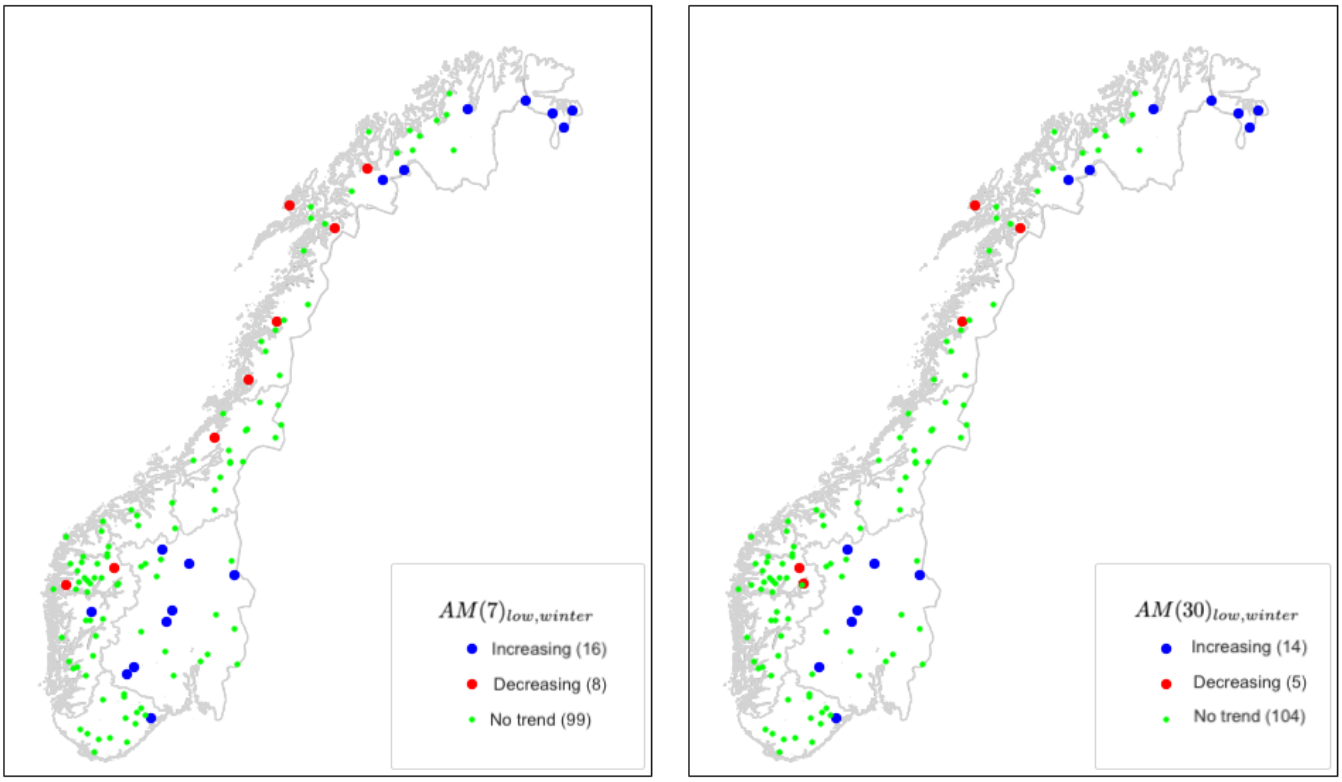

(a) (b)

Figure 4.4: Winter low flow trends calculated for the months October-May over the period 01.01.1991-31.12.2019 with 5% significance level. Trends are calculated over a 7-day minimum moving average (left), or a 30-day minimum moving average (right).

4.1.3 Seasonal trends in high flow

Trends for AM7 spring high flow ($AM(7)_{high,spring}$) is seen in Figure 4.5a, showing only three strong positive trends, two in Vestlandet and one in Trøndelag. One negative trend is found, in Austlandet. The two strongly positive trends in Vestlandet belong to measuring stations in catchments with high percentage of glacier (ca. 30% and ca. 70%, see Figure 2.6c). The 30% significance level revealed an additional 13 weak positive trends and 10 weak negative trends. The negative trends are found in Troms and Finnmark and at the coast of northern Vestlandet. There are two weak positive trends in Nordland, one in an area with high glacier percentage. Four weak positive trends in southern Norway are located along the mid-country mountain range, two on the coast of Sørlandet, and five in Vestlandet.

Figure 4.5b show the trend results for $AM(30)_{high,spring}$ (AM30 spring high flow). Here, we see a cluster of strong negative trends in Troms and Finnmark. Two strongly positive trends are found, in Vestlandet, at the same locations as for the $AM(7)_{high,spring}$ trends. The 30% significance level reveal two weak positive trends, both in Vestlandet, while 21 weak negative trends appear. Five are in Troms and Finnmark, adding to the cluster of negative trends here. Four trends form a cluster in Nordland, where one is a glacier station. The last cluster of four weak negative trends are located at the coast of Vestlandet. The remaining weak negative trends are scattered.

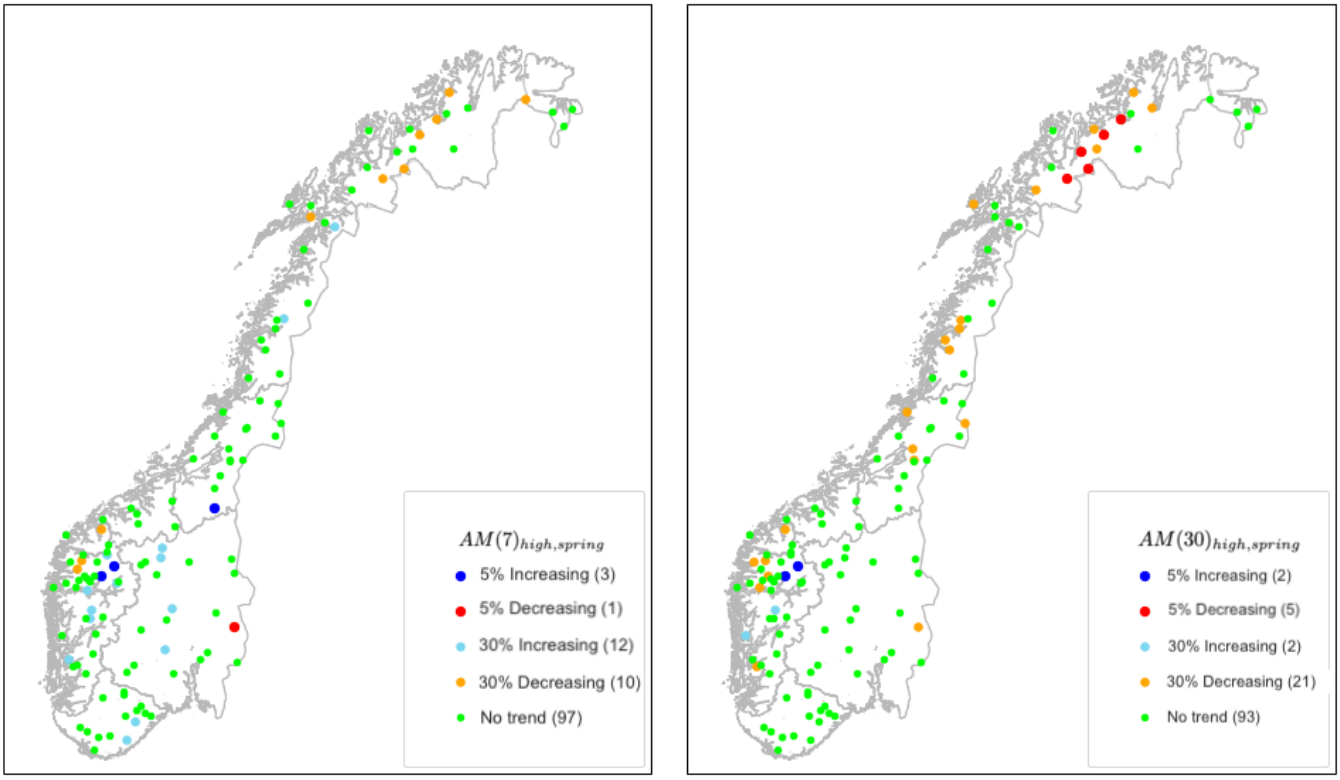

(a) (b)

Figure 4.5: Spring high flow trend calculated for the months March-July, over the period 01.01.1991-31.12.2019 with both a 5% and a 30% significance level. Trends are calculated over a 7-day maximum moving average (left), or a 30-day maximum moving average (right).

The trends for AM7 autumn high flow ($AM(7)_{high,autumn}$) can be seen in Figure 4.6a. This is a special case since we have no strong negative trends and 18 strongly positive trends in western and southern Norway. There is a cluster around north Vestlandet, including stations with no glacier and high percentage of glacier. When adding the trends with 30% significance level, a divide between trends in the north and the south appears. Southern Norway shows no negative trends, while northern Norway have 7 weak negative trends, most at the coast of northern Nordland and Troms and Finnmark. Multiple weak positive trends are shown, mostly in southern Norway, which now have more stations showing a positive trend than no trend. Two stations in northern Norway show weak positive trends, one is a glacier station in Nordland, and one an inland station in Troms and Finnmark.

Trends for $AM(30)_{high,autumn}$ (AM30 autumn high flow) have more strongly positive trends than $AM(7)_{high,autumn}$, 22 of them, and one strongly negative trend in Troms and Finnmark (Figure 4.6b). The cluster of strong positive trends in north Vestlandet have increased in number of stations from the $AM(7)_{high,autumn}$. There is also a new cluster of strong positive trends in southeast Sørlandet, and one in east Austlandet. Just as the $AM(7)_{high,autumn}$, there are more stations with weak positive trends than no trend stations in southern Norway for the $AM(30)_{high,autumn}$.

However, now there are two weak negative trends in Trøndelag.

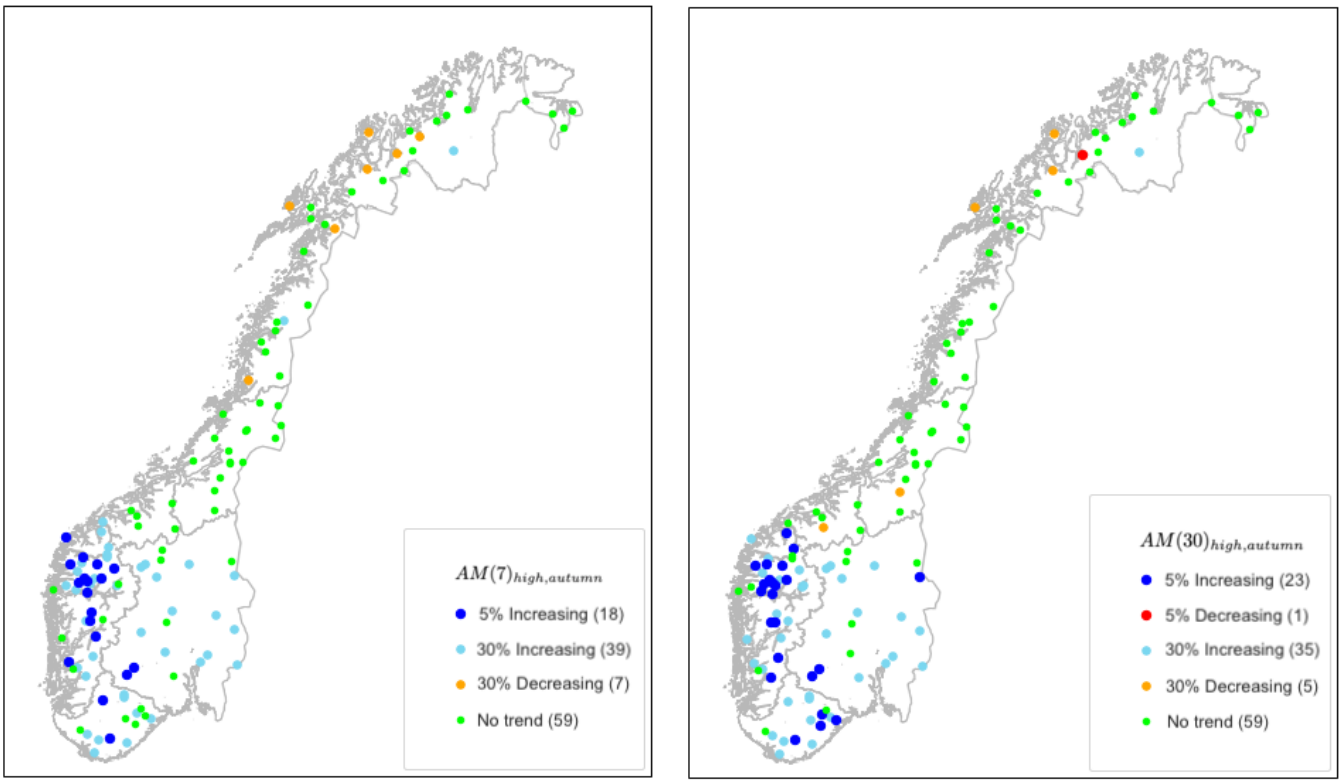

(a) (b)

Figure 4.6: Autumn high flow trend calculated for the months September-February, over the period 01.01.1991-31.12.2019 with both a 5% and a 30% significance level. Trends are calculated over a 7-day maximum moving average (left), or a 30-day maximum moving average (right).

4.1.4 Co-occurrence of trends in mean annual streamflow, seasonal low flow and seasonal high flow

Figure 4.7 shows trends sorted by measuring stations, north to south. In the northernmost stations, the trend pattern show mostly decreasing trends, with the exception of the winter low flow trends and one catchment displaying weak positive trends in summer low flow and autumn high flow. In Nordland there is mostly decreasing trends, except two catchments. For Trøndelag trends are decreasing, especially in summer low flow. Moving southward from Trøndelag, the main trend direction change from decreasing to increasing. Decreasing 5% significant trends are only found in four catchments, for decreasing winter low flow and one decreasing spring high flow. Yearly flow, summer low flow and autumn high flow only display increasing trends in southern Norway.

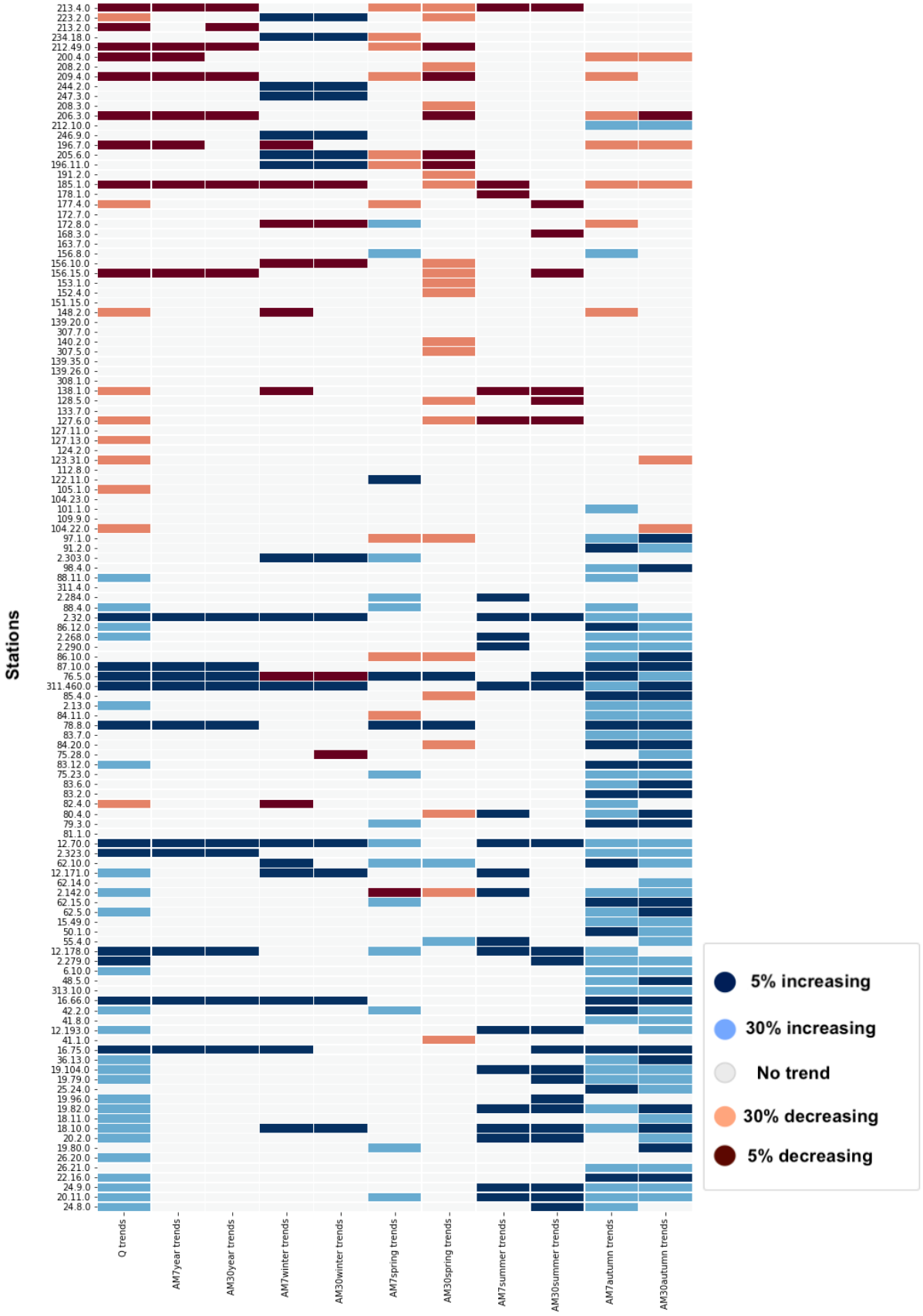

Figure 4.7: Heatmap showing the trends belonging to catchment sorted from north (top) to south (bottom).

4.2 Causing factors of low and high flow trends

4.2.1 Correlations between all trends and predictors

The correlation matrix computed using all trend results, catchment characteristics and climate indices can be seen in Figure 4.8. Dark blue signifies signifies a strong positive correlation (value close or equal to 1), while dark red signifies a strong negative correlation (value close or equal to -1). White mean the features are not correlated (value close or equal to 0). Some correlations are worth commenting on, such as mean and maximum precipitation are that strongly correlated, as well as mean discharge and the 5% exceedance frequency of discharge. Mean precipitation and specific discharge are strongly correlated as well. Maximum catchment height is strongly negatively correlated with mean and maximum temperature, as well as mean snow melt and mean evaporation. Percentage of forest and percentage of mountain in the catchments are strongly negatively correlated. Mean snow melt and mean evaporation correlates with mean and maximum temperature.

4.2.2 Model Accuracy

Table 4.1: Table showing the accuracy score from the Decision tree model (left) and the random forest model (right).

-	Decision Tree	Random Forest
$AM(7)_{low,summer}$	0.7714	0.7632
$AM(30)_{low,summer}$	0.7714	0.7632
$AM(7)_{low,winter}$	0.6571	0.8158
$AM(30)_{low,winter}$	0.8286	0.8421
$AM(7)_{high,spring}$	0.6857	0.7105
$AM(30)_{high,spring}$	0.5429	0.8158
$AM(7)_{high,autumn}$	0.6857	0.8421
$AM(30)_{high,autumn}$	0.7429	0.8158

Accuracy scores for each of the models for each trend is seen in Table 4.1. The closer the value is to 1, the better the prediction. The decision tree scored best when predicting summer and winter low flow, and performed the worst with the $AM(30)_{high,spring}$. The random forest model predicted winter low flow and autumn high flow best, with an overall worst performance when predicting the summer low flow.

As there in all of the trend calculations are an overweight of “no trend” catchments, there is a possibility that the model will get a good accuracy score even if it only predicts “no trend”, and no increasing or decreasing trends. To make sure this is not the case, it is controlled that all results from machine learning on the test data set include at least one correctly assigned trend from one of the “increasing” or “decreasing” classes.

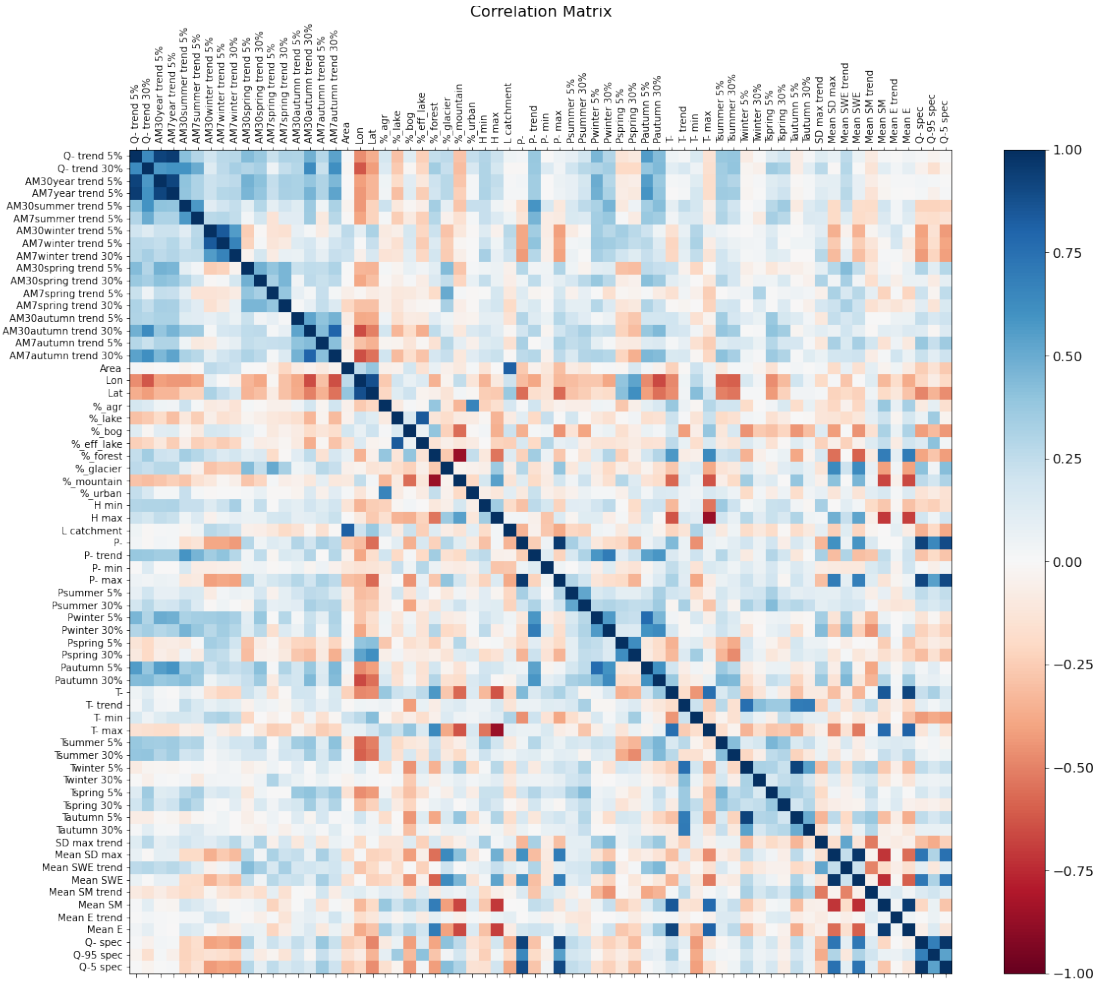

Figure 4.8: Correlation Matrix of all trends and predictors used in the machine learning analysis. Blue color mean strong positive correlation, white color is no correlation and red color means strong negative correlation.

4.2.3 Model results from predicting low and high flow trends

Here results from the decision tree and random forest is presented. The decision tree belonging to each trend is shown first, followed by feature importances calculated for both the decision tree method and the random forest method. Results for summer and winter low flow are shown first followed by the results from spring and autumn high flow.

Low flow

Figure 4.9 presents the $AM(7)_{low,summer}$ decision tree while Figure 4.10 present the $AM(30)_{low,summer}$ decision tree. Figure 4.11 show the corresponding feature importance from each decision tree method, with $AM7$ on the left and $AM30$ on the right (grey), and the random forest method (black) as a bar plot. The $AM(7)_{low,summer}$ decision tree start with a training dataset of 3 decreasing trends, 61 no trend catchments, and 11 increasing trends. $\bar{Q}_{s,95}$ (the 95% exceedance frequency of specific discharge) is the chosen as the root node, and the first split is decided by if $\bar{Q}_{s,95}$ is greater or smaller than 1.504. 7 increasing trends is smaller and moves on to the left. The next split is again $\bar{Q}_{s,95}$, and here 6 increasing trends have $\bar{Q}_{s,95}$ greater than 1.143 and is placed in a leaf node, resulting in no further splits. The last increasing trend on this left-path of the tree is decided by percentage of bog in the catchment. The right-path of the tree is much longer and more complicated. Some of the splits were decided by $\bar{P}$, $\bar{Q}_s$, latitude, longitude and percentage forest.

The tree for $AM(30)_{low,summer}$ is shorter and less complicated than for $AM(7)_{low,summer}$. The root node of the tree divides the training set (5 decreasing trends, 60 no trend and 10 increasing trends) by precipitation trend. This result in all the decreasing trends of the training set following the left path, with most of the no trends. The next split in this branch is T_{max}, and if its above 18.9 °C, all decreasing trends move to the right, to be split by mean SD_{max}. If that is above 1333.8 mm, the next split is T_{max} again, and if that is below 19.99 °C all decreasing trends is sorted into one leaf node. From the root node, 9 out of 10 increasing trends went to the right branch. Next, 7 of these has more than 0.01% urban area within their catchment which resulted in a leaf node. The ones with less urban area were split by P_{min}, and if it was more than 0.001 mm, two more increasing trends ended in a leaf node.

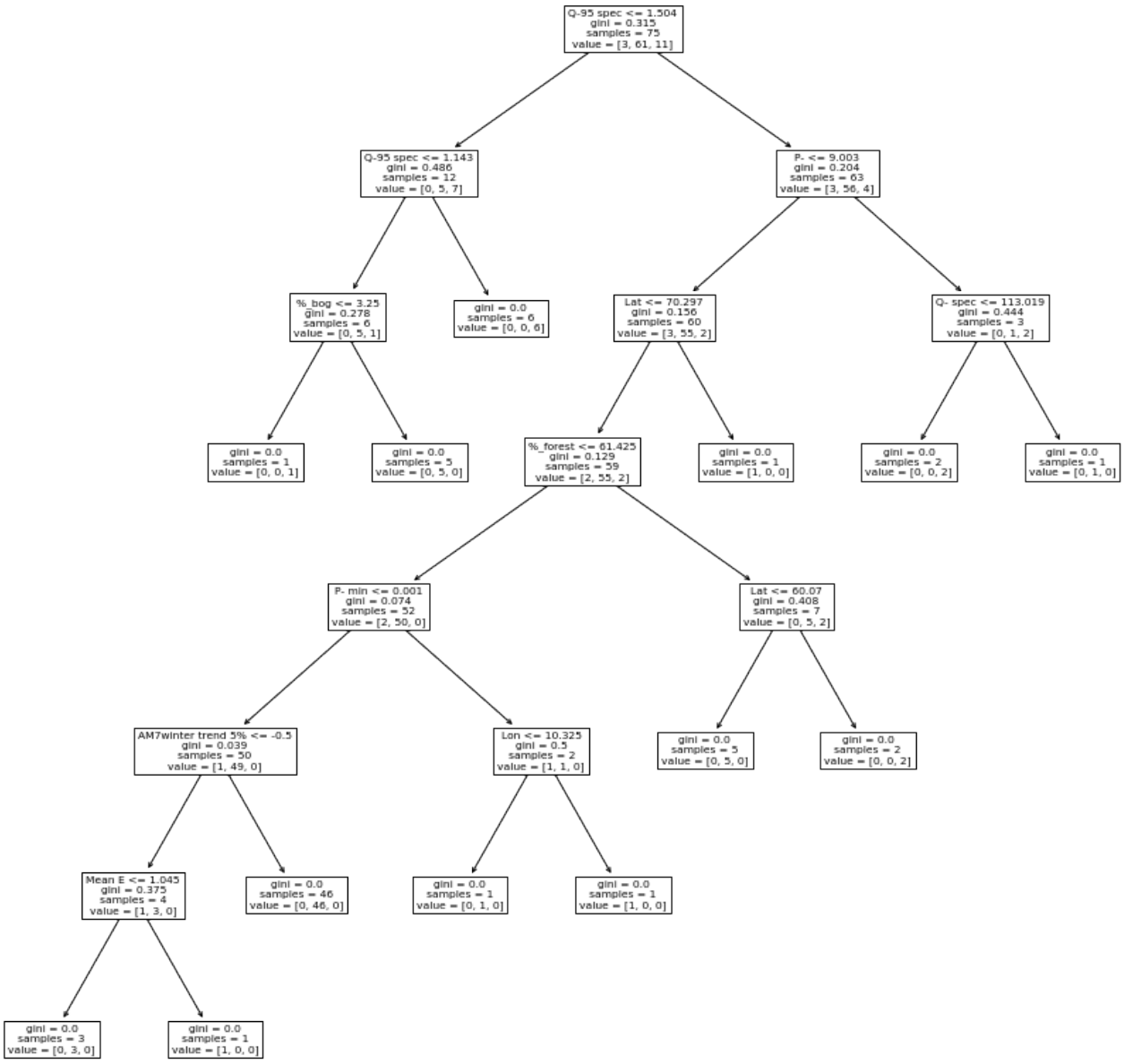

Figure 4.9: Decision Tree for $AM7_{low,summer}$

Looking at the corresponding feature importance in Figure 4.11, we see the most important predictors correspond for both the DT (decision tree) and RF (random forest) methods. The number on the x-axis on this plot show the feature importance, or the mean decrease in impurity this predictor add to the model. The predictors with the longest bars are therefore the most important predictors for each model. For $AM(7)_{low,summer}$, the two most important predictors for both DT and RF are $\bar{Q}_{s,95}$ and latitude. The DT model show $\bar{P}$, $\%bog$ and $\bar{Q}_s$ as the next three, while the RF have $\bar{P}_{min}$, percentage mountain and H_{max} in the top five. $AM(30)_{low,summer}$ have trend in $\bar{P}$ as most important, followed by mean SD_{max}, $\%urban$, T_{max} and P_{min} for the DT, and $\%urban$, latitude, $\bar{Q}_{s,95}$ and

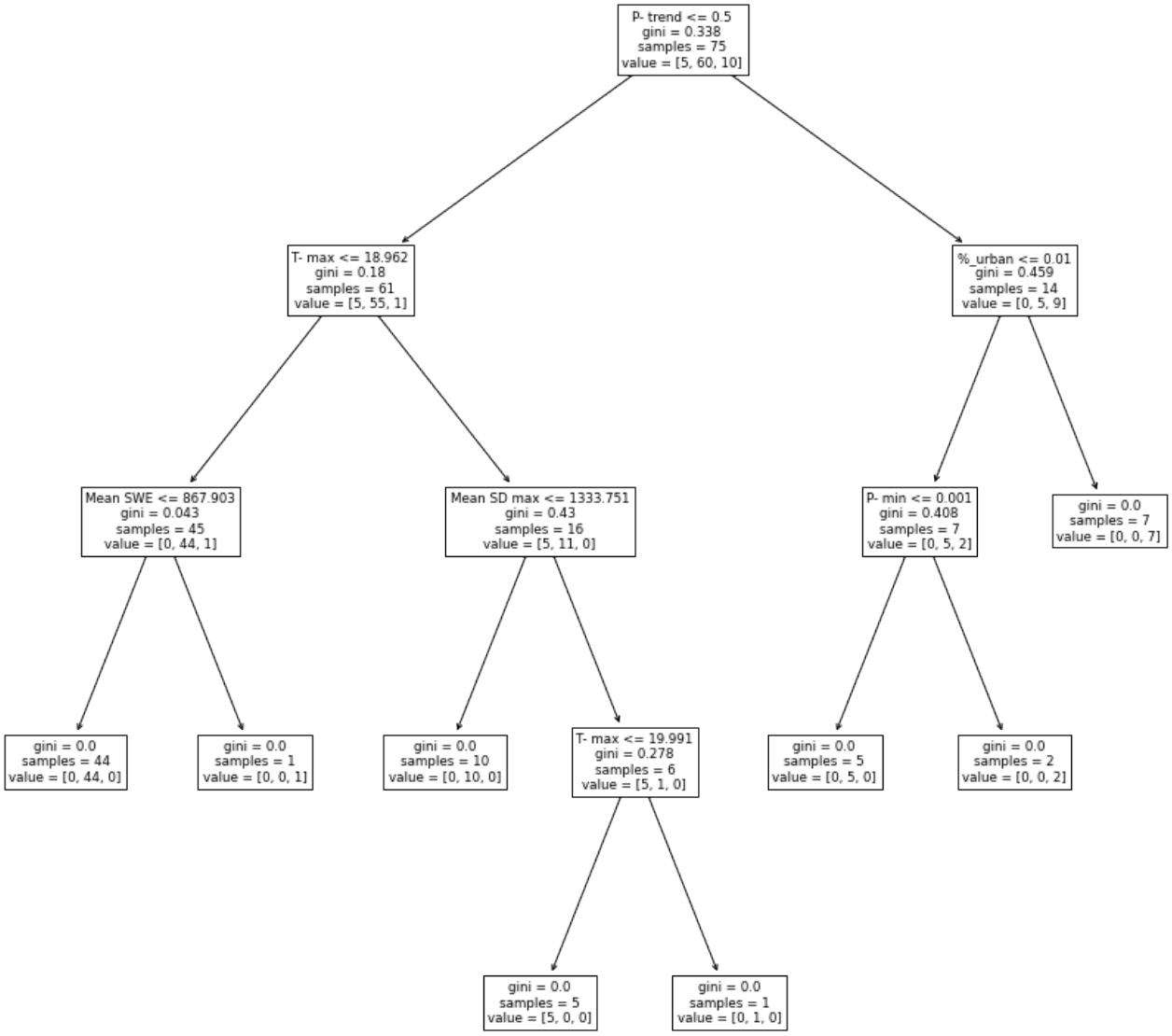

Figure 4.10: Decision Tree for $AM(30)_{low,summer}$

mean SM for the RF method.

The $AM(7)_{low,winter}$ tree is showed in Figure 4.12.The root node of this tree is $\bar{Q}_s \leq 21.931$, splitting the training

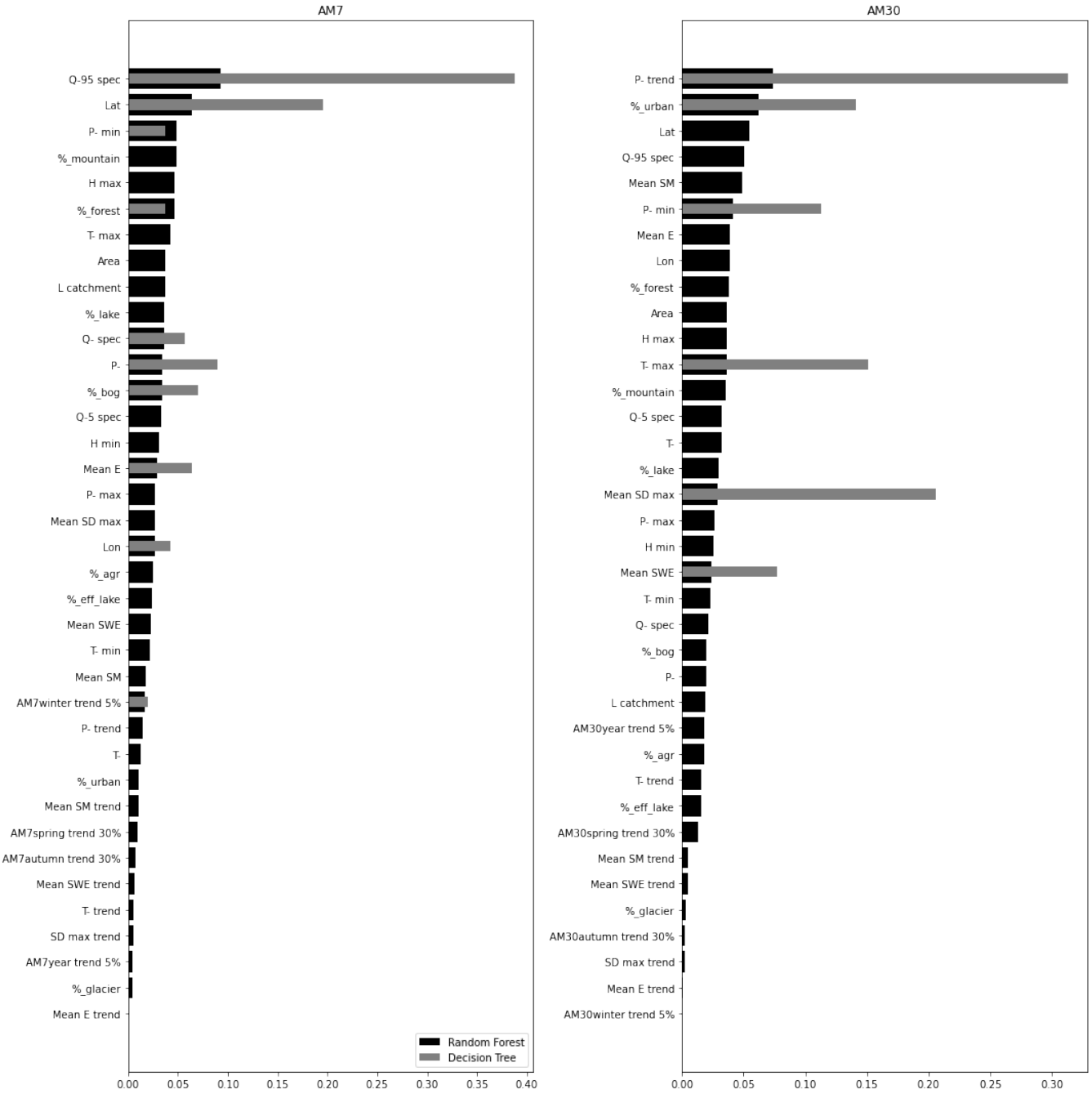

Figure 4.11: Feature importances for the $AM(7)_{low,summer}$ (left) and $AM(30)_{low,summer}$ (right).

dataset (5 decreasing, 59 no trend, 11 increasing) such that most increasing trend catchments move to the left along with 4 no trend catchments, while the rest move to the right branch. The left branch is short, sorting most increasing trends by high mean SD_{max}, and the rest by $\%lake$. The right branch is long and complicated, deciding on one increasing or decreasing trend one leaf node at the time. The importance of the first split and the left branch is reflected in Figure 4.14, where $\bar{Q}_s$ and $\%lake$ clearly are the predictors of most importance for the DT model. They

are followed by mean SD_{max}, $\%bog$, $L_{catchment}$ and mean SWE. The RF model have the same top predictors, $\bar{Q}_s$, but it is followed by $\bar{Q}_{s,5}$, $\%bog$, $\bar{T}_{min}$ and $\bar{P}_{max}$.

The $AM(30)_{low,winter}$ tree (Figure 4.13) starts off with a root node dividing the training set (2 decreasing, 63 no trend, 9 increasing) by longitude, where 4 out of 9 increasing trends end up in a leaf node to the right. If the catchment have a longitude less than 24.198, the next split is $\%bog$. Further down this branch there are many leaf nodes, each only deciding one or two increasing or decreasing trend at the time. This is reflected in the feature importance plot (Figure 4.14) where longitude is by far the predictor with highest importance for the DT. The following predictors for the DT are mean SD_{max}, $\bar{P}_{max}$, $\%bog$ and $\%glacier$. The RF method rules $\bar{P}$ as most important, followed by longitude, $\bar{Q}_s$, $\bar{T}$ and $\bar{Q}_{s,5}$.

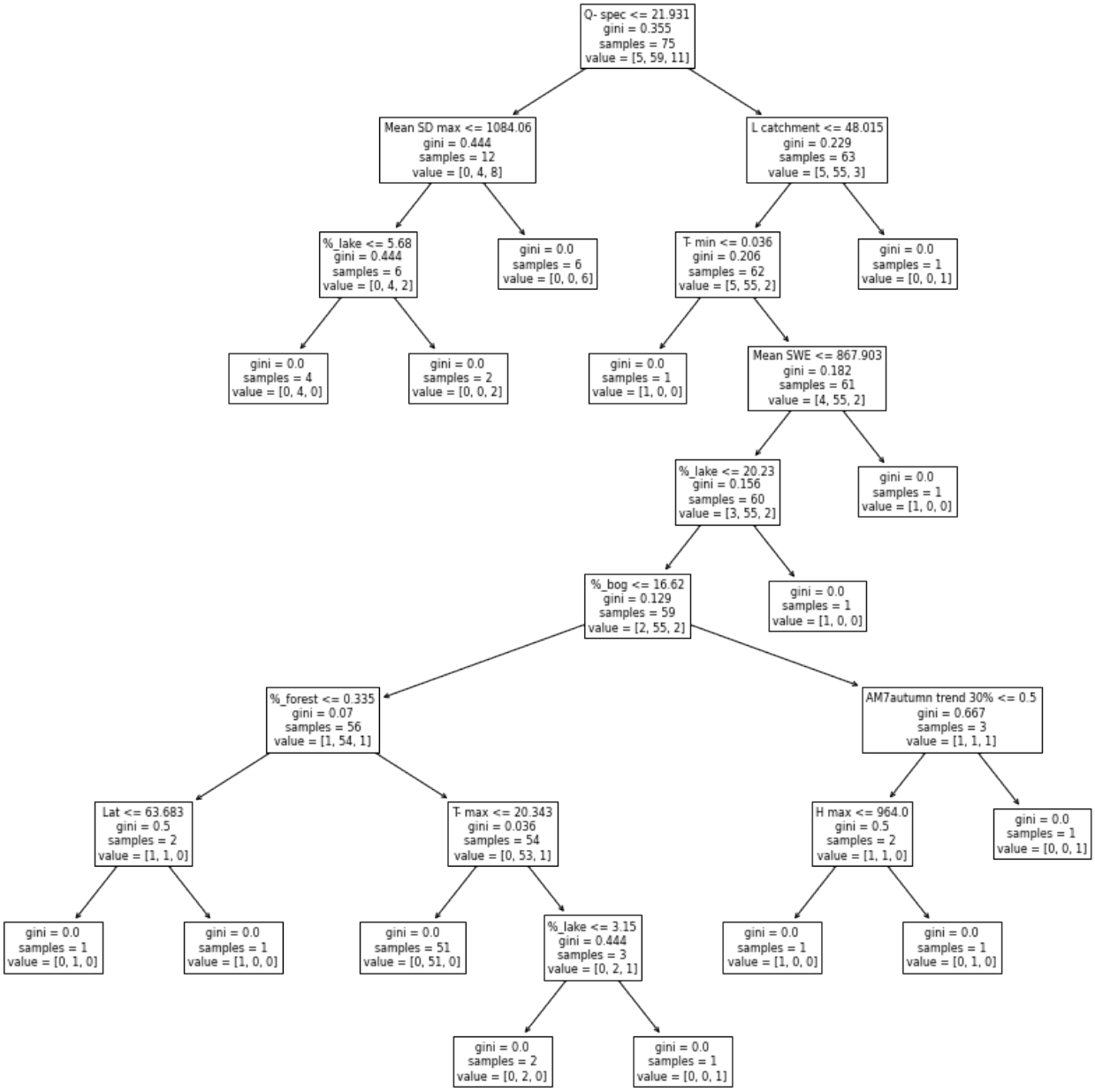

Figure 4.12: Decision Tree for $AM7_{low,winter}$

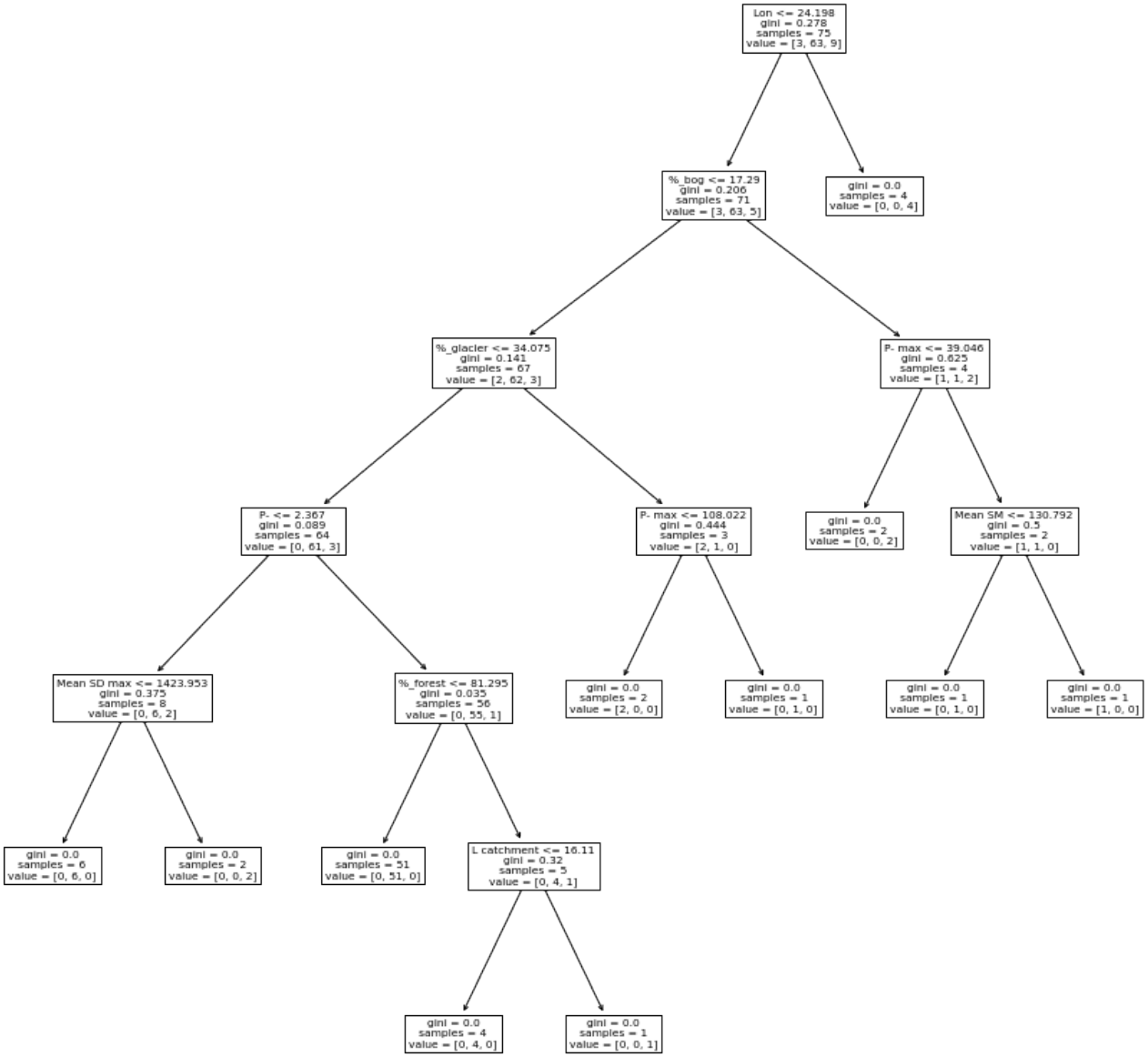

Figure 4.13: Decision Tree for $AM(30)_{low,winter}$

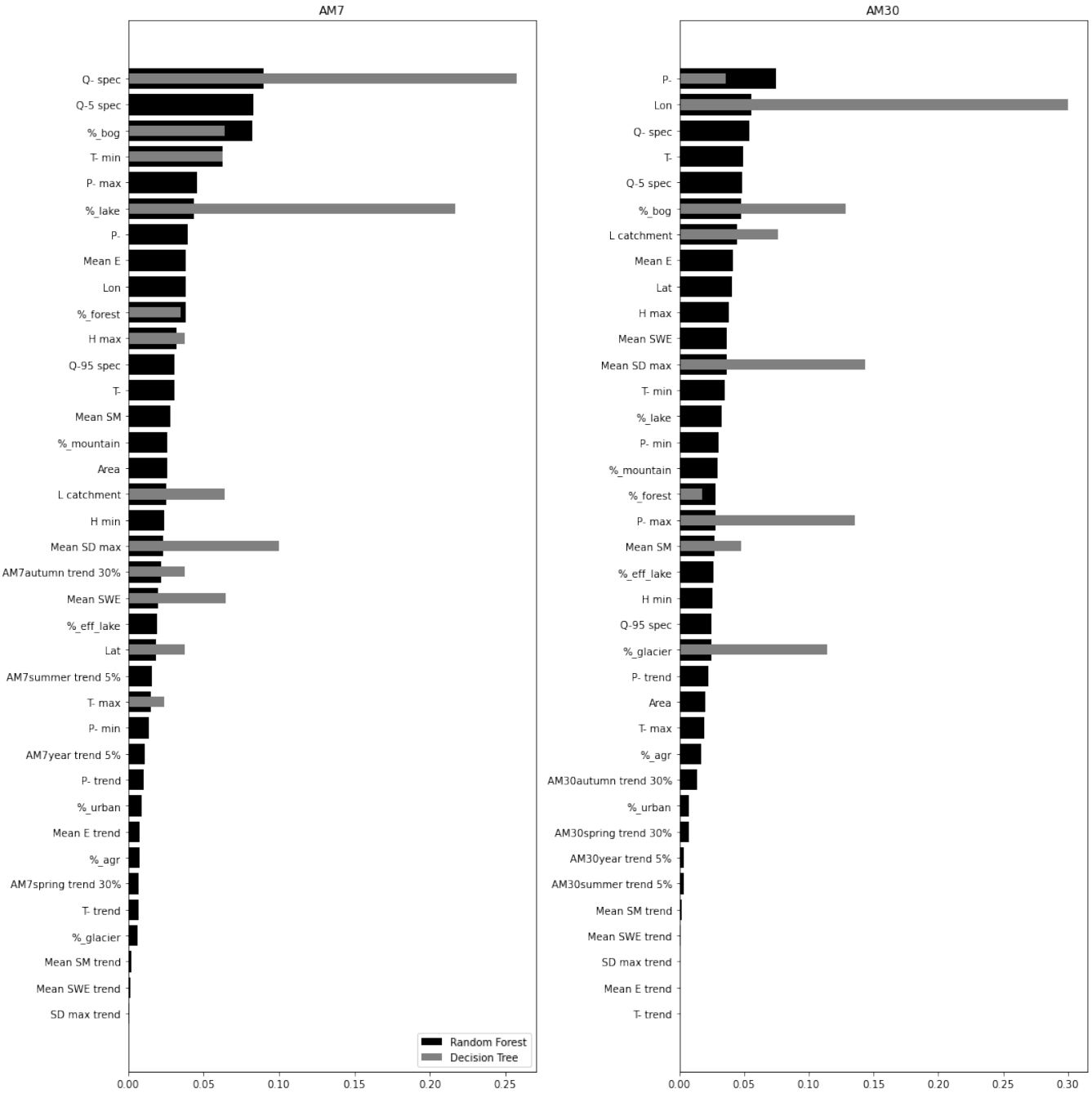

Figure 4.14: Feature importances for the $AM(7)_{low,winter}$ (left) and $AM(30)_{low,winter}$ (right).

High flow

The $AM(7)_{high,spring}$ decision tree (Figure 4.15) starts with a training set of 11 decreasing trends, 51 no trends and 13 increasing trends. The root node is a split decided by $\bar{P}_{max} \leq 37.688$, where 11 out of 13 increasing trends move to the right, and 8 out of 11 decreasing trends move to the left. Both branches have at least two more splits before deciding on a leaf node. 7 decreasing trends are decided by $\%agriculture > 0.105$ followed by $H_{min} \leq 227.5$ on the left branch. 6 increasing trends are decided by $\bar{T}_{min} > 0.062$ and $\bar{Q}_{s,95} \leq 2.03$ on the right branch. The rest of the trends are decided so that each leaf node have one increasing or decreasing trend each.

The root node in the $AM(30)_{high,spring}$ decision tree (Figure 4.16) is longitude ($Lon \leq 11.406$). The training set consists of 15 decreasing trend, 53 no trend, and 7 increasing trends. Following this split, all increasing trends move to the left branch, while all but one decreasing trend move to the right branch, making this a highly effective split between increasing and decreasing trends. On the left branch, 5 out of 7 increasing trend is found by $\bar{P} > 7.236$ followed by $\%mountain \leq 35.97$. On the right branch, 10 out of 14 decreasing trends are found by $\bar{P}_{min} \leq 0.0$ (not real zero, but very low) and $\%bog \leq 4.405$.

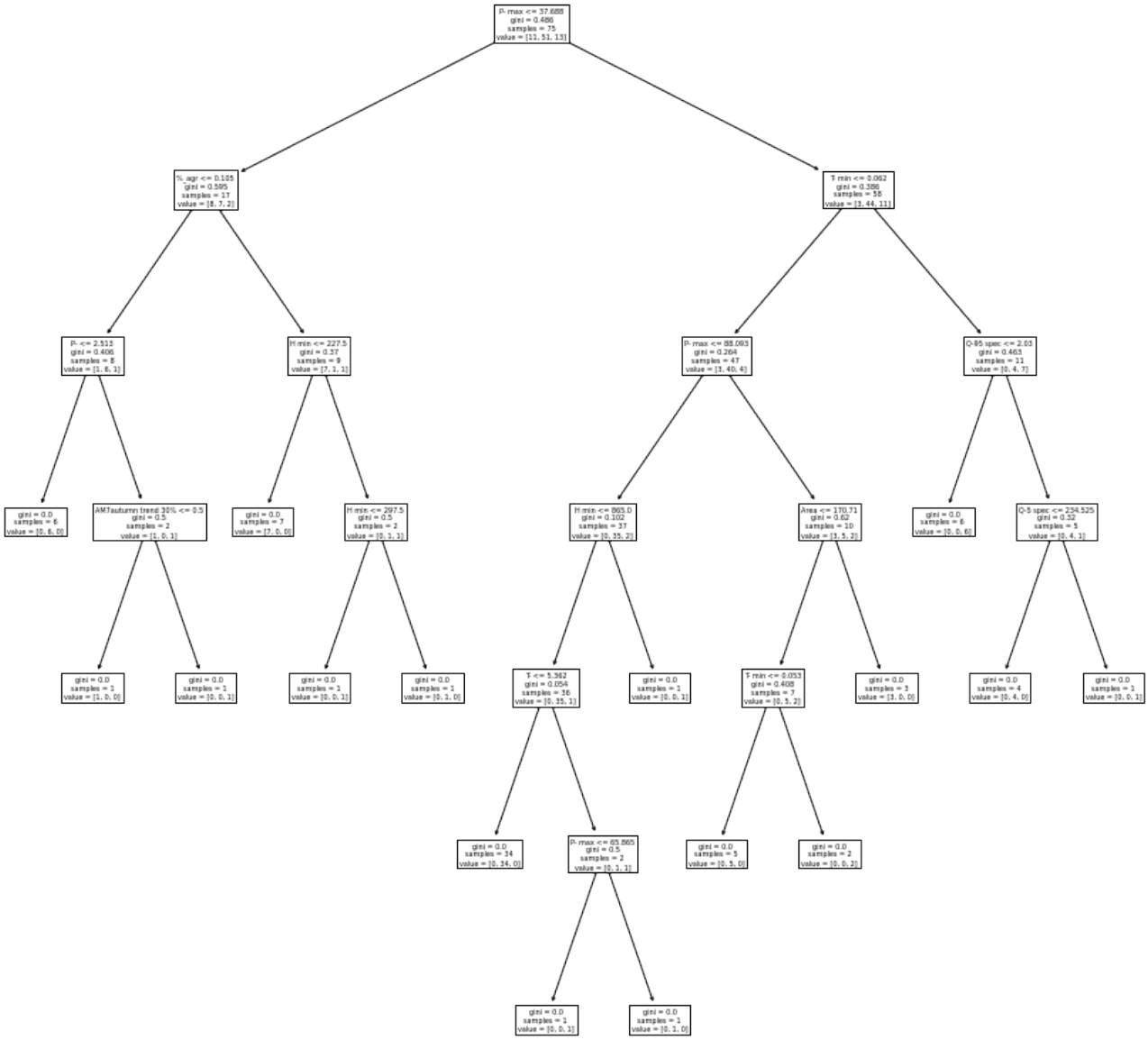

Figure 4.15: Decision Tree for $AM7_{high,spring}$

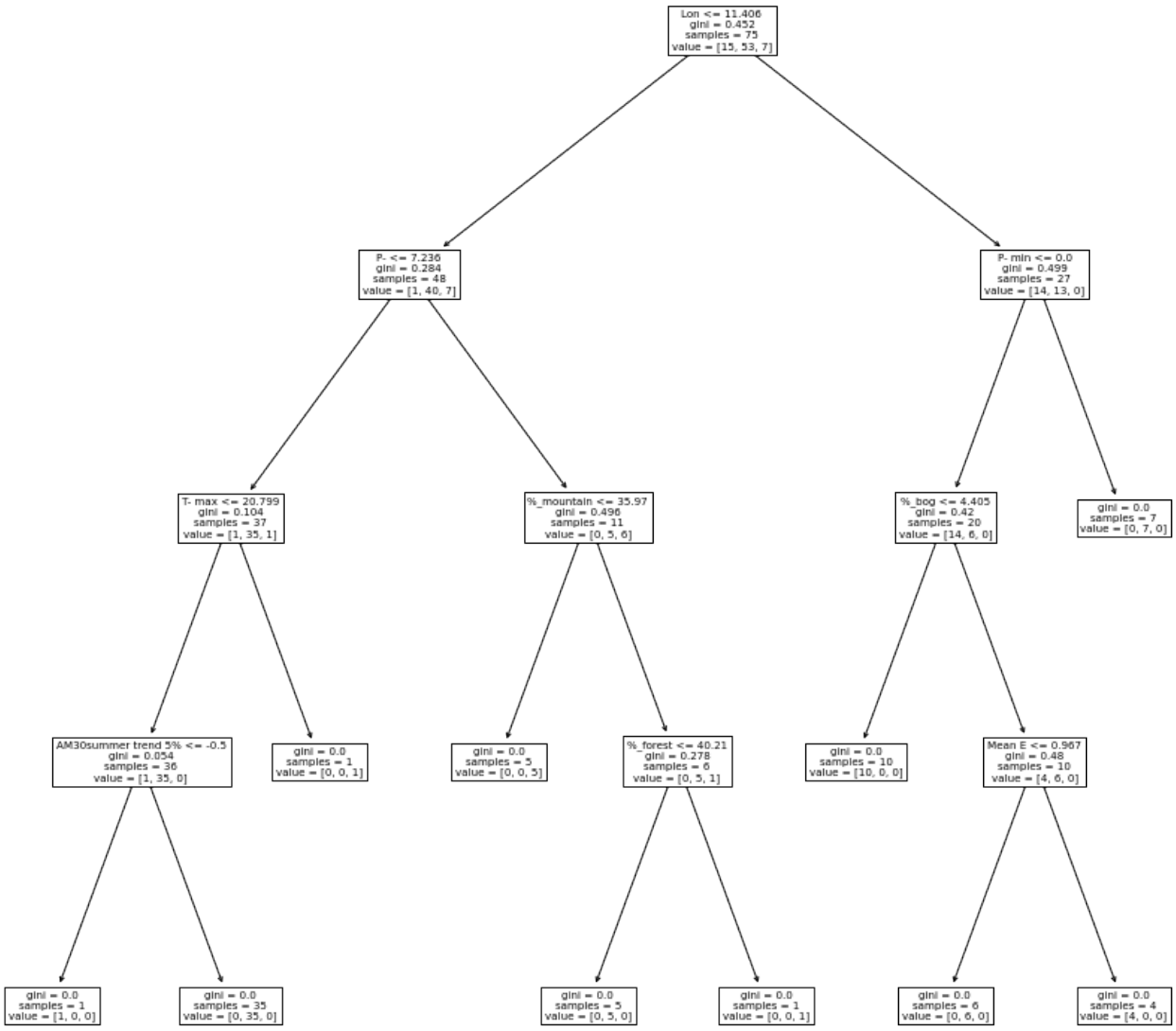

Figure 4.16: Decision Tree for $AM(30)_{high,spring}$

Looking at the feature importances in Figure 4.17, the splits from the decision tree are reflected in the corresponding bars (grey). For $AM(7)_{high,spring}$, $\bar{T}_{min}$ has the longest bar, followed by $\bar{P}_{max}$, H_{min}, Area, $\bar{Q}_{s,95}$ and $\%agriculture$. Since $AM(7)_{high,autumn}$ decided a split further down the tree, it has some importance as predictor. The RF method has $\bar{P}_{max}$ as top predictor, followed by longitude, area, $\bar{P}$ and $\bar{Q}_s$. $AM(30)_{high,spring}$ show longitude as the most important predictor for both the DT and RF model. For the DT model, the following four most important predictors were $\bar{P}_{min}$, mean E, $\bar{P}$ and $\%mountain$, while for the RF model it was latitude, mean SM, $\bar{P}_{min}$ and temperature. $AM30summer_{low,summer}$ are a moderately important predictor for both models as well.

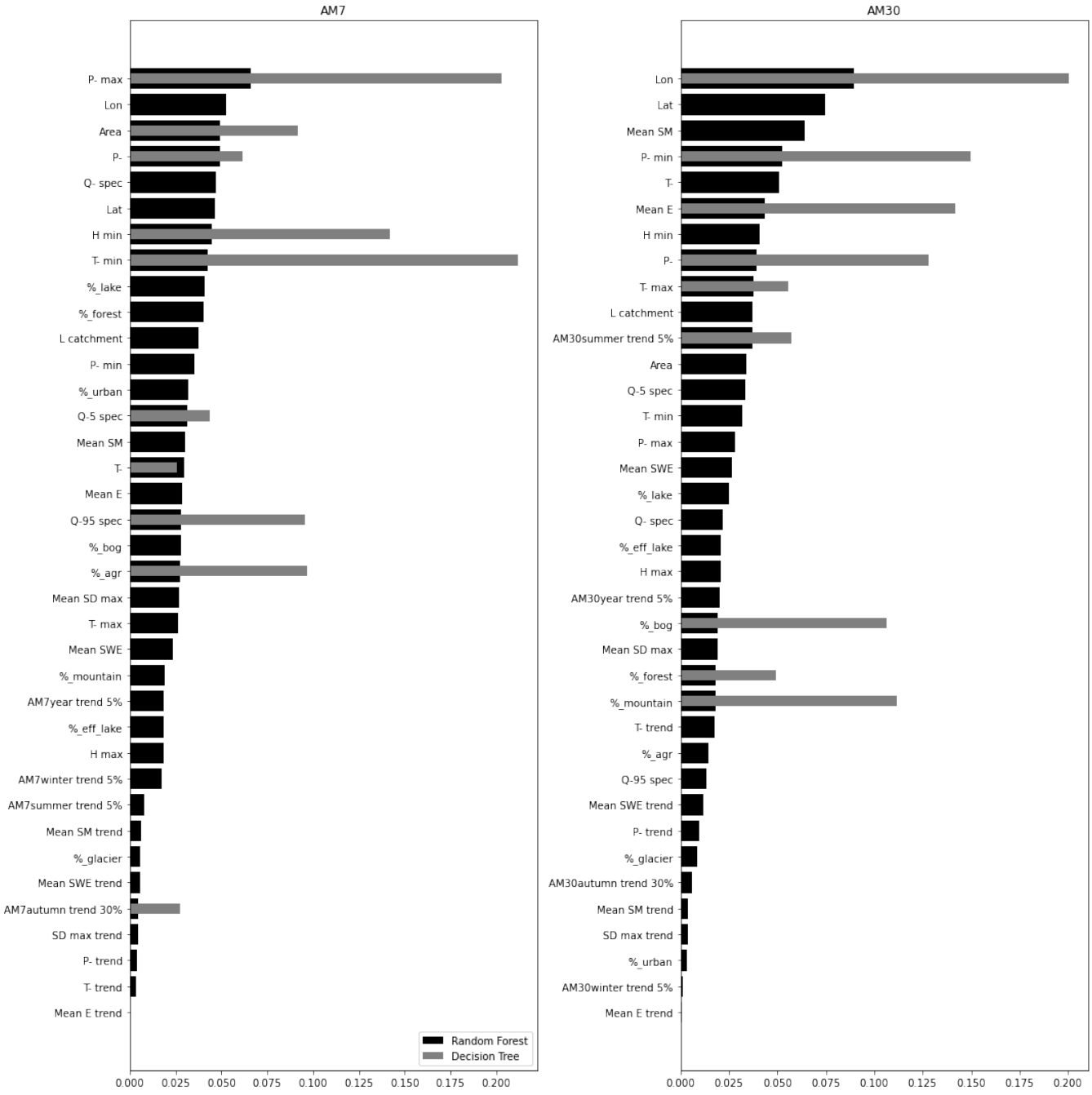

Figure 4.17: Feature importances for the $AM(7)_{high,spring}$ (left) and $AM(30)_{high,spring}$ (right).

The decision tree for $AM(7)_{high,autumn}$ is in Figure 4.18. The training set consists of 4 decreasing trends, 36 no trend and 35 increasing trends. The root node split is decided by latitude ($Lat \leq 62.614$). This effectively sort all the decreasing stations to the right and 32 out of 35 increasing trends to the left. 3 out of the 4 decreasing trends are then decided by $\%efflake > 9.105$ and $H_{min} \leq 17.5$. 29 of the 32 increasing trends in the left branch are decided by $\bar{Q}_{s,95} > 1.458$, $\%lake \leq 10.395$ and $\%mountain \leq 84.155$.

The root node of the $AM(30)_{high,autumn}$ decision tree (Figure 4.19) is also latitude ($Lat \leq 61.837$). Out of the 3 decreasing, 36 no trend and 36 increasing trends in the training dataset, all 3 decreasing are sorted to the right branch, while 30 increasing trends are sorted to the left branch. The 3 decreasing trends are further decided by $\%efflake > 9.105$ and longitude above 13.042. 27 out of the 30 increasing trends in the left branch are sorted by $\bar{T}_{min} \leq 0.085$, $Area > 3.443$ and latitude greater than 58.714.

The feature importance plots for the autumn trends show latitude as the most important predictor for both $AM(7)_{high,autumn}$ and $AM(30)_{high,autumn}$, for both the DT and RF models. The RF models agree that longitude is the next most important predictor for both smoothing intervals as well. The following top predictors the RF model picked for $AM(7)_{high,autumn}$ were longitude, $\bar{P}$, $\%lake$ and $\%efflake$, where as it picked longitude, $\%efflake$, $\%lake$ and mean E for $AM(30)_{high,autumn}$. The DT model picked $\bar{Q}_{s,95}$, $\%efflake$, H_{min} and $L_{catchment}$ for $AM(7)_{high,autumn}$, where as it picked $\bar{T}_{min}$, $\%efflake$, H_{min} and longitude for $AM(30)_{high,autumn}$.

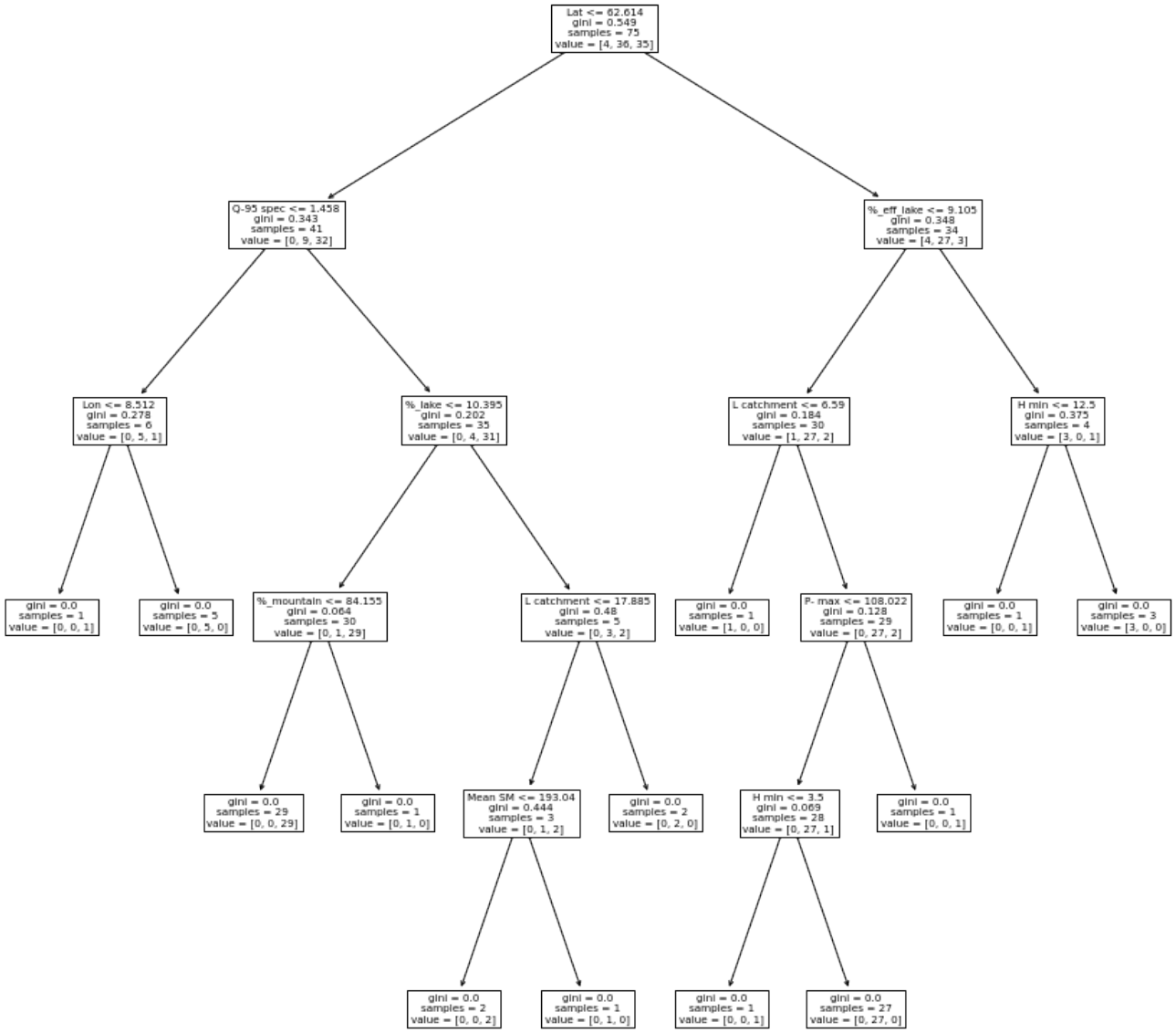

Figure 4.18: Decision Tree for $AM7_{high,autumn}$

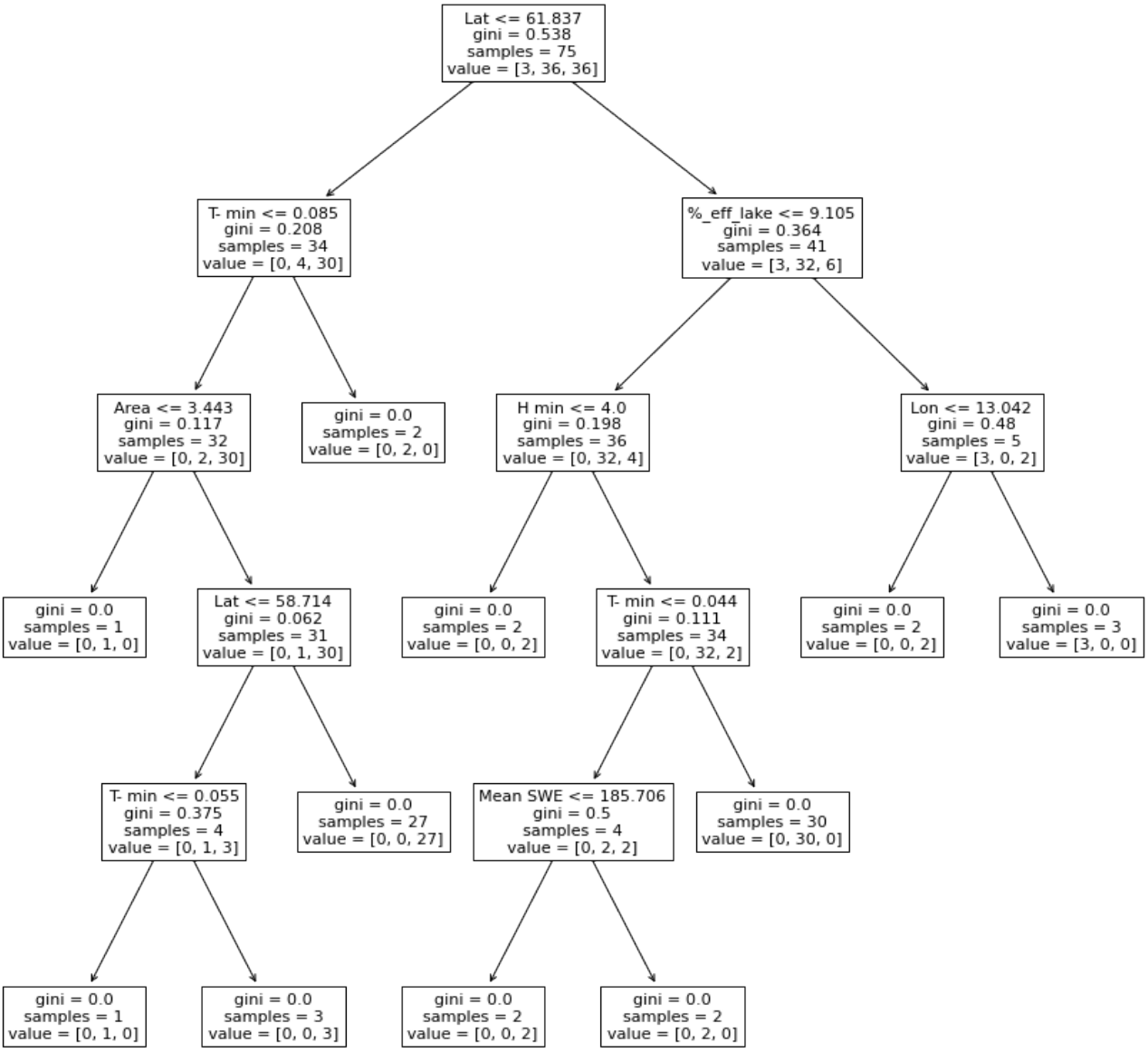

Figure 4.19: Decision Tree for $AM(30)_{high,autumn}$

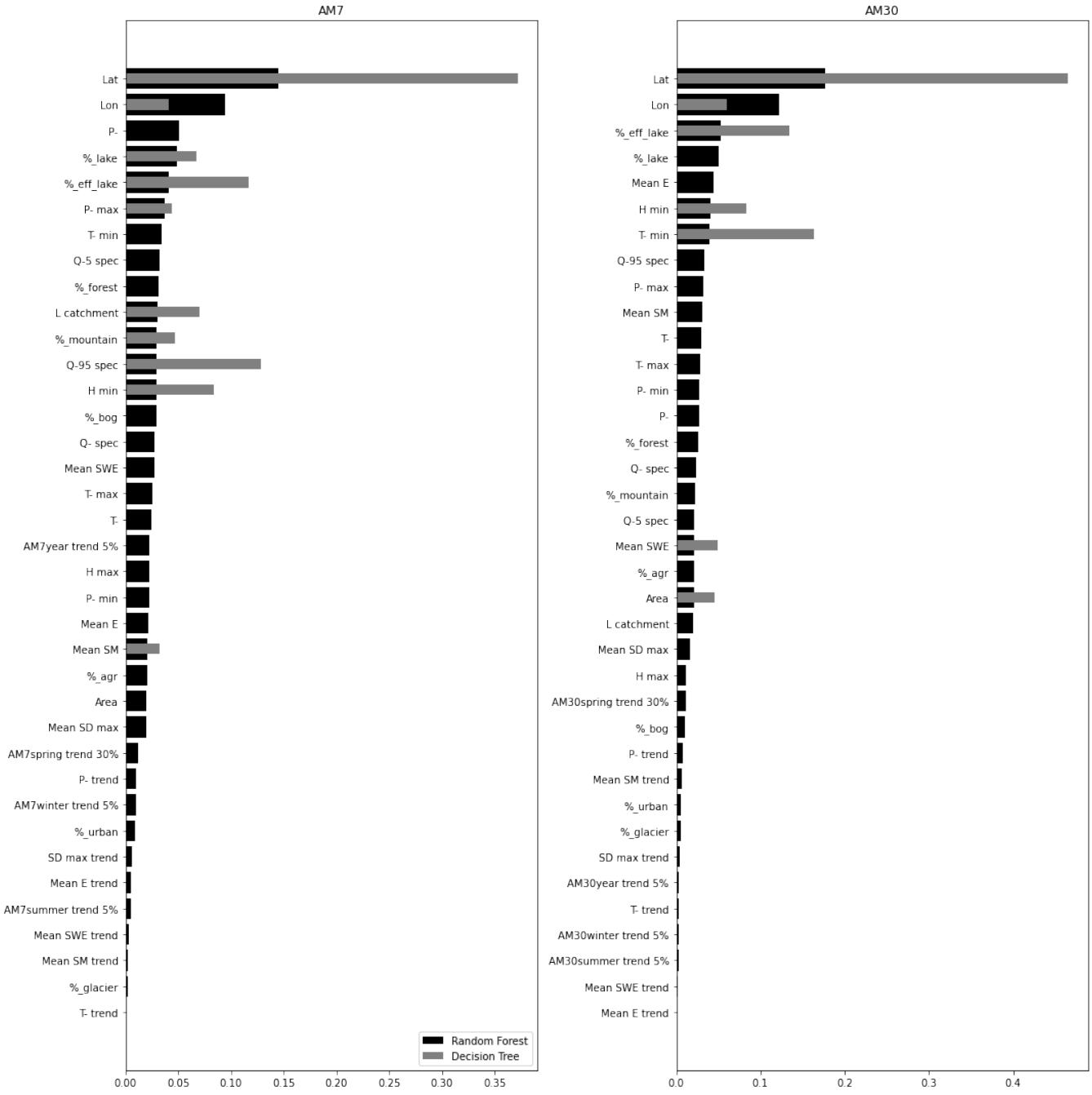

Figure 4.20: Feature importances for the $AM(7)_{high,autumn}$ (left) and $AM(30)_{high,autumn}$ (right).

5 Discussion

This chapter will be divided into three main parts. Firstly, the results from the trend analysis will be discussed, both one their own and their co-occurrence. This is followed by a discussion of the main trend predictors and performance of the machine learning methods. Lastly, a short discussion of the data and methods used.

5.1 Trends

5.1.1 Trends in mean annual streamflow and mean moving average streamflow

Both Figure 4.1 and Figure 4.2 shows the 5% significant trends for $\bar{Q}$, $AM(7)_{year}$ and $AM(7)_{year}$ in roughly the same catchments for both smoothing intervals. Negative trends (towards decrease in streamflow) in mean streamflow are located in northern Norway, while positive trends (towards increase in streamflow) are located in southern Norway. As mentioned in Section 1.1.3, previous studies have found that streamflow in Vestlandet and mountainous regions of Austlandet, were increasing in the periods 1961-2000 and 1962-2004 (Stahl et al., 2010; Wilson et al., 2010). One study also found decreasing streamflow trends in coastal Trøndelag and Nordland, with an increasing trend in Troms and Finnmark (Stahl et al., 2010). This matches the pattern in streamflow trends found in this study. A bachelor thesis from 2020 looked at trends in $\bar{Q}$ for the period 1984-2019, and found mainly increasing trends in catchments in southern Norway, as well as in inland Troms and Finnmark. The study also found decreasing trends from Trøndelag and northward (Nordeide, 2020). This solidifies the results in this thesis, as trends of the same direction have been found in the same areas, for different time intervals.

5.1.2 Low flow trends

The trends in $AM(7)_{low,summer}$ and $AM(30)_{low,summer}$ showed a divide between trend direction in northern Norway and southern Norway (Figure 4.3), with the three southern runoff regions only having increasing trends in summer low flow, while the three northern regions only have decreasing trends. Most of the increasing trends are in Sørlandet and Austlandet. Processes controlling summer low flow is less precipitation combined with higher evaporation. The increasing trends in summer low flow may indicate higher precipitation levels in summer. According to the Climate in Norway 2100 report (CiN2100) (Hanssen-Bauer et al., 2017), summer precipitation in Norway have increased between the periods 1971-2000 and 1985-2014, and it is expected to further increase. The recorded linear trends for summer precipitation in the CiN2100 are not significant at a 1% level (according to the Mann-Kendall trend test), except for in inland Troms and Finnmark. However, in the precipitation regions for Austlandet and Sørlandet, there is a +7% deviation in rainfall between the periods 1971-2000 and 1985-2014.

This increase in summer precipitation does not explain the decreases in summer low flow in Northern Norway. Looking at the mean summer streamflow for the past normal period 1961-1990 (Figure 2.4c), we see streamflow in Nordland during this period was high. However, the CiN2100 found that between the period 1971-2000 and 1985-2014 the summer runoff in Nordland decreased by 12%. A decrease in summer runoff was also found in Trøndelag (-10%) and Troms and Finnmark (-4%) (Hanssen-Bauer et al., 2017). An explanation to this may be decreasing snow cover extent in the late spring/early summer months, and increasing summer temperatures on a 1% significance level in Nordland (Rizzi et al., 2017);(Hanssen-Bauer et al., 2017).

In the Bachelor thesis by Nordeide [2020], trends in summer low flow was calculated over the period 01.01.1984-31.12.2019 using the same 7-day and 30-day moving average as in this thesis. Due to the different research periods and a somewhat different dataset, the results are different and not directly comparable, but some similarities can be seen in the results. Firstly, for $AM(7)_{low,summer}$ there are fewer increasing trends at the 5% significance level in the longer period (7 in the bachelor thesis, where as there were 18 here), and more decreasing trends (11 against 5). The spatial distribution of the trends are quite similar, with increasing trends in the south of Norway and decreasing trends in Trøndelag and northward. The cluster of decreasing trends in Trøndelag consist of 5 trends, and north Vestlandet has two decreasing trends. For the $AM(30)_{low,summer}$ there are still less increasing trends (9 against 17), but the amount of decreasing trends are the same (5). In the bachelor thesis they are all clustered in Trøndelag, and in Figure 4.3 they are scattered from Trøndelag and northward. Three trends in 4.3 are clustered in Trøndelag, solidifying the trend pattern here.

Interestingly enough, summer low flow for southern Norway all show increasing trends. This may seem strange since the past Norwegian summers have been dry, especially summer 2018, when southern Norway experienced a

long drought (Bakke et al., 2020). Increasing summer low flow and increasing winter low flow does both happen in multiple catchments.

The winter low flow trends show a similar pattern to the summer low flow trends and the trends in mean annual streamflow. Since both the $AM(7)_{low,winter}$ and the $AM(30)_{low,winter}$ trends are located mainly in the same regions, they will be discussed together. As opposed to the summer low flow trends, Troms and Finnmark have increasing winter low flow trends, and some decreasing trends are found in Vestlandet. It could seem the trend directions are decided by how close the catchment are to the coast. The positive trends are located at Austlandet and inland Finnmark, while the negative trends are on the coast of Vestlandet and Nordland.

The increasing trends both in Austlandet and Troms and Finnmark are in regions with increasing mean precipitation. Precipitation in Troms and Finnmark deviated from the 1971-2000 normal by +15% in the period 1985-2014. Austlandet and eastern Sørlandet deviated with +11% and +17%, respectively. According to the CiN2100, inland Troms and Finnmark are in a different temperature and precipitation region than the coastal catchments (Hanssen-Bauer et al., 2017). This is also clear from Figure 2.2a and 2.2b with both temperature and precipitation being below the country's mean.

An increase in winter low flow in Troms and Finnmark, usually cold and low-precipitation areas, could be a result of milder winters. According to the Arctic Monitoring and Assessment Programme (AMAP, 2021) the winter temperature in the Arctic regions are increasing at a rate three times faster than the global average, with an increase of 3.1 °C from 1971-2019. During the same period total Arctic precipitation increased by 9%, and precipitation as rain increased by 24% with the largest increase in the winter period, October-May.

Increase in winter low flow in Austlandet could come from the fact that the snow layer is thinner than before, and melts and refreezes more often. Looking at the trend maps from our snow indices in Appendix B, we see maximum snow depth is decreasing, while mean snow melt is increasing. Higher temperatures in the autumn and winter may lead to less snow accumulating in the winter (Rizzi et al., 2017). A thinner snow layer is more sensitive to changing temperatures and melt faster.

The decreasing trends in $AM(7)_{low,winter}$ and $AM(30)_{low,winter}$ are located in Vestlandet, Trøndelag and Nordland. The trends are all, except one, in catchments close to the coast. Decreasing winter low flow can be a result of decreasing precipitation, or more of the precipitation being stored as snow upstream in the catchment. Mean monthly SWE in Norway has decreased between the periods 1961-1990 and 1981-2010 in all winter months except October (Rizzi et al., 2017). Snow cover extent decreased in Nordland during the winter months, but increased in

mountainous parts of Vestlandet. CiN2100 found some small deviations in precipitation from the 1971-2000 normal to 1985-2014 of +1% (Trøndelag/southern Nordland) and -1% (northern Nordland) (Hanssen-Bauer et al., 2017). Rizzi et al. (2017) also calculated trend in temperature for Norway over the period 1981-2010, and found significantly increasing temperatures for parts of Nordland in January and April, while large parts of the area had non-significant increases in temperature.

5.1.3 High flow trends

Both the $AM(7)_{high,spring}$ and the $AM(30)_{high,spring}$ trends showed two increasing trends at 5% significance level belonging to glacier catchments in western Norway. From 1989-1995 glaciers in Norway had surplus of snow, but the 2000's had the four years with most melt during the measured period (Hanssen-Bauer et al., 2017). All glaciers in Norway are presently receding (Ketzler et al., 2021). This probably leads to an increased melting trend in these catchments during spring melting.

One additional 5% significant trend appeared for $AM(7)_{high,spring}$ in Trøndelag. This trend is alone in its runoff region and does not match the $AM(30)_{high,spring}$ trends for the runoff region. According to CiN2100 Trøndelag show no deviation from the normal period 1971–2000 to 1985–2014 (Hanssen-Bauer et al., 2017) However the area does have a significantly negative trend in days with snow covered ground and maximum daily snow depth increase, as well as significantly increasing temperature in April (Hanssen-Bauer et al., 2017; Rizzi et al., 2017) A possible explanation for this trend is a larger, more fast moving snow melt period, leading to spring high flow happening over a shorter, but more intense period.

$AM(7)_{high,spring}$ has a higher number of increasing trends at a 30% significance level, most of them in southern Norway. One is in Nordland, at a catchment with high glacier percentage, and may be subject to the same changes as discussed above. The others in Austlandet, Sørlandet and Vestlandet are all located in or near catchment experiencing increased winter low flow. According to CiN2100 spring discharge in Vestlandet and Austlandet has increased by 8% and 6%, respectively. The spring precipitation is also increasing (Hanssen-Bauer et al., 2017). Spring high flow in these areas may increase because the main FGP cross from being purely snow melt to being rain-on-snow processes.

Five 5% significant negative trends are found in Troms and Finnmark for $AM(30)_{high,spring}$. This cluster of trends, along with the other 30% significant decreasing trends from Trøndelag and northward show that traditionally snow melt driven spring high flows are decreasing. Increasing winter and spring temperatures and increasing winter low flows contribute to lower snow melt in the spring. The figures in Appendix B show the climate index trends from

Table 3.1. In Troms and Finnmark, mean SWE and mean SD max are decreasing while mean snow melt is increasing. This indicates that the snow layer is thinning during our research period, while there is no defined melt period at the end of the season, but melting is happening more during the winter.

Autumn high flow have the most significant trend results out of all the result, with 5% and 30% trends combined being equal to the amount of no trend results. The $AM(7)_{high,autumn}$ and the $AM(30)_{high,autumn}$ largely show the same result, with most increasing trends in southern Norway and the 5% significant ones mainly in Vestlandet. Autumn high flow period was classified based on it being largely rainfall dominated. Increasing precipitation in Vestlandet in autumn is found significant by CiN2100, even though the deviation between the normal period 1971-2000 and 1985-2014 were decreasing (Hanssen-Bauer et al., 2017). Although, since the autumn and winter period overlap, increasing precipitation in the winter months may skew the flood season from late autumn to early winter. A study from 2017 (Blöschl et al., 2017) confirmed just this, that rainfall dominated floods in western Norway have shifted to later in the year due to a shift in timing in extreme winter precipitation.

5.1.4 Co-occurrence of high and low flow trends

The heatmap (Figure 4.7) shows all trends for each catchment, sorted by the latitude position of each catchment from north to south. As commented on in the results, the main finding in this figure is the clear divide between the trends in northern Norway and southern Norway. North of Trøndelag most trends are decreasing, while southern of Trøndelag most trends are increasing. This result is not only within each trend season, but over all seasonal trends within each catchment, the yearly mean specific discharge and the $AM(7,30)_{year}$ trends, indicating some co-occurrence of trends.

For Troms and Finnmark, the winter low flow trends are positive (increasing) while the rest of the trends are negative (decreasing). Although, only two of the catchments displaying increasing trends also have an 5% significant decreasing trend. Looking at Figure 4.4, we see all the catchments displaying increasing winter low flow trends are located in inland Troms and Finnmark. Increasing winter low flow trends may be, as discussed previously, due to increasing temperature and precipitation levels. Inland Troms and Finnmark display one increasing autumn high flow trend, which may have been caused by these same processes. In addition, the trends for spring high flow and summer low flow in the area is decreasing. As mentioned in Section 1.2, increasing winter low flow may lead to a decrease in snow melt volume in the spring. This, combined with earlier snow melt in the spring, can lead to less water available in the rivers in summer. During the past 50 years snow melt floods in Troms and Finnmark have been occurring between 2 to 8 days earlier, with flood peaks between May and July (Blöschl et al., 2017). A decreasing annual streamflow does not match the changes calculated in CiN2100 for Troms and Finnmark between 1971–2000 and

1985–2014 (increase of 2.5%), but it does match the trend patterns found in the 2020 bachelor thesis (Nordeide, 2020).

Nordland has a few catchments with multiple trends, mostly decreasing trends. When the trends are decreasing in all seasons and yearly, the reason can not only be co-occurrence but also climatic. As previously mentioned, the CiN2100 found a decrease in runoff of 4.5% in Nordland between the periods 1971–2000 and 1985–2014, with most of this being decrease in summer runoff (Hanssen-Bauer et al., 2017). This overall decrease in Nordland is interesting since the CiN2100 does not find a decrease in precipitation over Nordland, rather an increase. One previous streamflow study which have included catchments in Nordland found increasing streamflow trends in the area (Wilson et al., 2010), while another found decreasing summer low flow in Nordland (Stahl et al., 2010). In my own bachelor study I found multiple 5% significant trend in mean summer streamflow, $AM(7)_{low,summer}$ and $AM(30)_{low,summer}$ (Nordeide, 2020).

The Trøndelag runoff region does not show many trends, but include a cluster of 5% significant trends in summer low flow. This pattern was also discovered in my bachelor thesis (Nordeide, 2020), but is less apparent in this shorter time period. Earlier streamflow studies have also found decreasing trends inn summer low flow in this area, in one case combined with earlier timing of spring floods (Stahl et al., 2010; Wilson et al., 2010). There is two catchments with 30% significant decreasing trends in spring high flow, meaning these may be connected.

Moving south from Trøndelag, the most trends are now increasing. It seems to be a general trend direction for all of southern Norway, not just the individual runoff regions. The exception is three catchments with decreasing trends in winter low flow and some decreasing trends in spring high flow. Three catchments with decreasing winter low flow also has increasing autumn high flow trends, although some at 30% significance level. At 30% significance level, almost all catchments in southern Norway display increasing trends in autumn high flow. This despite the CiN2100 finding a decrease in autumn precipitation in almost all of Norway's precipitation regions (Hanssen-Bauer et al., 2017). However, winter precipitation has increased, and rainfall dominated catchments in Vestlandet experience floods timed later in the year (Blöschl et al., 2017; Hanssen-Bauer et al., 2017). The catchments with 5% significantly increasing autumn high flow are not always the same catchments as the ones with increasing winter low flow, disproving this increase is only caused by increasing winter precipitation.

On catchment with 70% glacier in Vestlandet show decreasing trends in winter low flow, while having increasing trends in almost all other seasons. This region experience increasing precipitation and temperature for the whole year (Hanssen-Bauer et al., 2017), and some decrease in SCE during the winter months (Rizzi et al., 2017). Mass balance in Norwegian glaciers have decreased since the early 2000's, with four of the year with highest melt in recorded history happening within this decade (Hanssen-Bauer et al., 2017). Decreasing trends in winter low flow combined

with increasing trends for the other seasons may reflect the size and melt of the glacier. Base flow in winter from the glacier decreases because the glacier has decreased in size during the study period, while both high and low flow increases in the other seasons due to higher melt and increasing precipitation.

5.2 Causing factors of low and high flow trends

5.2.1 Co-occurrence of trends in mean annual streamflow, seasonal low flow and seasonal high flow

The correlation matrix in Figure 4.8 showed, as expected, that each trend calculated on the different moving average period highly correlates, and most of them show some positive correlation to each other. This is reflected in the trend heatmap in Figure 4.7, where trends in northern and southern Norway generally moves in the same direction. An exception is the spring trends negatively correlation to the winter trends. This is probably because of the relatively high number of strongly decreasing trends in Troms and Finnmark for $AM(7)_{high,spring}$, compared to the increasing trends in the area for $AM(7)_{low,winter}$ and $AM(30)_{low,winter}$ as discussed earlier.

Other correlating values were more surprising, such as mean annual precipitation and annual maximum precipitation correlating strongly, or mean annual specific discharge and its 5% exceedance frequency, as well as the precipitation and specific discharge strong correlation with each other. This correlation is highlighted by Figure 2.2b and Figure 2.3, showing mean annual precipitation and streamflow over Norway. However, the strong correlation between mean and maximum precipitation, as well as mean specific discharge and its 5% exceedance frequency is expected.

5.2.2 Model accuracy

The accuracy scores for the model performances (Table 4.1) all were in the range 0.65-0.85, except the decision tree model for $AM(30)_{high,spring}$ at 0.5429. The latter score is similar to the score one would get using a random model (i.e. 0.5). This might be because of the low number of increasing trends to train the model on in the training dataset. However, the random forest model performed well on this same trend set. This might be due to the random forest model being more robust and not too prone to overfitting. The other accuracy scores are not perfect, but they are better than random. As for the actual scores, a score between 70-90% from a machine learning model is considered good enough that continuing with the analysis from these numbers would show sufficiently good results. When paired with the fact that each model have placed at least one trend from each classification correctly, the model accuracy is suitable for its purpose in this thesis, being showing what predictors stand out as important when predicting trend directions.

5.3 The most dominant predictors

Since the trends are for different seasons regarding different drivers for the flow types, they have different predictors. Even so, some predictors are more apparent than others. Mean specific discharge, mean temperature and mean precipitation are frequently appearing predictors, as are latitude and longitude. That the hydroclimatic predictors show importance is no surprise, since precipitation and runoff have a clear connection (Figure 2.2 and 2.3). That latitude and longitude show up as important predictors is not surprising either, since the heatmap (Figure 4.7) showed a clear divide between the trends of northern Norway and southern Norway.

Looking at the individual predictions for each season, the variability in which predictor is chosen as main driver is high. This is good, indicating different processes lead to the trends in different seasons. For the $AM(7)_{low,summer}$ latitude is the second most important predictor, which is clear to see from Figure 4.3. In the figure, all increasing trends are in southern Norway and all decreasing trends are in northern Norway. $\bar{Q}_{s,95}$, which can be used as a low flow threshold, is the most important predictor for summer low flow. According to Figure 1.1, the decreasing trends in coastal Trøndelag and Nordland are in summer process driven low flow regions, while the increasing trends in southern Norway are all in winter process driven low flow regions. Which process is the main driver of low flow may affect the 95% exceedance frequency in the catchment, which again help the machine learning algorithm sort the catchments by trends.

The precipitation trend and percentage urban area are interesting choices as important predictors for $AM(30)_{low,summer}$. However, looking at Figure B.2b in Appendix B, many catchments with increasing precipitation trends align with catchments with increasing summer low flow. This aligns with what was discussed in Section 5.1.1, that summer precipitation in southern Norway has increased. That catchments with higher percentage of urban area show increase in summer low flow may be due to more surface runoff in these areas. A higher percentage urban area usually mean more surfaces covered with asphalt or buildings, leading to less precipitation percolating the ground, and rather flow on the surface to the nearest drainage point. Therefore, a direct link between higher precipitation and higher runoff is common in urban areas.

The $AM(7)_{low,winter}$ trends have $\bar{Q}_s$ a the most important predictor, followed by % lake for the DT model and $\bar{Q}_{s,5}$ for the RF model. For the $AM(30)_{low,winter}$ DT, all important predictors were climate indices except for % agriculture. Its RF method instead highlighted latitude and %bog as the most important predictors. Both of these catchment percentages are within the DT for $AM(7)_{low,winter}$, as well as % forest and longitude. Climate indices are important regarding winter low flow, since the causing factors behind is controlled by temperature and precipitation. The amount of snow falling is controlled by whether us is cold enough for precipitation to fall as snow, and if it stays cold to hinder snow from melting.

Results from $AM(7)_{high,spring}$ and $AM(30)_{high,spring}$ are very different from each other, and will therefore be discussed separately. The most important predictor for the $AM(7)_{high,spring}$ DT is $\bar{P}_{max}$, and as discussed in Section 5.1.3, spring precipitation in the regions with positive trends is increasing. That the decision trees divide almost all increasing trends by high maximum precipitation indicate that the increasing trends in spring high flow is caused by snow melt floods happening at the same time as high precipitation events, leading to a rain-on-snow flood as mentioned in Section 1.3. These events usually happen at the end of the winter period (Merz & Blöschl, 2003). $\bar{P}_{max}$ is not a predictor for $AM(30)_{high,spring}$, which indicate that the high flow events following rain-on-snow floods may be of a shorter time duration of the AM30 smoothing interval to pick up.

The most important predictor for $AM(30)_{high,spring}$ is longitude, which also is the second most important predictor for $AM(7)_{high,spring}$. The difference between Figure 4.5a and 4.5b is less weak increasing trends in southern Norway and more weak decreasing trends in northern Norway. Since northern Norway, containing most of the decreasing trends, is further to the east longitude is pointed out as an important predictor. Mean snow melt is the third most important predictor for the RF model for $AM(30)_{high,spring}$. In Section 5.1.1 we discussed that the decreasing trends in this area could be caused by increasing winter low flow and the snow melting more during the winter, leading to smaller snow melt volumes in the spring. Snow melt showing importance as a predictor is therefore expected, even if it did not show up for the DT model.

The most important predictors for the $AM(7)_{high,autumn}$ and $AM(30)_{high,autumn}$ trends are overwhelmingly latitude. Looking at Figure 4.6 the divide between trends in northern and southern Norway is prominent, and the decision trees and random forest methods picking this attribute as leading predictor is no surprise. Percentage effective lake is an important predictor for all models as well. $\%effflake$ differs from $\%lake$ in that $\%lake$ is the area of the catchment covered by the lake, while $\%effflake$ is the weighted lake percentage of the catchment. $\%effflake$ is an indication of storage capacity within a catchment. Large $\%effflake$ indicate decreasing trends in the catchments while small percentages indicate increasing trends. This is probably due to the catchment's response time to incoming precipitation being slowed by having a lake in the catchment.

Interestingly enough, neither precipitation not temperature does not seem to have a large effect on the DT method for either of the smoothing intervals of autumn high flow. As discussed in Section 5.1.3, increasing precipitation in the western part of the country may explain some of the trends found in the area. However, $\bar{T}_{min}$ have some significance for $AM(30)_{high,autumn}$, and $\bar{P}_{max}$ for the $AM(7)_{high,autumn}$ DT. The DT model highlight more catchment characteristics than climate indices, and no other trends, neither of the seasonal trends or the climatic trends show importance.

5.3.1 Co-occurrence as indicated by the machine learning models

In most of the cases, one or more of the other trend results was used by one or both machine learning methods to predict the other trend. This was usually more significant in the case of decision tree method than random forest. But since they were used as predictors, they must have been important enough for the model to by some degree divide between the different trends. As previously mentioned, $AM(7)_{year}$ and $AM(30)_{year}$ are the two trend most often present as important predictors. The yearly trends show the same north-south division in trends as the seasonal trends, and the trends more often belong to the same catchments that are showing seasonal trends. This makes the yearly trends better predictors for the seasonal trends than the seasonal trends are to each other.

Throughout all of the trend predictors, the other trends were not often high up on the list of most important predictors, except for $AM(30)_{low,summer}$ for $AM(30)_{high,spring}$. This is an interesting result, as the heatmap in Figure 4.7 show a great clustering of trends within the different regions. As commented earlier, often the catchments with strong trends in one season did not show trends during the other seasons.

5.3.2 Possible Improvements to the models

Since I assumed all predictors would be interesting and may show importance for the seasonal trends, a cross-validation was not performed. A cross-validation might have further improved the models' predictions by removing predictors not necessary for the analysis. This might have removed parameters which are usually far down on the feature importances plots, such as the snow indices and evaporation trends. That these were not picked as predictors may be because the significant trends had the same directions for the whole country, with no latitude or longitude divisions.

To improve the model, one could add more predictors, such as distance from the coast, height percentiles of the catchment, more snow indices e.g., which may have lead to a better analysis.

Another procedure to make the machine learning better would be to fine-tune the model for each of the trends, resulting in a different final model for each seasonal trend and smoothing interval. Since all models were now evaluated based on the same method, some performed worse than others, for example the $AM(30)_{high,spring}$ decision tree, as seen in Table 4.1. If each model had been given their own hyperparameters best suited for them, the models' predictions might have been better. For the decision trees, it probably would have lead to more concise trees, with fewer leaf nodes and less of the splits resulting in one and one decided trend.

5.4 Uncertainties of the study

5.4.1 Data uncertainties

A consequence of choosing to add many catchments to the machine learning dataset, opposed to following the data quality of the new HRD (Dahl & Pedersen, 2021) is that many of the gauging stations included in the final dataset are not recommended for use in winter low flow studies. In most cases this recommendation is the result of the discharge data being corrected due to backwater from snow and ice, but for some cases, other reasons are listed. Added metadata and new data analysis resulted in more than half of the new HRD being unfit for our research goals. Since I chose to use the old HRD as reference the gauging stations not recommended for winter low flow use, but which still fills our other criteria, is used in this dataset.

5.4.2 Method uncertainties

In this thesis, when a machine learning method found a characteristic or index important, it is used as fact that it must be important for the trend. However, in machine learning, it could be just a coincidence that this parameter suddenly has something to say about this trend direction. Still, in this thesis it was used as causing factors, since we believe that catchment characteristics and climate indices do have some importance.

In this thesis the original goal was to find trends at only the 5% significance level, before comparing the seasonal trend patterns and their top predictors from the machine learning methods. However, since the high flow trends showed so few significant trends at this level, another significance level of 30% had to be added. This lead to a difference in the significance level of most trends predicted by the machine learning models for low and high flow.

6 Conclusion

Trend analysis have been performed over seasonal low and high flow in Norway over the period 01.01.1991-31.12.2019. Low flow periods were defined as: winter low flow driven by precipitation stored as snow and ice (September-May) and summer low flow driven by low precipitation and high evaporation (June-August). High flow periods were defined by: spring high flow driven by snow melt (March-July) and autumn/winter high flow driven by high precipitation (August-February). Machine learning by the methods decision trees and random forest were then used to see if the found trends could be predicted accurately, and which predictors amongst catchment characteristics and climate indices showed the highest importance to the predictions. Based on the findings in this study, the answer the research questions from Section 1.4 is as follows:

i) How has low and high flow for Norwegian unregulated catchments changed during the period 01.01.1991 - 31.12.2019?

Both summer and winter low flow increased in southern Norway and decreased in parts of Nordland. Summer low flow in Troms and Finnmark is decreasing, while winter low flow in the region is increasing. High flow in the autumn period is increasing in southern Norway and decreasing in northern Norway. Spring high flow is increasing in most of southern Norway, and decreasing in northern Norway.

(ii) If there are changes, do they display co-occurrence in their location and directions?

The trends do display some co-occurrence in both their locations and directions. Overall, southern Norway show increasing trends, Trøndelag and Nordland mostly show decreasing trends and Troms and Finnmark show decreasing trends, except for winter low flow.

(iii) Can we, using machine learning, find which of the climate indices, catchment characteristics or other trends available are the most important predictors?

The two machine learning methods applied to predict the trends performed sufficiently good (model accuracy between 0.65 and 0.85, with one exception of 0.54). Latitude and longitude were among the predictors showing highest importance for the majority of the trends. Among the climate indices, precipitation and temperature were frequently

among the most important predictors, as was mean streamflow and its 5% and 95% exceedance frequencies.

Further study of trends in streamflow in Norway and their co-occurrence is needed to understand how climate change has impacted, and will continue to impact the water cycle. Changes in the period one calculate the streamflow trends over can change the result of the trend analysis. Only one definition of high and low flow was used in this study. Other methods to define high and low flow than used in this study may affect the results as well. Using multiple definitions would provide insight in how the definition of the flows affect the trend results. In this thesis only trend magnitude and slope was calculated for seasonal low and high flow. Calculating trends in timing for low flow and high flow periods may help further understanding on the co-occurrence of the trends, and clarify the connection between trend directions in the seasonal trends. Using machine learning to define trends in seasonal streamflow is, to the authors knowledge, not previously done, and by the results of this study, a possible way to define changes in streamflow in a catchment. However, small datasets restrict the machine learning. Only two machine learning methods was applied in this thesis, both classification methods applying if-else testing to sort data into categories. Using other methods, such as linear or regression methods, or using the calculated slope of the trend as the target variable, may have presented different results.

This thesis looked at seasonal trends in high and low flow in Norway and their co-occurrence, and which main predictors explained the observed changes. To the author's knowledge, this is the first study to use machine learning methods to predict trends in high and low flow in Norwegian unregulated catchments. These findings help further the understanding of the changing water cycle in Norway, how it has impacted flow in unregulated catchments, and highlight important drivers of high and low flow.

References

AMAP. (2021). *Arctic climate change update 2021: Key trends and impacts. summary for policy-makers.* Arctic Monitoring; Assessment Programme (AMAP).

Bakke, S. J., Ionita, M., & Tallaksen, L. M. (2020). The 2018 northern european hydrological drought and its drivers in a historical perspective. *Hydrology and Earth System Sciences*, *24*(11), 5621–5653. https://doi.org/10.5194/hess-24-5621-2020

Beldring, S., Engeland, K., Roald, L. A., Sælthun, N. R., & Voksø, A. (2003). Estimation of parameters in a distributed precipitation-runoff model for norway. *Hydrology and Earth System Sciences*, *7*(3), 304–316. https://doi.org/10.5194/hess-7-304-2003

Bergström, S. (1995). The hbv model. In V. P. Singh (Ed.). Water Resources Publications.

Blauhut, V., Stoelzle, M., Ahopelto, L., Brunner, M. I., Teutschbein, C., Wendt, D. E., Akstinas, V., Bakke, S. J., Barker, L. J., Bartošová, L., Briede, A., Cammalleri, C., De Stefano, L., Fendeková, M., Finger, D. C., Huysmans, M., Ivanov, M., Jaagus, J., Jakubınský, J., ... Živković, N. (2021). Lessons from the 2018–2019 european droughts: A collective need for unifying drought risk management. *Natural Hazards and Earth System Sciences Discussions*, *2021*, 1–26. https://doi.org/10.5194/nhess-2021-276

Blöschl, G., Hall, J., Parajka, J., Perdigão, R. A. P., Merz, B., Arheimer, B., Aronica, G. T., Bilibashi, A., Bonacci, O., Borga, M., Čanjevac, I., Castellarin, A., Chirico, G. B., Claps, P., Fiala, K., Frolova, N., Gorbachova, L., Gül, A., Hannaford, J., ... Živković, N. (2017). Changing climate shifts timing of european floods. *Science*, *357*(6351), 588–590. https://doi.org/10.1126/science.aan2506

Catto, J. L., & Dowdy, A. (2021). Understanding compound hazards from a weather system perspective. *Weather and Climate Extremes*, *32*, 100313. https://doi.org/10.1016/j.wace.2021.100313

CCCS. (2018). The nordic gridded climate dataset stable release. https://surfobs.climate.copernicus.eu/documents/C3S_M311a_Lot4.2.3.3_201809_report_stable_release_v1.pdf

Dahl, M.-P. J., & Pedersen, A. I. (2021). Norwegian streamflow reference dataset for climate change studies. https://www.nve.no/media/13177/norwegian-streamflow-reference-dataset-for-climate-change-studies-2021-kombinert.pdf

Dingman, S. L. (2015). *Physical hydrology* (3rd ed.). Waveland Press Inc.

Engeland, K., & Hisdal, H. (2009). A comparison of low flow estimates in ungauged catchments using regional regression and the hbv-model. *Water Resource Management*, *23*, 2567–2586. https://doi.org/10.1007/s11269-008-9397-7

Fleig, A., Andreassen, L. M., Barfod, E., Haga, J., Haugen, L. E., Hisdal, H., Melvold, K., & Saloranta, T. (2013). Norwegian hydrological reference dataset for climate change studies. http://publikasjoner.nve.no/rapport/2013/rapport2013_02.pdf

Gottschalk, L., Jensen, J. L., Lundquist, D., R., S., & Tollan, A. (1979). Hydrologic regions in the nordic countries. *Nordic Hydrology*, *10*, 273–286.

Hannaford, J., & Marsh, T. J. (2006). High and low flow trends in a national network of undisturbed indicator catchments in the uk. *IAHS Publishing*, *308*, 496–501. https://iahs.info/uploads/dms/13710.90-496-501-13-308-Hannaford-new.pdf

Hannaford, J., & Marsh, T. J. (2008). High-flow and flood trends in a network of undisturbed catchments in the uk. *International Journal of Climatology*, *28*(10), 1325–1338. https://doi.org/10.1002/joc.1643

Hanssen-Bauer, I., Førland, E. J., Haddeland, I., Hisdal, H., Mayer, S., Nesje, A., Nilsen, J., Sandven, S., Sandø, A., Sorteberg, A., & Ådlandsvik, B. (2017). Climate in norway 2100: A knowledge base for climate adaptation.

IPCC. (2021). *Climate change 2021: The physical science basis. contribution of working group i to the sixth assessment report of the intergovernmental panel on climate change* (Vol. In Press). Cambridge University Press. https://doi.org/10.1017/9781009157896

Jenicek, M., & Ledvinka, O. (2020). Importance of snowmelt contribution to seasonal runoff and summer low flows in czechia. *Hydrology and Earth System Sciences*, *24*(7), 3475–3491. https://doi.org/10.5194/hess-24-3475-2020

Kendall, M. G. (1975). *Rank correlation methods* (2nd ed.). Charles Griffin.

Ketzler, G., Römer, W., & Beylich, A. A. (2021). The climate of norway. In A. A. Beylich (Ed.), *Landscapes and landforms of norway* (pp. 7–29). Springer International Publishing. https://doi.org/10.1007/978-3-030-52563-7_2

Konapala, G., & Mishra, A. (2020). Quantifying climate and catchment control on hydrological drought in the continental united states. *Water Resources Research*, *56*(1), e2018WR024620. https://doi.org/10.1029/2018WR024620

Laimighofer, J., Melcher, M., & Laaha, G. (2022). Parsimonious statistical learning models for low-flow estimation. *Hydrology and Earth System Sciences*, *26*(1), 129–148. https://doi.org/10.5194/hess-26-129-2022

Lawrence, D. (2020). Uncertainty introduced by flood frequency analysis in projections for changes in flood magnitudes under a future climate in norway. *Journal of Hydrology: Regional Studies*, *28*, 100675. https://doi.org/10.1016/j.ejrh.2020.100675

Lussana, C., Tveito, O. E., Dobler, A., & Tunheim, K. (2019). Senorge_2018, daily precipitation, and temperature datasets over norway. *Earth System Science Data*, *11*(4), 1531–1551. https://doi.org/10.5194/essd-11-1531-2019

Lussana, C., Tveito, O. E., & Uboldi, F. (2018). Three-dimensional spatial interpolation of 2m temperature over norway. *Quarterly Journal of the Royal Meteorological Society*, *144*(711), 344–364. https://doi.org/10.1002/qj.3208

Mann, H. B. (1945). Nonparametric test against trend. *Econometrica*, *13*, 254–259. https://www.jstor.org/stable/1907187

Merz, R., & Blöschl, G. (2003). A process typology of regional floods. *Water Resources Research*, *39*(12). https://doi.org/10.1029/2002WR001952

Nordeide, S. (2020). *Trendar i lågvassføring i noreg*. Universitetet i Oslo.

Pedregosa, F., Varoquaux, G., Grramfort, A., Michel, V., & Thirion, B. (2011). Skikit-learn: Machine learning in python. *Journal of Machine Learning Research*, *12*, 2825–2830.

Poff, N. L., Allan, J. D., Bain, M. B., Karr, J. R., Prestegaard, K. L., Richter, B. D., Sparks, R. E., & Stromberg, J. C. (1997). The natural flow regime. *BioScience*, *47*(11), 769–784. Retrieved May 7, 2022, from http://www.jstor.org/stable/1313099

Rizzi, J., Nilsen, I. B., Stagge, J. H., Gisnås, K., & Tallaksen, L. M. (2017). Five decades of warming: impacts on snow cover in Norway. *Hydrology Research*, *49*(3), 670–688. https://doi.org/10.2166/nh.2017.051

Roald, L. A. (2020). *Floods in norway*. NVE.

Saloranta, T. (2014). New version (v1.1.1) of the senorge snow model and snow maps for norway. https://publikasjoner.nve.no/rapport/2014/rapport2014_06.pdf

Saloranta, T. M. (2012). Simulating snow maps for norway: Description and statistical evaluation of the senorge snow model. *The Cryosphere*, *6*(6), 1323–1337. https://doi.org/10.5194/tc-6-1323-2012

Skålevåg, A., & Vormoor, K. (2021). Daily streamflow trends in western versus eastern norway and their attribution to hydro-meteorological drivers. *Hydrological Processes*, *35*(8), e14329. https://doi.org/10.1002/hyp.14329

Smakhtin, V. U. (2001). Low flow hydrology: A review. *Journal of hydrology*, *240*(3-4), 147–186.

Stahl, K., Hisdal, H., Hannaford, J., Tallaksen, L. M., van Lanen, H. A. J., Sauquet, E., Demuth, S., Fendekova, M., & Jódar, J. (2010). Streamflow trends in europe: Evidence from a dataset of near-natural catchments. *Hydrology and Earth System Sciences*, *14*(12), 2367–2382. https://doi.org/10.5194/hess-14-2367-2010

Tallaksen, L. M., & Van Lanen, H. A. (2004). Hydrological drought: Processes and estimation methods for streamflow and groundwater.

Van Loon, A., & Laaha, G. (2015). Hydrological drought severity explained by climate and catchment characteristics [Drought processes, modeling, and mitigation]. *Journal of Hydrology*, *526*, 3–14. https://doi.org/10.1016/j.jhydrol.2014.10.059

Wilson, D., Fleig, A. K., Lawrence, D., Hisdal, H., Pettersson, L.-E., & Holmqvist, E. (2011). A review of nve's flood frequency estimation procedures . https://publikasjoner.nve.no/report/2011/report2011_09.pdf

Wilson, D., Hisdal, H., & Lawrence, D. (2010). Has streamflow changed in the nordic countries? – recent trends and comparisons to hydrological projections. *Journal of Hydrology*, *394*(3), 334–346. https://doi.org/10.1016/j.jhydrol.2010.09.010

WMO. (2009). *Manual on low-flow estimation and prediction. operational hydrology report no. 50.* World Meteorological Organization (WMO).

Yang, D., Yang, Y., & Xia, J. (2021). Hydrological cycle and water resources in a changing world: A review. *Geography and Sustainability*, *2*(2), 115–122. https://doi.org/10.1016/j.geosus.2021.05.003

A Table of gauging stations

Table A.1: Gauging stations measuring discharge for each of the catchments used in this thesis. Stations are sorted by regine number (left). Gauging station name, coordinate position and catchment area is included.

Stations	Name	Area [km^2]	Lat	Lon
2.13.0	Nedre Sjodalsvatn	480.7	61.56064	8.91856
2.32.0	Atnasjø	463.3	61.85194	10.22212
2.142.0	Knappom	1643.02	60.64117	12.04712
2.268.0	Akslen	789.27	61.79955	8.44722
2.279.0	Kråkfoss	435.21	60.13345	11.0801
2.284.0	Sælatunga	457.52	61.88439	9.06212
2.290.0	Brustuen	254	61.7262	8.29597
2.303.0	Dombås	493.62	62.08677	9.10108
2.323.0	Fura	36.41	60.88483	11.32496
6.10.0	Gryta	7.03	59.98723	10.80066
12.70.0	Etna	568.53	60.95353	9.62442
12.171.0	Hølervatn	79.4	60.70962	9.45899
12.178.0	Eggedal	310.59	60.15247	9.43342
12.193.0	Fiskum	51.54	59.69721	9.7902
15.49.0	Halledalsvatn	59.19	60.49297	8.47906
16.66.0	Grosettjern	6.547	59.83555	8.32061
16.75.0	Tannsvatn (Lognvikvatnet)	118.016	59.67317	8.06739
18.10.0	Gjerstad	235.89	58.88361	9.03327
18.11.0	Tjellingtjernbekk	1.95	58.93208	8.85938
19.79.0	Gravå	6.301	59.23484	8.03641
19.80.0	Stigvassåi	14.486	58.74981	8.51559
19.82.0	Rauåna	8.908	58.96851	8.50818

19.96.0	Storgama ovf.	0.584	59.05231	8.65362
19.104.0	Songedalsåi	65.633	59.29985	7.9851
20.2.0	Austenå	276.42	58.83963	8.10052
20.11.0	Tveitdalen	0.44	58.38541	8.24237
22.16.0	Myglevatn ndf.	182.2	58.44589	7.58499
24.8.0	Møska (Skolandsvatnet)	121.41	58.16056	7.06623
24.9.0	Tingvatn (Lygne)	272.16	58.40114	7.22335
25.24.0	Gjuvvatn	96.98	59.15918	7.21481
26.20.0	Årdal	77.25	58.54367	6.49791
26.21.0	Sandvatn	27.5	58.48967	6.77313
36.13.0	Grimsvatn	34.41	59.5815	6.53967
41.1.0	Stordalsvatn	130.73	59.68285	6.01001
41.8.0	Hellaugvatn	27.49	59.72001	6.18786
42.2.0	Djupevad	30.965	59.81744	5.84441
48.5.0	Reinsnosvatn	120.5	59.96939	6.72526
50.1.0	Hølen	231.38	60.35738	6.74625
55.4.0	Røykenes	50.09	60.24881	5.4419
62.5.0	Bulken (Vangsvatnet)	1091.65	60.62868	6.29254
62.10.0	Myrkdalsvatn	157.75	60.79921	6.50157
62.14.0	Slondalsvatn	41.86	60.69053	6.948
62.15.0	Kinne	511.38	60.63039	6.49937
75.23.0	Krokenelv	45.92	61.34702	7.39822
75.28.0	Feigumfoss	48.04	61.38168	7.44511
76.5.0	Nigardsbrevatn	65.29	61.66655	7.24191
78.8.0	Bøyumselv	40.46	61.4487	6.74268
79.3.0	Nessedalselv	30	61.15987	6.27839
80.4.0	Ullebøelv	8.31	61.20324	5.78553
81.1.0	Hersvikvatn (Hagevatnet)	7.13	61.1352	4.93712
82.4.0	Nautsundvatn	218.96	61.2529	5.38535
83.2.0	Viksvatn (Hestadfjorden)	508.13	61.33306	5.88626
83.6.0	Byttevatn	104.54	61.34341	6.34683
83.7.0	Grønengstølsvatn	65.65	61.44324	6.46896
83.12.0	Haukedalsvatn ndf.	205.55	61.36569	6.23159

84.11.0	Hovefoss	233.74	61.53279	5.75214
84.20.0	Holsenvatn	71.48	61.43177	6.06488
85.4.0	Straumstad (Solheimsvatnet)	109.68	61.6484	5.44487
86.10.0	Åvatn (Ommedalsvatnet)	162.13	61.71941	5.9213
86.12.0	Skjerdalselv	23.66	61.81564	5.93555
87.10.0	Gloppenelv v/Bergheim	218.6	61.7186	6.52064
88.4.0	Lovatn	234.88	61.85897	6.88935
88.11.0	Strynsvatn	482.04	61.9306	6.87882
91.2.0	Dalsbøvatn	25.72	62.16243	5.16649
97.1.0	Fetvatn (Fitjavatnet)	89.05	62.33236	6.59336
98.4.0	Øye ndf.	138.78	62.06826	6.93157
101.1.0	Engsetvatn	39.91	62.53123	6.61772
104.22.0	Midtre Mardalsvatn	13.681	62.5095	8.07138
104.23.0	Vistdal	66.51	62.69773	7.96078
105.1.0	Osenelv v/Øren	137.59	62.7932	7.72607
109.9.0	Driva v/Risefoss	745.99	62.51138	9.59264
112.8.0	Rinna	87.83	62.98495	9.4071
122.11.0	Eggafoss	655.18	62.89011	11.18388
123.31.0	Kjeldstad i Garbergelva	142.98	63.26617	11.1311
124.2.0	Høggås bru	494.5	63.49292	11.35831
127.6.0	Grunnfoss	880.42	63.79118	11.80969
127.11.0	Veravatn	176.13	63.78934	12.32654
127.13.0	Dillfoss	479.64	63.7642	11.76507
128.5.0	Støafoss	477.08	64.01762	11.71813
133.7.0	Krinsvatn (Kringsvatnet)	206.61	63.80409	10.23191
138.1.0	Øyungen	239.41	64.24378	11.08169
139.20.0	Moen	64.06	64.92564	13.07912
139.26.0	Embrethølen	494.24	64.38757	12.44005
139.35.0	Trangen	852.25	64.43047	12.48165
140.2.0	Salsvatn	431.9	64.70538	11.45436
148.2.0	Mevatnet	108.47	65.36555	12.5381
151.15.0	Nervoll	653.36	65.43757	13.98604
152.4.0	Fustvatn	525.69	65.90524	13.30759

153.1.0	Storvatn	48	66.09342	13.11638
156.8.0	Svartisdal	121.98	66.48089	14.22483
156.10.0	Berget	210.69	66.45672	13.87848
156.15.0	Forsbakk	56.3	66.29299	13.81261
163.7.0	Kjemåvatn	36.39	66.76917	15.40877
168.3.0	Lakså bru	26.67	67.79663	15.29608
172.7.0	Leirpoldvatn	18.72	68.28318	16.42874
172.8.0	Rauvatn	21.23	68.20586	16.88333
177.4.0	Sneisvatn	29.25	68.40743	15.70544
178.1.0	Langvatn	18.41	68.61924	15.71249
185.1.0	Gåslandsvatn	7.7	68.67283	14.62927
191.2.0	Øvrevatn	526.02	68.85762	17.94107
196.7.0	Ytre Fiskeløsvatn	54.42	69.26298	18.88207
196.11.0	Lille Rostavatn	638.38	69.02298	19.58108
200.4.0	Skogsfjordvatn	136.01	69.98093	19.10412
205.6.0	Didnojokka	110.87	69.17903	20.77847
206.3.0	Manndalen bru	200.4	69.52389	20.52562
208.2.0	Oksfjordvatn	265.83	69.90022	21.37681
208.3.0	Svartfossberget	1932.29	69.52854	21.38166
209.4.0	Lillefossen	330.6	69.78563	21.91785
212.10.0	Masi	5620.81	69.42004	23.63504
212.49.0	Halsnes	145.05	70.02644	22.94164
213.2.0	Leirbotnvatn	135.47	70.10667	23.55344
213.4.0	Kvalsund	124.8	70.48684	23.95331
223.2.0	Lombola	877.14	70.13985	24.76063
234.18.0	Polmak nye	14161.4	70.07034	28.01601
244.2.0	Neiden	2947.19	69.70071	29.32131
246.9.0	Sametielv	255.69	69.40015	29.71704
247.3.0	Karpelva	128.89	69.65991	30.38412
307.5.0	Murusjø	345.62	64.4867	14.01565
307.7.0	Landbru	61.37	64.88673	13.91636
308.1.0	Lenglingen	449.98	64.24487	13.76031
311.4.0	Femundsenden (Femunden)	1794.03	61.91996	11.94004

311.460.0	Engeren	394.83	61.66524	12.01897
313.10.0	Magnor	357.86	59.95464	12.18729

B Mean values and trends for temperature, precipitation, evaporation and snow indices

Temperature and precipitation

The following are maps covering Norway showing the calculated mean annual values for temperature [°C] (Figure B.1a and precipitation (Figure B.1b. Description of the calculation is in Section 2.2.1.

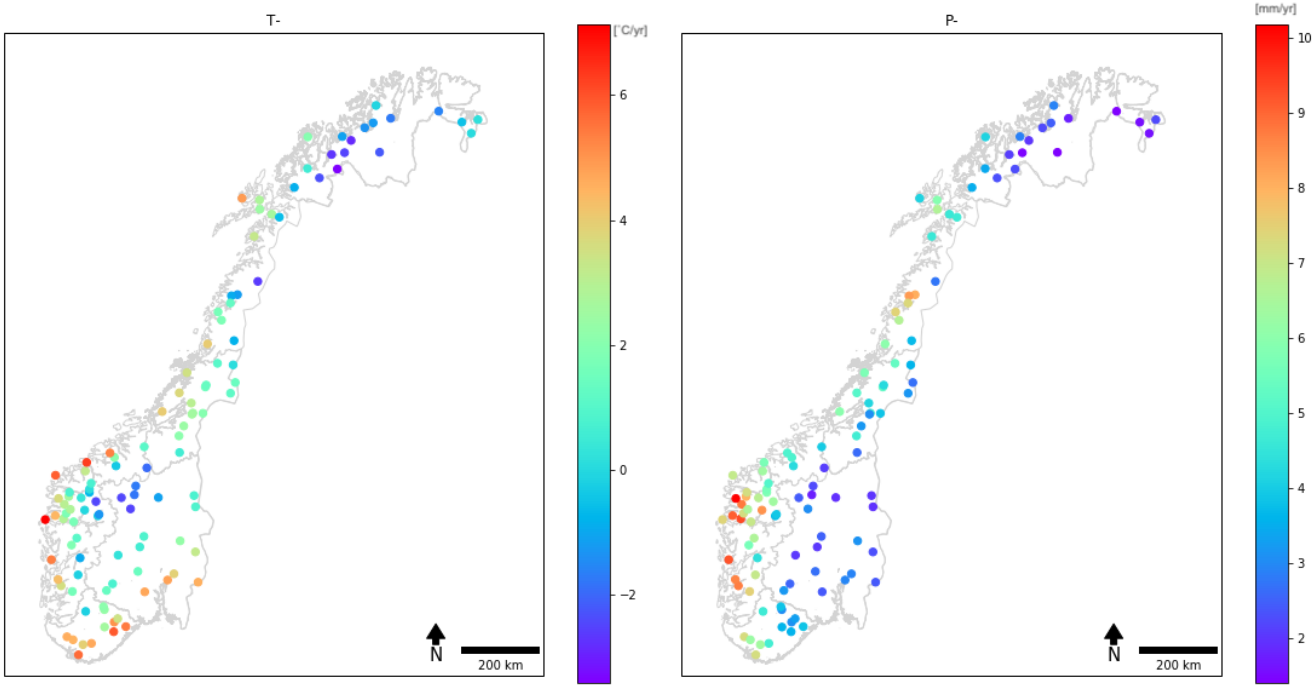

(a) (b)

Figure B.1: Mean annual temperature (a) and precipitation (b) over Norway calculated for the period 01.01.1991-31.12.2019.

Figure B.2 show the corresponding trend calculation for the mean yearly values for temperature and precipitation over the period 01.01.1991-31.12.2019.

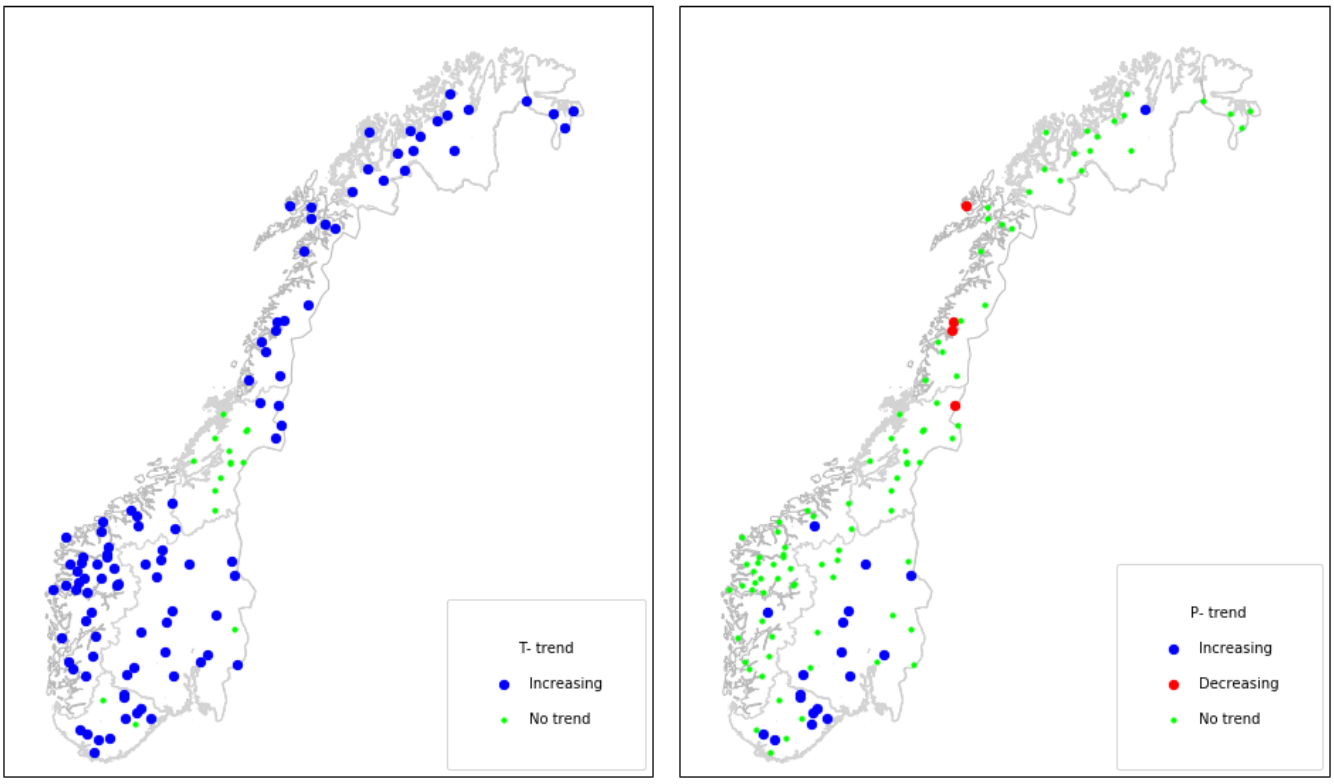

(a) (b)

Figure B.2: Trend in mean annual temperature (a) and precipitation (b) over Norway calculated at 5% significance level over the period 01.01.1991-31.12.2019. Blue dots are 5% significantly increasing trends, red dots are 5% significantly decreasing trends, while green dots mean no significant trend.

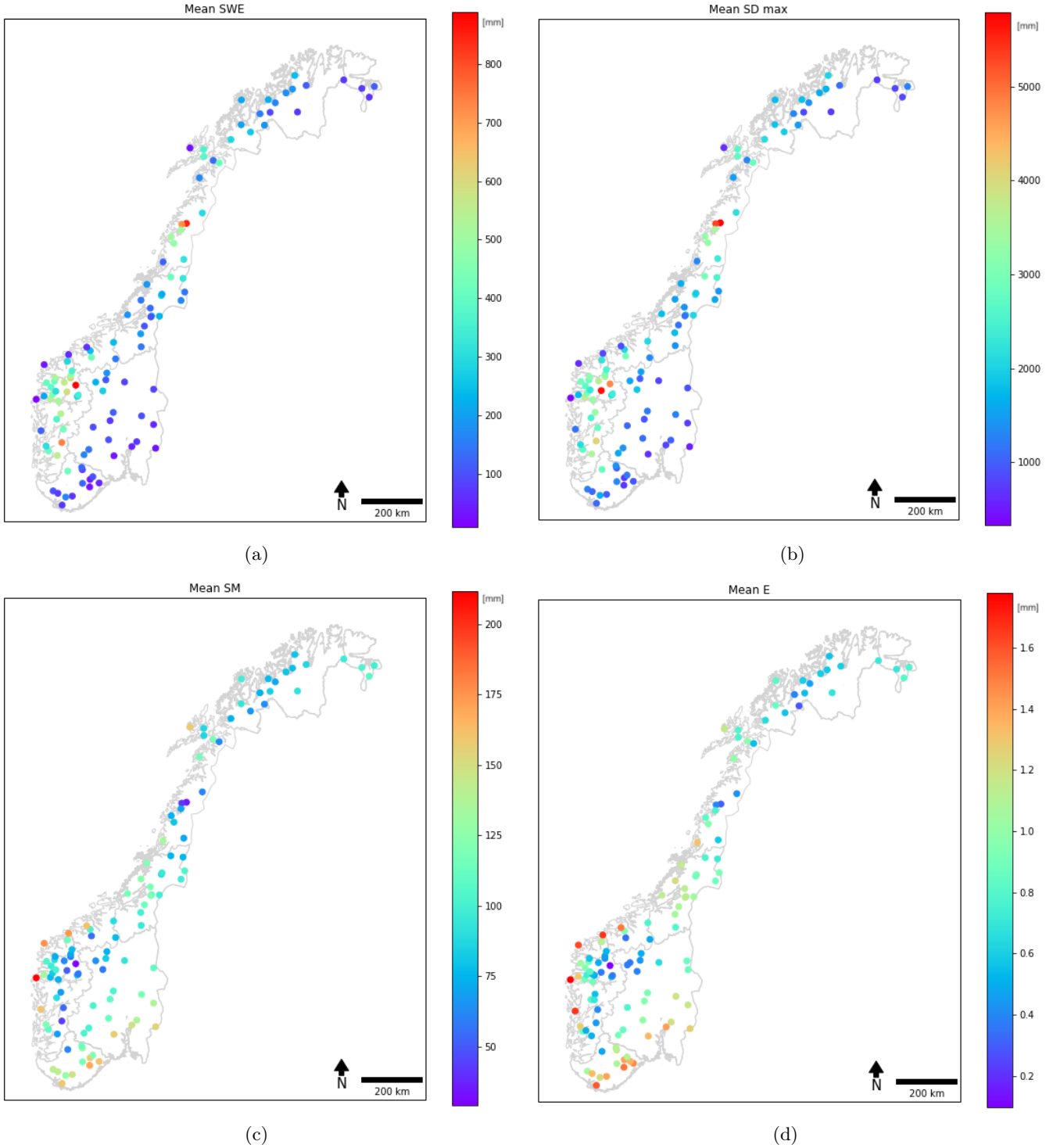

Figure B.3: Mean annual snow water equivalent [mm] (a), mean annual maximum snow depth [mm] (b), mean annual snow melt [mm] (c) and mean annual evaporation [mm] (d) over Norway calculated for the period 01.01.1991-31.12.2019.

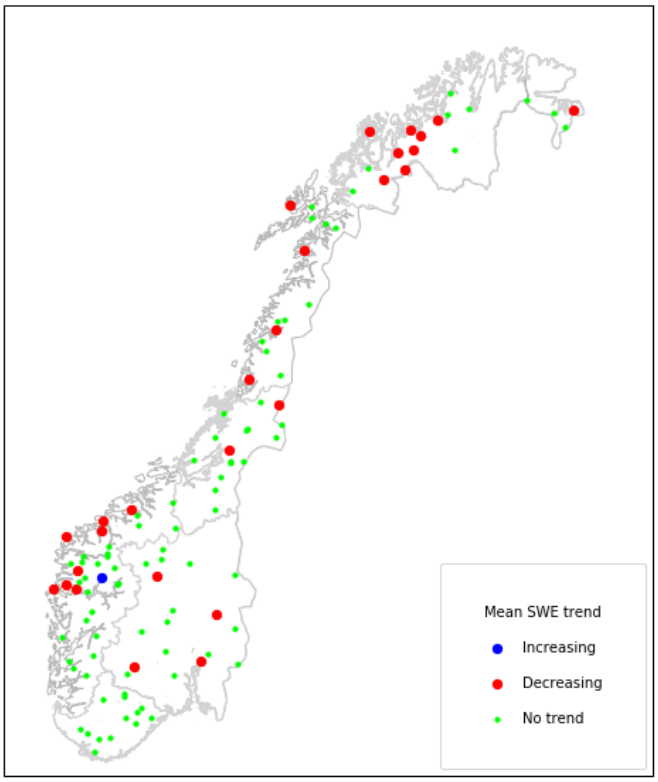

(a)

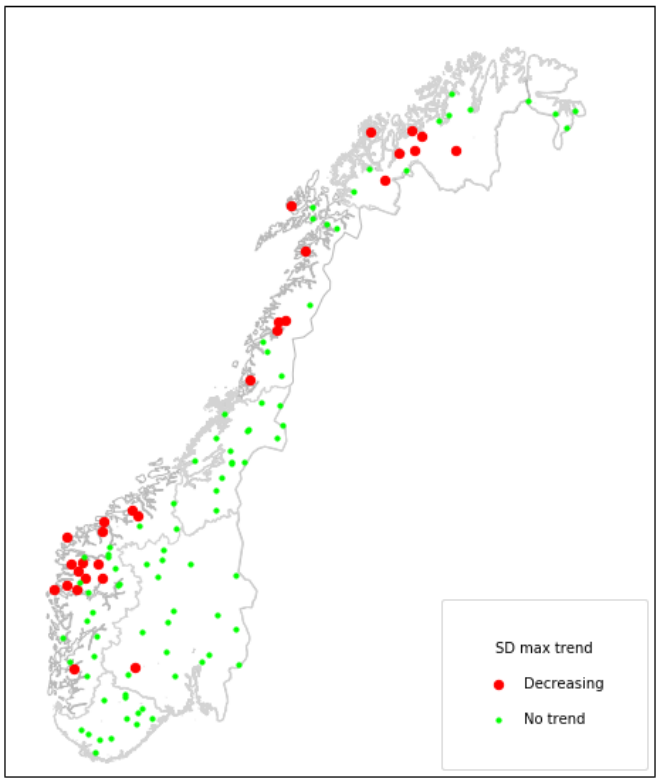

(b)

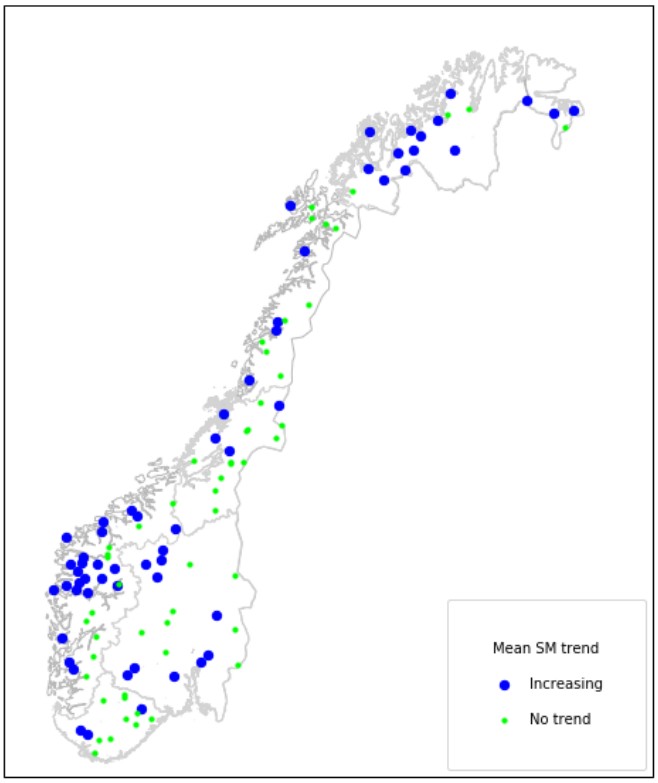

(c)

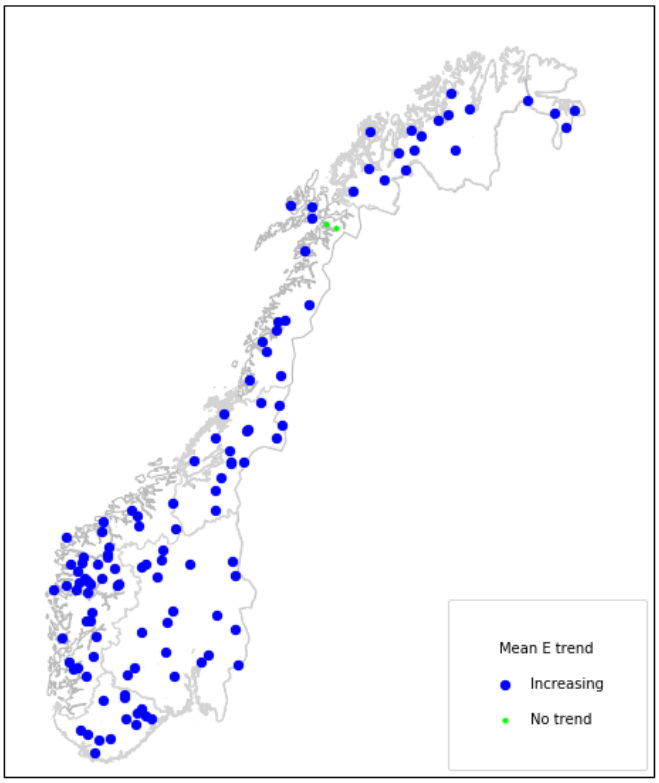

(d)

Figure B.4: Trend results for mean annual snow water equivalent [mm] (a), mean annual maximum snow depth [mm] (b), mean annual snow melt [mm] (c) and mean annual evaporation [mm] (d) over Norway calculated for the period 01.01.1991-31.12.2019. Blue dots are 5% significantly increasing trends, red dots are 5% significantly decreasing trends, while green dots mean no significant trend.

C Additional catchment characteristics

Here are maps of the catchment characteristics listed in Table 3.1 not included in Figure 2.6.

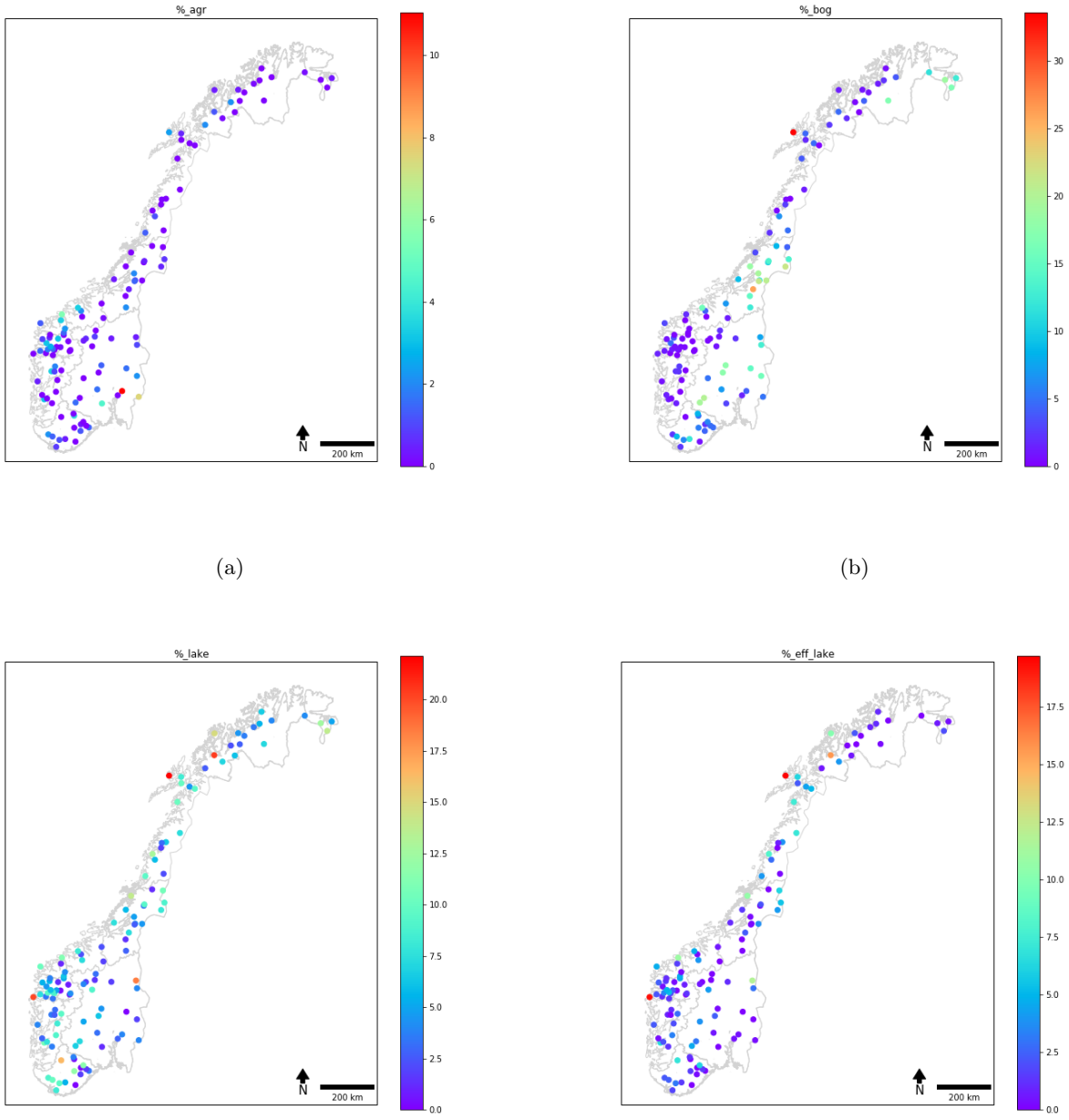

(a) (b)

(c) (d)

Figure C.1: Percentage agriculture (a), percentage bog (b), percentage lake (c) and percentage effective lake (d) in each catchment. Data from NVE's database Hydra II, via the HydAPI: https://hydapi.nve.no/UserDocumentation

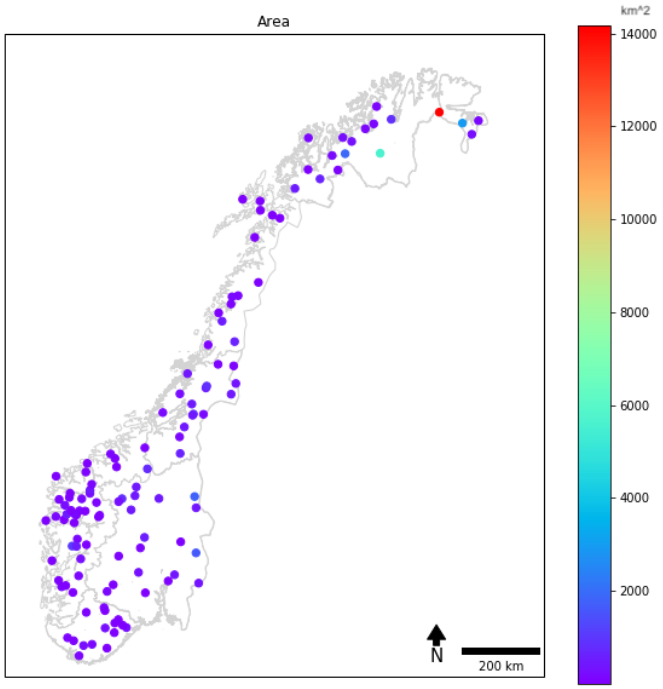

(a)

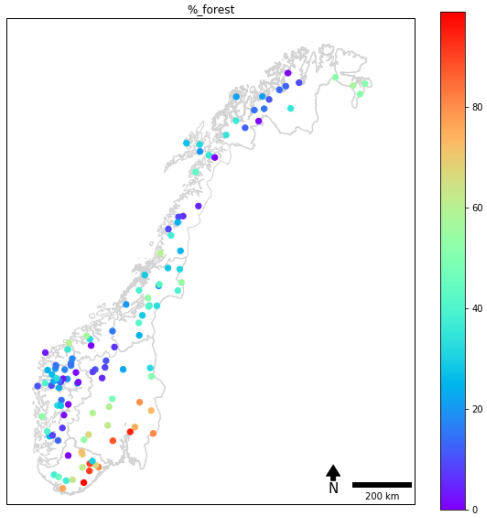

(b)

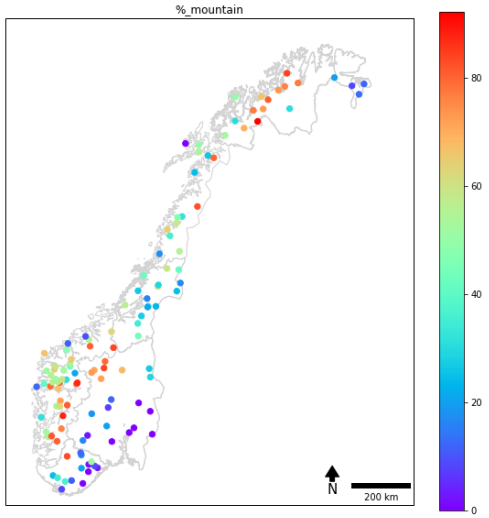

(c)

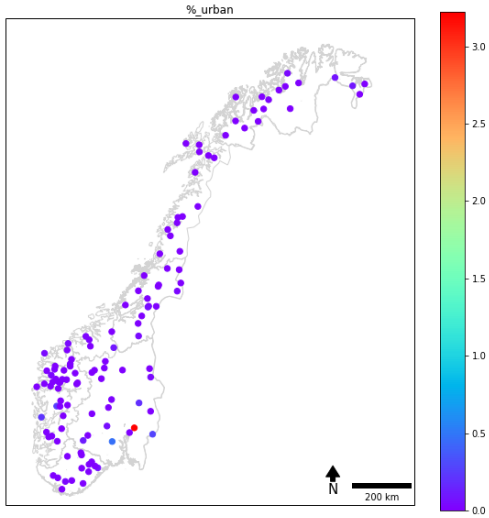

(d)

Figure C.2: Catchment area [km^2] (a), percentage forest (b), percentage mountain (c) and percentage urban (d) in each catchment. Data from NVE's database Hydra II, via the HydAPI: https://hydapi.nve.no/UserDocumentation

D Snow simulation calculations

The seNorge snow model v1.1 calculates if precipitation is classified as liquid (P_L) or solid (P_S) based on whether the air temperature T is above or below the snowfall threshold temperature T_S. If $T \leq T_S$, the amount of snowfall is calculated by $P_S = f_S * P$ and rainfall as $P_L = 0$.

If $T \leq T_S$:

$$\begin{aligned} P_S &= f_S * P \\ P_L &= 0 \end{aligned} \tag{D.1}$$

If $T > T_S$, the amount of rainfall is $P_L = f_R * P$ and snowfall is $P_S = 0$. The parameters f_S and f_R are correction factors for the input precipitation.

If $T > T_S$:

$$\begin{aligned} P_L &= f_R * P \\ P_S &= 0 \end{aligned} \tag{D.2}$$

The melt algorithm was previously based on the temperature-dependent degree-day method. A degree-day factor of potential daily melting rate, C_M [mm d-1 °C-1], varies seasonally between its minimum and maximum as a sinus wave, with its maximum at the summer solstice.

$$C_M = C_{Mmin} + ((C_{Mmax} - C_{Mmin}) * 0.5 * (sin(2\pi((N_d - 81.5)/366)) + 1 \tag{D.3}$$

Where N_d is the Julian day number. The snow then melts or refreezes, depending on whether the temperature T is above or below the melting threshold temperature T_M, which calculate the potential daily melting (positive) or refreezing (negative) M^* [mmd^{-1}]. If $T > T_M$, daily potential melt is $M^* = C_M(T - T_M)$ and actual daily melt is $M = min(M^*,\ W_I^{t-1} + P_S)$, where W_I is the ice content in the snow in water equivalents [mm].

If $T > T_M$:

$$M^* = C_M(T - T_M) M = min(M^*,\ W_I^{t-1} + P_S) and \tag{D.4}$$

If $T < T_M$, daily potential refreezing is $M^* = C_{rf}(T - T_M)$ and actual daily refreezing is $M = max(M^*,\ -W_L^{t-1})$, where C_{rf} is a degree-day factor for refreezing while W_L^t is the actual liquid water content in the snow.
If $T < T_M$:

$$M^* = C_{rf}(T - T_M) M = max(M^*,\ -W_L^{t-1}) \tag{D.5}$$

The ice content in the snowpack W_I can be found by:

$$W_I^t = W_I^{t-1} + P_S - M \tag{D.6}$$

while the potential (W_{Lpot}^t) and actual (W_L^t) water liquid content can be found by the equations:

$$W_{Lpot}^t = W_L^{t-1} + P_L + M \tag{D.7}$$

$$W_L^t = min(W_{Lpot}^t,\ r_{max} * W_I^t) \tag{D.8}$$

where r_{max} is maximum liquid water to ice ratio in the snowpack ($W_L W_I$).

The snow and ice water equivalent SWE [mm] and the runoff out of the snowpack Q_{out} [mm d-1] are then derived as follows:

$$SWE^t = W_I^t + W_L^t \tag{D.9}$$

$$Q_{out} = W_{Lpot}^t - W_L^t \tag{D.10}$$

The snowpack compaction and density routine start with calculating changes in snow depth SD [mm] in three steps. Firstly, net decrease in SWE since the last step due to melting:

$$SD_0 = SD^{t-1} * min\left(\frac{max(SWE^t - P_S,\ 0)}{SWE^{t-1}},\ 1\right) \tag{D.11}$$

Secondly, how compaction of the old snowpack lowers the snow depth because of weight of new snow at the current time step:

$$\Delta SD_1 = -\frac{P_S}{SWE^t - P_S} * (\frac{SD_0}{b_1})^{b_{exp}} * SD_0 \tag{D.12}$$

Thirdly, after compaction and added new snow, the snow depth is:

$$SD_1 = SD_0 + \Delta SD_1 + \frac{min(SWE, P_S)}{\rho_{ns}} \tag{D.13}$$

ρ_{ns} is the density of the new snow at the current time step if there is any. A gradual compaction of the snowpack during the third step due to the assumption that snow is a viscous medium is calculated by:

$$\Delta SD_2 = -\frac{kc * g * \rho c * (0.001 * SWE)}{\eta_0 * exp^{-C_5 * T_{snow} + C_6 * \rho_1} * SD_1 * \Delta t} \tag{D.14}$$

Snow depth and density is finally calculated by:

$$SD^t = SD_1 + \Delta SD_2 and \rho^t = \frac{SWE^t}{SD^t} \tag{D.15}$$

The melt rate was revised for the snow model v1.1.1 with the help of approximately 3350 observations from 31 snow-pillow stations across Norway, providing melt rates from daily snow water equivalent time series. This was also used to develop a temperature-independent melt term which that only depend on solar radiation. The final melt equation is:

$$M = b_0 T + c_0 S^* \tag{D.16}$$

The first term in the equation depends on whether the temperature is above or below a threshold, the second term depends on c_0, a constant, and S^*, potential extraterrestrial solar radiation on a horizontal plane, depends on day of year and latitude normalized by the maximum value at the latitude 60°N. The value of b_0 and c_0 are determined (calibrated) using multiple regression analysis, where values of c_0 is based on data of M from spring and summer only.

E Link to GitHub

The code used to produce the results is this thesis is available on GitHub from this url: https://github.com/sunnivan/master-thesis/tree/master.